Progress Energy

Crystal River Nuclear Plant
Docket No. 50-302
Operating License No. DPR-72

Ref: 10 CFR 50.90

February 26, 2009
3F0209-05

U.S. Nuclear Regulatory Commission
Attn: Document Control Desk
Washington, DC 20555-0001

Subject: Crystal River Unit 3 – License Amendment Request #307, Revision 0
Methodology for Rod Ejection Accident Analysis Under Extended Power Uprate Conditions

Dear Sir:

Pursuant to 10 CFR 50.90, Florida Power Corporation (FPC), doing business as Progress Energy Florida, Inc., hereby requests approval of the subject License Amendment Request (LAR). The proposed amendment for Crystal River Unit 3 (CR-3), requests approval for a new methodology, developed by AREVA NP, to analyze the rod ejection accident (REA) under Extended Power Uprate (EPU) conditions. The adoption of the new methodology is reflected in a change to the CR-3 Operating License and Improved Technical Specifications (ITS). ITS Section 5.6.2.18.b is being revised to add this new methodology to the list of approved methods used in developing the Core Operating Limits Report. Additionally, Operating License Condition 2.C.(12), which was a one cycle license condition, is being deleted.

FPC requests approval of the proposed license amendment by June 30, 2009 with the amendment to be implemented during Refuel 17, scheduled for Fall 2011. This LAR is required to support submittal of the EPU LAR. It has been determined to be a linked submittal for the EPU LAR per Office of Nuclear Reactor Regulation (NRR) Office Instruction LIC-109, "Acceptance Review Procedures."

This letter establishes no new regulatory commitments.

A report describing the new methodology is provided in Attachment E. In the attached report, a bounding sample problem analysis is presented to demonstrate that the process, computer codes, boundary conditions, uncertainties, and results for the REA event are applicable to CR-3. The results from the sample problem demonstrate that the new methodology provides acceptable results relative to the interim Reactivity Insertion Accident criteria specified in NUREG-0800, Revision 3, "Standard Review Plan for the Review of Safety Analysis Reports for Nuclear Power Plants" (SRP), Section 4.2.

Attachment E contains proprietary information. AREVA NP Inc. requests the proprietary information be withheld from public disclosure in accordance with 10 CFR 2.390(a)(4). An

Progress Energy Florida, Inc.
Crystal River Nuclear Plant
15760 W. Powerline Street
Crystal River, FL 34428

A001
NRR

Affidavit supporting the request is provided in Attachment D. A non-proprietary version of the report is attached in Attachment F.

In accordance with 10 CFR 50.91, a copy of this application with enclosures is being provided to the designated State of Florida Official.

The CR-3 Plant Nuclear Safety Committee has reviewed this request and recommended it for approval.

If you have any questions regarding this submittal, please contact Mr. Dan Westcott, Supervisor, Licensing and Regulatory Programs at (352) 563-4796.

Sincerely,

JON A. FRANKE, for

Dale E. Young
Vice President
Crystal River Nuclear Plant

DEY/rt/par

Attachments:
A. Description of the Proposed Change, Background, Justification for the Request, Determination of No Significant Hazards Consideration, and the Environmental Assessment

B. Proposed Improved Technical Specification Page Changes – Strikeout and Shadowed Text Format

C. Proposed Improved Technical Specification Changes – Revision Bar Format

D. Affidavit for Withholding Proprietary Information from Public Disclosure

E. ANP-2788P, Revision 0, Crystal River Unit 3 Rod Ejection Accident Methodology Report (Proprietary)

F. ANP-2788NP, Revision 0, Crystal River Unit 3 Rod Ejection Accident Methodology Report (non-Proprietary)

cc: NRR Project Manager
Regional Administrator, Region II
Senior Resident Inspector
State Contact

STATE OF FLORIDA

COUNTY OF CITRUS

Jon A. Franke states that he is the Director Site Operations, Crystal River Nuclear Plant for Florida Power Corporation, doing business as Progress Energy Florida, Inc.; that he is authorized on the part of said company to sign and file with the Nuclear Regulatory Commission the information attached hereto; and that all such statements made and matters set forth therein are true and correct to the best of his knowledge, information, and belief.

Jon A. Franke
Director Site Operations
Crystal River Nuclear Plant

The foregoing document was acknowledged before me this 26 day of February, 2009, by Jon A. Franke.

Signature of Notary Public
State of Florida

CAROLYN E. PORTMANN
Notary Public - State of Florida
My Commission Expires Mar 1, 2010
Commission # DD 520330
Bonded By National Notary Assn.

(Print, type, or stamp commissioned Name of Notary Public)

Personally Known ✓ -OR- Produced Identification _____

PROGRESS ENERGY FLORIDA, INC.

CRYSTAL RIVER UNIT 3

DOCKET NUMBER 50-302/LICENSE NUMBER DPR-72

LICENSE AMENDMENT REQUEST #307, REVISION 0

ATTACHMENT A

Description of the Proposed Change, Background, Justification for the Request, Determination of No Significant Hazards Consideration, and the Environmental Assessment

DESCRIPTION OF THE PROPOSED LICENSE AMENDMENT REQUEST, BACKGROUND, JUSTIFICATION FOR THE REQUEST, DETERMINATION OF NO SIGNIFICANT HAZARDS CONSIDERATION, AND THE ENVIRONMENTAL ASSESSMENT

1.0 DESCRIPTION OF PROPOSED LICENSE AMENDMENT REQUEST

Florida Power Corporation (FPC) hereby submits License Amendment Request (LAR) #307, Revision 0, requesting approval of a new methodology, developed by AREVA NP, to analyze the rod ejection accident under Extended Power Uprate conditions for Crystal River Unit 3 (CR-3).

The resulting changes to the CR-3 Operating License and Improved Technical Specifications (ITS) [Reference 1] are presented in Attachments B and C. These changes are:

- Operating License 2.C.(12) is being deleted because it is an obsolete License Condition.

- ITS Section 5.6.2.18.b is being revised to add ANP-2788P, "Crystal River 3 Rod Ejection Accident Methodology Report," to the list of approved methods used in developing the Core Operating Limits Report.

2.0 BACKGROUND

CR-3 is currently preparing the necessary supporting documentation for an Extended Power Uprate (EPU) License Amendment Request. NRC guidance documents, RS-001, "Review Standard for Extended Power Uprates," and Office of Nuclear Reactor Regulation Office Instruction LIC-109, "Acceptance Review Procedures," include two requirements that are key to the need for and timing of this LAR. First, it is the NRC staff's expectation that the EPU LAR not rely on unapproved methods. Second, it is the NRC staff's expectation that linked submittals be resolved prior to the subsequent submittal, avoiding concurrent reviews or presumed acceptance. This LAR requests approval of a new methodology and is a linked submittal for the CR-3 EPU LAR. Once approved, this methodology will be used in developing the Cycle 18 core operating limits at 3014 MWt.

The rod ejection accident (REA) is one of the current licensing bases accidents outlined in Chapter 14 of the CR-3 FSAR [Reference 2]. AREVA NP is analyzing the plant response to the current licensing bases accidents as part of the overall EPU Project. In general, reactivity sensitive events (REA, Main Steam Line Break, overcooling, etc.) are affected more by EPU than those that are sensitive to thermal-hydraulic (T-H) conditions. This is because EPU directly and significantly impacts the net reactivity of the core whereas the EPU required changes in Reactor Coolant System (RCS) T-H conditions are much less significant.

Section 4.2 of NUREG 0800, "Fuel System Design," [Reference 3] was revised in March 2007 to reflect the current NRC position for the review of Safety Analysis Reports for new nuclear power plants. The requirements of Reference 3 have not been imposed on operating plants, but

FPC and AREVA NP factored the current NRC staff positions into the evaluation of this event due to the significant increase in core power associated with an EPU.

The EPU thermal power level would challenge the current CR-3 FSAR acceptance criteria (cal/g and departure from nucleate boiling ratio (DNBR) fuel failure criteria) using the currently approved ejected rod methodology and standard inputs. FPC is concerned that under EPU conditions, the analyses utilizing the current methodology will not provide successful results without sacrificing significant margin. Therefore, it was determined that future analyses utilizing a more robust methodology would be required to achieve acceptable results. This new methodology will maintain, to the extent possible, the current CR-3 safety analysis margins and fuel management flexibility.

AREVA NP has already developed, submitted, and has been working with the NRC on review and approval of an alternate rod ejection analysis methodology [Reference 4] as part of the licensing of the US EPR (Evolutionary Pressurized Reactor). Rather than develop a different alternate methodology for CR-3, it was considered more appropriate to simply adopt the US EPR methodology [Reference 4] for use at CR-3 for the EPU REA. The review of the US EPR methodology has progressed well; but, approval does not appear likely in time to support the CR-3 EPU submittal. Further, the EPR Topical was not proposed for operating plants. Therefore, FPC is proposing to use the methodology described in Reference 4, using a bounding sample problem to demonstrate applicability to CR-3 [Reference 5].

While the NRC has not imposed the revised SRP requirements on operating plants, the proposed method will be shown to meet the revised SRP for the CR-3 EPU core designs. It is worth noting that the new methodology will use a conservative maximum clad temperature limit as one of the additional acceptance criterion in order to meet the coolability requirement identified in SRP Section 4.2.

3.0 EVALUATION

The deletion of the CR-3 Operating License (OL) Condition 2.C.(12) is due to a one cycle condition becoming obsolete. The OL Condition identified specific vendor documents that were used in developing the Cycle 14 Core Operating Limits Report (COLR). This one cycle condition has become obsolete since those specific documents were merged into an updated version of the document that is currently used in developing COLRs. The NRC permitted CR-3 to utilize the methods but required a one cycle OL Condition. With the approval of Amendment 211 (Accession No. ML032930435), the NRC approved the additional methods which were subsequently incorporated into BAW-10179P-A, "Safety Criteria and Methodology for Acceptable Cycle Reload Analyses." Therefore, the OL Condition is no longer required.

The methodology described in ANP-2788P, Revision 0, "Crystal River Unit 3 Rod Ejection Accident Methodology Report" (Attachment E), is capable of explicitly modeling rod ejections with 3-dimensional kinetics to facilitate the consideration of a wider range of ejected rod worths and more accurate peaking. The new methodology described in Attachment E includes the use of a nodal 3-D kinetics solution with both T-H and fuel temperature feedback and a separate peak rod thermal evaluation with an open channel T-H and fuel thermal model. These models

provide more precise localized neutronic and thermal conditions than previous methods to show compliance with the revised SRP [Reference 3]. The criteria and guidance specified in Appendix B of SRP Section 4.2 [Reference 3] was applied in this new methodology for demonstration purposes.

This new methodology described in Attachment E is the same as the methodology described in Reference 4, except that it is applied to CR-3. In the attached report, a bounding sample problem analysis is presented to demonstrate the process, computer codes, boundary conditions, uncertainties, and results for the REA event are applicable to CR-3. Section 2 of the report describes the regulatory requirements for cladding failure and core coolability. Section 3 describes the requirements of the Computer Codes. Section 4 addresses the boundary conditions and uncertainties considered for the REA. Section 5 provides the CR-3 REA methodology with a sample problem to demonstrate applicability to CR-3, and describes the overall calculational flow among various computer codes and data process linkages during the Ejected Rod Accident Analysis. Section 6 describes the details of various computer codes that are used for REA simulation. Section 7 describes the boundary conditions and uncertainties that are applied to the specific analyses. Section 8 provides the results from the sample problem. These results demonstrate that new methodology provides acceptable results relative to the regulatory requirements described in Section 2. In Section 9, this methodology also provides the static conditions that a future cycle must meet for this analysis to remain valid. A cycle specific analysis can be repeated for those cycle parameters that do not meet the REA design parameters or a complete re-analysis can be performed to meet more challenging fuel designs.

The first step of the methodology is to choose the regulatory requirements to define the specific criteria that the REA analysis will meet. This methodology uses the requirements in Reference 3 for cladding failure, core coolability, and radiological consequences. The requirements for radiological assessment and the maximum system pressure are not addressed by this methodology.

The overall REA sample problem results for CR-3 are within the limiting criteria for this REA methodology.

Conclusion

The sample calculations discussed in Attachment E demonstrate that the proposed new methodology provides acceptable results using sample problem inputs both from an operational and regulatory perspective. Therefore, the acceptance criterion discussed in SRP Section 4.2 will be satisfied. This methodology will be utilized in support of the EPU LAR which is currently scheduled to be submitted to NRC on or before June 30, 2009. The addition of this methodology to the list of documents used in developing the CR-3 COLR will enable its utilization in developing the COLR for Cycle 18.

4.0 NO SIGNIFICANT HAZARDS CONSIDERATION

The proposed change is incorporation of a new methodology into Section 5 of the CR-3 ITS. This methodology will be used in developing the reactor core operating limits and will be added into the COLR. As such, this methodology is an analytic tool which will be used to analyze a spectrum of rod ejection events and to show that those events will be safely terminated without harming the reactor core. NRC review and approval is required for a new analytical tool that specifically addresses the rod ejection accident. This new methodology more accurately models core dynamics results for a range of rod ejection scenarios. Further, the methodology was explicitly developed to address the new, more conservative acceptance criteria addressed in Section 4.2 of the Standard Review Plan.

The adoption of the new methodology results in changes to both the CR-3 Operating License and ITS [Reference 1]. ITS Section 5.6.2.18, COLR is revised to include this new methodology in the list of methods used to develop the COLR. Additionally, Operating License Condition 2.C.(12) is being deleted. This one cycle condition identified specific vendor documents that were used in developing the Cycle 14 COLR. This one cycle condition has become obsolete since those specific documents were merged into an updated version of the document that is currently used in developing COLRs. Neither of these changes will have any impact on the operation or maintenance of the plant.

Florida Power Corporation (FPC) has evaluated the proposed License Amendment Request (LAR) against the criteria of 10 CFR 50.92(c) to determine if any significant hazards consideration is involved. FPC has concluded that this proposed LAR does not involve a significant hazards consideration. The following is a discussion of how each of the 10 CFR 50.92(c) criteria is satisfied.

(1) Does not involve a significant increase in the probability or consequences of an accident previously evaluated.

This amendment addresses analytical tools. A spectrum of Rod Ejection Accident events will be analyzed using this methodology and the results will be factored into developing the Core Operating Limits Report. The improved methods have no impact on any actual event probability. No change to any installed plant components is required to utilize this methodology. The improved methods more accurately predict accident consequences, but cannot increase them.

Therefore, granting this LAR does not involve any increase in the probability or consequences of the Rod Ejection Accident (REA).

(2) Does not create the possibility of a new or different kind of accident from any accident previously evaluated.

This amendment addresses analytical tools and therefore, it has no impact on plant performance. Plant systems, structures, or components will not be altered or replaced in order to utilize this methodology. Plant software used to control equipment or monitor plant parameters will not be affected by this methodology change. Thus, it cannot create the possibility of a new or different kind of accident.

The improved methods do address aspects of rod ejection methods that current methods do not address. Additionally, the methodology continues to evaluate the range of rod ejection accidents against similar but more limiting acceptance criteria (dose, energy deposition and peak clad temperature).

Therefore, the proposed change will not create the possibility of a new or different kind of accident from any previously evaluated.

*(3) **Does not involve a significant reduction in a margin of safety.***

The new methodology evaluates the Rod Ejection Accident against substantially more limiting acceptance criteria. Specifically, the peak radial average fuel enthalpy limit is reduced from the previous limit of 280 cal/g [Reference 2] to the Standard Review Plan, Section 4.2, Revision 3, limit of less than 230 cal/g [Reference 3]. This peak radial average fuel enthalpy limit is further reduced to 150 cal/g in the new methodology [Reference 4]. The dose limit has not been changed. However, an additional conservative peak clad temperature limit has been added to preclude the potential for rod ballooning. This limit is significantly below the value expected for incipient fuel melt. The methodology includes consideration of appropriate conservatisms, benchmarks, and uncertainties. If applied to the same input conditions, the proposed methodology would predict lower results than the current methodology because of the increased thoroughness and rigorous consideration of a number of factors. The actual margin of safety is not negatively affected by application of a more robust model. Therefore, the proposed change does not reduce the margin of safety.

5.0 ENVIRONMENTAL IMPACT EVALUATION

10 CFR 51.22(c)(9) provides criteria for and identification of licensing and regulatory actions eligible for categorical exclusion from performing an environmental assessment. A proposed amendment to an operating license for a facility requires no environmental assessment if the amendment changes a requirement with respect to use of a facility component within the restricted area provided that:

(i) the amendment involves no significant hazards consideration,
(ii) there is no significant change in the types or significant increase in the amounts of any effluents that may be released offsite, and
(iii) there is no significant increase in individual or cumulative occupational radiation exposure.

Florida Power Corporation (FPC) has reviewed this License Amendment Request (LAR) and has

determined that it meets the eligibility criteria for categorical exclusion set forth in 10 CFR 51.22(c)(9). Pursuant to 10 CFR 51.22, no environmental impact statement or environmental assessment needs to be prepared in connection with the issuance of the proposed license amendment. The basis for this determination is that for this amendment:

(i) The proposed license amendment does not involve a significant hazards consideration, as described in the significant hazards evaluation.

(ii) As discussed in the Justification for the Request and the No Significant Hazards Consideration, this change does not result in a significant change or significant increase in the release associated with any Design Basis Accident. Likewise, there will be no significant change in the types or a significant increase in the amounts of any effluents released offsite during normal operation.

(iii) The proposed LAR does not result in a significant increase to the individual or cumulative occupational radiation exposure.

6.0 APPLICABLE REGULATORY REQUIREMENTS/CRITERIA

FPC and AREVA NP have evaluated the Regulatory Requirements applicable to the proposed LAR. FPC and AREVA NP have determined that the proposed LAR is consistent with the following applicable regulatory requirements, guidance or criteria:

1. NUREG-0800, Revision 3, "Standard Review Plan for the Review of Safety Analysis Reports for Nuclear Power Plants" (SRP), Section 15.4.8, "Spectrum of Rod Ejection Accidents (PWR)," March 2007

2. NUREG-0800, Revision 3, Section 4.2, "Fuel System Design," Appendix B, March 2007

3. NUREG/CR-6742, LA-UR-99-6810, "Phenomenon Identification and Ranking Tables (PIRTs) for Rod Ejection Accidents in Pressurized Water Reactors Containing High Burnup Fuel," Los Alamos National Laboratory, September 2001

7.0 REFERENCES

1. Crystal River Unit 3, "Improved Technical Specifications" through Amendment 230 and Bases Revision 77
2. Crystal River Unit 3, "Final Safety Analysis Report (FSAR)," Rev. 31.2
3. NUREG-0800, "Standard Review Plan" (SRP), Section 4.2, "Fuel System Design," (Revision 3), March 2007
4. ANP-10286P, U.S. EPR Rod Ejection Accident Methodology Topical Report
5. ANP-2788P, Crystal River 3 Rod Ejection Accident Methodology Report, Revision 0

PROGRESS ENERGY FLORIDA, INC.

CRYSTAL RIVER UNIT 3

DOCKET NUMBER 50-302/LICENSE NUMBER DPR-72

LICENSE AMENDMENT REQUEST #307, REVISION 0

ATTACHMENT B

PROPOSED IMPROVED TECHNICAL SPECIFICATION PAGE CHANGES

STRIKEOUT AND SHADOWED TEXT FORMAT

2.C.(6) Deleted per Amendment No. 21, 7-3-79

2.C.(7) Prior to startup following the first regularly scheduled refueling outage, Florida Power Corporation shall modify to the satisfaction of the Commission, the reactor coolant system flow indication to meet the single failure criterion with regard to pressure sensing lines to the flow differential pressure transmitters.

2.C.(8) Within three months of issuance of this license, Florida Power Corporation shall submit to the Commission a proposed surveillance program for monitoring the containment for the purpose of determining any future delamination of the dome.

2.C.(9) Fire Protection

Florida Power Corporation shall implement and maintain in effect all provisions of the approved fire protection program as described in the Final Safety Analysis Report for the facility and as approved in the Safety Evaluation Reports, dated July 27, 1979, January 22, 1981, January 6, 1983, July 18, 1985, and March 16, 1988, subject to the following provisions:

The licensee may make changes to the approved fire protection program without prior approval of the Commission only if those changes would not adversely affect the ability to achieve and maintain safe shutdown in the event of a fire. *{Amdt. #147, 1-22-93}*

2.C.(10) The design of the reactor coolant pump supports need not include consideration of the effects of postulated ruptures of the primary reactor coolant loop piping and may be revised in accordance with Florida Power Corporation's amendment request of April 24, 1986. *{Added per Amdt. #89, 5-23-86}*

2.C.(11) A system of thermocouples added to the decay heat (DH) drop and Auxiliary Pressurizer Spray (APS) lines, capable of detecting flow initiation, shall be operable for Modes 4 through 1. Channel checks of the thermocouples shall be performed on a monthly basis to demonstrate operability. If either the DH or APS system thermocouples become inoperable, operability shall be restored within 30 days or the NRC shall be informed, in a Special Report within the following fourteen (14) days, of the inoperability and the plans to restore operability. *{Amdt. #164, 1-27-98}*

2.C.(12) ~~Florida Power Corporation shall assure that the Cycle 14 core for CR-3 is designed using the methods specified in and operated within the Core Operating Limits Report limits developed from Topical Reports BAW-10164P-A, Revision 4, and BAW-10241P, Revision 0, in addition to those methods allowed by Improved Technical Specification 5.6.2.18.~~

5.6 Procedures, Programs and Manuals

5.6.2.18 COLR (continued)

LCO 3.2.3 AXIAL POWER IMBALANCE Operating Limits
LCO 3.2.4 QUADRANT POWER TILT
LCO 3.2.5 Power Peaking Factors
LCO 3.3.1 Reactor Protection System (RPS) Instrumentation
SR 3.4.1.1 Reactor Coolant System Pressure DNB Limits
SR 3.4.1.2 Reactor Coolant System Temperature DNB Limits
SR 3.4.1.3 Reactor Coolant System Flow DNB Limits
LCO 3.9.1 Boron Concentration

b. The analytical methods used to determine the core operating limits shall be those previously reviewed and approved by the NRC:

BAW-10179P-A, "Safety Criteria and Methodology for Acceptable Cycle Reload Analyses" (the approved revision at the time the reload analyses are performed) and License Amendment 144, SER dated June 25, 1992. The approved revision number for BAW-10179P-A shall be identified in the COLR.

ANP-2788P, "Crystal River 3 Rod Ejection Accident Methodology Report," Revision 0, and License Amendment , SER dated Month Day, 2009.

c. The core operating limits shall be determined such that all applicable limits (e.g., fuel thermal mechanical limits, core thermal hydraulic limits, Emergency Core Cooling System (ECCS) limits, nuclear limits such as SDM, transient analysis limits, and accident analysis limits) of the safety analysis are met.

d. The COLR, including any midcycle revisions or supplements, shall be provided upon issuance for each reload cycle to the NRC.

5.6.2.19 Reactor Coolant System (RCS) PRESSURE AND TEMPERATURE LIMITS REPORT (PTLR)

a. Other Applicable ITS:

3.4.3 RCS P/T Limits
3.4.11 Low Temperature Overpressure Protection

b. RCS pressure and temperature limits, including heatup and cooldown rates, criticality, and hydrostatic and leak test limits, shall be established and documented in the PTLR. The analytical methods used to determine the pressure and temperature limits including the heatup and cooldown rates shall be those previously reviewed and approved by the NRC in BAW-10046A, Rev. 2, "Methods of Compliance With Fracture Toughness and Operational Requirements of 10 CFR 50, Appendix G," June 1986. The analytical method used to determine vessel fluence shall be those reviewed by the NRC and documented in BAW-2241P, May 1997. The analytical method used to determine LTOP limits shall be those previously reviewed by the NRC based on ASME Code Case N-514. The Materials Program is in accordance with BAW-1543A, "Integrated Reactor Vessel Surveillance Program."

(continued)

PROGRESS ENERGY FLORIDA, INC.

CRYSTAL RIVER UNIT 3

DOCKET NUMBER 50-302/LICENSE NUMBER DPR-72

LICENSE AMENDMENT REQUEST #307, REVISION 0

ATTACHMENT C

PROPOSED IMPROVED TECHNICAL SPECIFICATION PAGE CHANGES

REVISION BAR FORMAT

2.C.(6) Deleted per Amendment No. 21, 7-3-79

2.C.(7) Prior to startup following the first regularly scheduled refueling outage, Florida Power Corporation shall modify to the satisfaction of the Commission, the reactor coolant system flow indication to meet the single failure criterion with regard to pressure sensing lines to the flow differential pressure transmitters.

2.C.(8) Within three months of issuance of this license, Florida Power Corporation shall submit to the Commission a proposed surveillance program for monitoring the containment for the purpose of determining any future delamination of the dome.

2.C.(9) Fire Protection

Florida Power Corporation shall implement and maintain in effect all provisions of the approved fire protection program as described in the Final Safety Analysis Report for the facility and as approved in the Safety Evaluation Reports, dated July 27, 1979, January 22, 1981, January 6, 1983, July 18, 1985, and March 16, 1988, subject to the following provisions:

The licensee may make changes to the approved fire protection program without prior approval of the Commission only if those changes would not adversely affect the ability to achieve and maintain safe shutdown in the event of a fire. *{Amdt. #147, 1-22-93}*

2.C.(10) The design of the reactor coolant pump supports need not include consideration of the effects of postulated ruptures of the primary reactor coolant loop piping and may be revised in accordance with Florida Power Corporation's amendment request of April 24, 1986. *{Added per Amdt. #89, 5-23-86}*

2.C.(11) A system of thermocouples added to the decay heat (DH) drop and Auxiliary Pressurizer Spray (APS) lines, capable of detecting flow initiation, shall be operable for Modes 4 through 1. Channel checks of the thermocouples shall be performed on a monthly basis to demonstrate operability. If either the DH or APS system thermocouples become inoperable, operability shall be restored within 30 days or the NRC shall be informed, in a Special Report within the following fourteen (14) days, of the inoperability and the plans to restore operability. *{Amdt. #164, 1-27-98}*

2.C.(12) Deleted per Amendment No.

5.6 Procedures, Programs and Manuals

5.6.2.18 COLR (continued)

LCO 3.2.3 AXIAL POWER IMBALANCE Operating Limits
LCO 3.2.4 QUADRANT POWER TILT
LCO 3.2.5 Power Peaking Factors
LCO 3.3.1 Reactor Protection System (RPS) Instrumentation
SR 3.4.1.1 Reactor Coolant System Pressure DNB Limits
SR 3.4.1.2 Reactor Coolant System Temperature DNB Limits
SR 3.4.1.3 Reactor Coolant System Flow DNB Limits
LCO 3.9.1 Boron Concentration

b. The analytical methods used to determine the core operating limits shall be those previously reviewed and approved by the NRC:

BAW-10179P-A, "Safety Criteria and Methodology for Acceptable Cycle Reload Analyses" (the approved revision at the time the reload analyses are performed) and License Amendment 144, SER dated June 25, 1992. The approved revision number for BAW-10179P-A shall be identified in the COLR.

ANP-2788P, "Crystal River 3 Rod Ejection Accident Methodology Report," Revision 0, and License Amendment , SER dated

c. The core operating limits shall be determined such that all applicable limits (e.g., fuel thermal mechanical limits, core thermal hydraulic limits, Emergency Core Cooling System (ECCS) limits, nuclear limits such as SDM, transient analysis limits, and accident analysis limits) of the safety analysis are met.

d. The COLR, including any midcycle revisions or supplements, shall be provided upon issuance for each reload cycle to the NRC.

5.6.2.19 Reactor Coolant System (RCS) PRESSURE AND TEMPERATURE LIMITS REPORT (PTLR)

a. Other Applicable ITS:

3.4.4 RCS P/T Limits
3.4.11 Low Temperature Overpressure Protection

b. RCS pressure and temperature limits, including heatup and cooldown rates, criticality, and hydrostatic and leak test limits, shall be established and documented in the PTLR. The analytical methods used to determine the pressure and temperature limits including the heatup and cooldown rates shall be those previously reviewed and approved by the NRC in BAW-10046A, Rev. 2, "Methods of Compliance With Fracture Toughness and Operational Requirements of 10 CFR 50, Appendix G," June 1986. The analytical method used to determine vessel fluence shall be those reviewed by the NRC and documented in BAW-2241P, May 1997. The analytical method used to determine LTOP limits shall be those previously reviewed by the NRC based on ASME Code Case N-514. The Materials Program is in accordance with BAW-1543A, "Integrated Reactor Vessel Surveillance Program."

(continued)

PROGRESS ENERGY FLORIDA, INC.

CRYSTAL RIVER UNIT 3

DOCKET NUMBER 50-302/LICENSE NUMBER DPR-72

LICENSE AMENDMENT REQUEST #307, REVISION 0

ATTACHMENT D

Affidavit for Withholding Proprietary Information from Public Disclosure

AFFIDAVIT

COMMONWEALTH OF VIRGINIA)
) ss.
CITY OF LYNCHBURG)

1. My name is Gayle F. Elliott. I am Manager, Product Licensing, for AREVA NP Inc. and as such I am authorized to execute this Affidavit.

2. I am familiar with the criteria applied by AREVA NP to determine whether certain AREVA NP information is proprietary. I am familiar with the policies established by AREVA NP to ensure the proper application of these criteria.

3. I am familiar with the AREVA NP information contained in the report, ANP-2788P, Revision 0, "Crystal River 3 Rod Ejection Accident Methodology Report," dated February 2009, and referred to herein as "Document." Information contained in this Document has been classified by AREVA NP as proprietary in accordance with the policies established by AREVA NP for the control and protection of proprietary and confidential information.

4. This Document contains information of a proprietary and confidential nature and is of the type customarily held in confidence by AREVA NP and not made available to the public. Based on my experience, I am aware that other companies regard information of the kind contained in this Document as proprietary and confidential.

5. This Document has been made available to the U.S. Nuclear Regulatory Commission in confidence with the request that the information contained in this Document be withheld from public disclosure. The request for withholding of proprietary information is made in accordance with 10 CFR 2.390. The information for which withholding from disclosure is

requested qualifies under 10 CFR 2.390(a)(4) "Trade secrets and commercial or financial information."

6. The following criteria are customarily applied by AREVA NP to determine whether information should be classified as proprietary:

(a) The information reveals details of AREVA NP's research and development plans and programs or their results.

(b) Use of the information by a competitor would permit the competitor to significantly reduce its expenditures, in time or resources, to design, produce, or market a similar product or service.

(c) The information includes test data or analytical techniques concerning a process, methodology, or component, the application of which results in a competitive advantage for AREVA NP.

(d) The information reveals certain distinguishing aspects of a process, methodology, or component, the exclusive use of which provides a competitive advantage for AREVA NP in product optimization or marketability.

(e) The information is vital to a competitive advantage held by AREVA NP, would be helpful to competitors to AREVA NP, and would likely cause substantial harm to the competitive position of AREVA NP.

The information in the Document is considered proprietary for the reasons set forth in paragraphs 6(b) and 6(c) above.

7. In accordance with AREVA NP's policies governing the protection and control of information, proprietary information contained in this Document have been made available, on a limited basis, to others outside AREVA NP only as required and under suitable agreement providing for nondisclosure and limited use of the information.

8. AREVA NP policy requires that proprietary information be kept in a secured file or area and distributed on a need-to-know basis.

9. The foregoing statements are true and correct to the best of my knowledge, information, and belief.

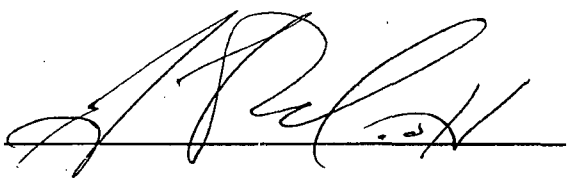

SUBSCRIBED before me this 16th
day of February 2009.

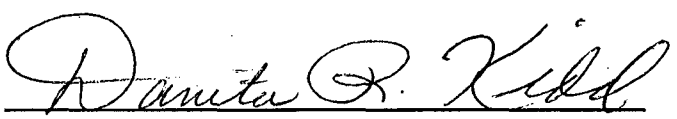

Danita R. Kidd
NOTARY PUBLIC, STATE OF VIRGINIA
MY COMMISSION EXPIRES: 12/31/12
Reg. # 205569

DANITA R. KIDD
Notary Public
Commonwealth of Virginia
Comm. Expires 12-31-12
Registration # 205569

PROGRESS ENERGY FLORIDA, INC.

CRYSTAL RIVER UNIT 3

DOCKET NUMBER 50-302/LICENSE NUMBER DPR-72

LICENSE AMENDMENT REQUEST #307, REVISION 0

ATTACHMENT F

ANP-2788NP, REVISION 0
Crystal River 3 Rod Ejection Accident Methodology Report

(non-Proprietary)

AREVA

ANP-2788NP
Revision 0

Crystal River 3 Rod Ejection Accident Methodology Report

February 2009

AREVA NP Inc.

Nature of Changes

Item	Section(s) or Page(s)	Description and Justification
Original Issue	NA	NA

Contents

List of Tables

List of Figures

Nomenclature

Acronym	Definition
β_{eff}	Beta effective (effective total delayed neutron fraction)
BOC	Beginning Of Cycle
BOL	Beginning Of Life (of a fuel rod)
cal/g	Calories per gram
CG/CP	Constant Gap/Constant Properties
CG/TDP	Constant Gap/Temperature Dependent Properties
CHF	Critical Heat Flux
DNBR	Departure From Nucleate Boiling Ratio
DTC	Doppler Temperature Coefficient
EOC	End Of Cycle
EOL	End Of Life (of a fuel rod)
FGR	Fission Gas Release
FGRF	Fission Gas Release Failures
FOP	Fraction Of Power
$F_{\Delta H}$	Peak rod power (in the core)
F_Q	Peak local power (in the core)
Gd_2O_3	Gadolinium Oxide
GWD/MTU	GigaWatt Days per Metric Ton Uranium
HCF	Hot Channel Factor
HFP	Hot Full Power
HZP	Hot Zero Power
IR	Importance Ratios
KR	Knowledge Ratios
LCO	Limiting Conditions for Operation
LHGR	Linear Heat Generation Rate
LOCA	Loss-Of-Coolant Accident
MDNBR	Minimum Departure from Nucleate Boiling Ratio
MTC	Moderator Temperature Coefficient
NEACRP	Nuclear Energy Agency Committee on Reactor Physics
pcm/°F	PerCent Milli-rho per degree Fahrenheit
PCMI	Pellet Cladding Mechanical Interaction
PIRT	Phenomena Importance Ranking Tables

Acronym	Definition
REA	Rod Ejection Accident
RIA	Reactivity Initiated Accident
SA	Safety Analysis
SAFDL	Specified Acceptable Fuel Design Limit
SRSS	Square Root Sum of the Squares
TFGR	Transient Fission Gas Release
T-H	Thermal Hydraulics
TS	Technical Specifications
μm	Micrometers
UO_2	Uranium Dioxide
VG/TDP	Variable Gap/Temperature Dependent Properties
VLPT	Variable Low Pressure Trip
w/o	Weight percent
2-D	Two Dimensional
3-D	Three Dimensional

1.0 INTRODUCTION

The methodology to analyze the rod ejection accident (REA) for Crystal River 3 is presented in this report. The methodology includes the use of a nodal 3-D kinetics solution with both thermal-hydraulic (T-H) and fuel temperature feedback and a separate peak rod thermal evaluation with an open channel T-H and fuel thermal model. These models provide more precise localized neutronic and thermal conditions than previous methods to show compliance with the interim Reactivity Initiated Accident (RIA) criteria in the SRP Section 4.2 (Reference 1). The boundary conditions and uncertainty values are defined for the REA methodology. The overall REA sample problem results for Crystal River 3 are within the limiting criteria for this REA methodology, with maximum Δcal/g less than 125 and failures less than 4.3 percent of the rods in the core. This report presents the REA regulatory requirements, followed by the code and model requirements, Crystal River 3 methodology, computer codes, application of boundary conditions and uncertainties, sample problem results, and conclusions.

2.0 REA REGULATORY REQUIREMENTS

The first step of the methodology is to choose the regulatory requirements to define the specific criteria that the REA analysis will meet. This methodology uses the requirements in Reference 1 for cladding failure, core coolability, and radiological consequences. This section defines the specific criteria that the REA analysis sample problem will meet. The requirements for radiological assessment and the maximum system pressure are not addressed by this methodology.

2.1 Cladding Failure

Reference 1 contains several criteria to determine whether the cladding is assumed failed. The failure criteria to be assumed for Crystal River 3 are provided for pellet cladding mechanical interaction (PCMI), total energy deposition, and departure from nucleate boiling ratio (DNBR). Each rod is examined to determine whether it has exceeded any of these criteria and is considered failed if it does.

2.1.1 PCMI Criteria for M5™ Cladding

The prompt PCMI cladding failure criteria (the change in radial average fuel enthalpy) for M5™ Cladding is based on Figure B-1 from Reference 1. The maximum corrosion expected for Crystal River 3 fuel cladding with M5™ at end of life is less than 33 μm. This oxide thickness is based on a conservative COPERNIC (Reference 2) analysis for a limiting rod using a bounding rod power history at burnups in excess of 62 GWD/MTU. The basis of this corrosion model is described in Section 8.1.3.2 of Reference 2. The corresponding oxide to wall thickness ratio is 0.052, which leads to a conservative PCMI failure limit of 125 cal/g.

The maximum prompt energy deposition in the REA simulations is shown to be less than 125 cal/g for all burnups. Hence, no cladding failures occur based on the PCMI criteria for all initial power levels from hot zero power (HZP) to hot full power (HFP).

In order to calculate the fuel enthalpy rise to assess PCMI failures, the prompt fuel enthalpy rise is defined as the radial average fuel enthalpy increase (Δcal/g) from the initial conditions to the time corresponding to one pulse width after the peak of the prompt pulse. The pulse width is defined as the time width of the power pulse at half the maximum power.

2.1.2 Cladding Failure Due to Total Energy Deposition

The peak radial average fuel enthalpy is shown to be less than 150 cal/g, which is the limit in Reference 1 for fuel rods above system pressure and powers less than or equal to 5 percent. It also is more conservative than the value of 170 cal/g for fuel rods below system pressure. The 150 cal/g limit is used for REA simulations beginning at powers less than or equal to 5 percent.

2.1.3 DNBR

For REA simulations beginning at powers greater than 5 percent rated thermal power, fuel cladding failure is assumed if the cladding surface heat flux exceeds the thermal design limits for MDNBR.

2.2 Coolability

The coolability requirements from Reference 1 are as follows:

1. Peak radial average fuel enthalpy must remain below 230 cal/g.
2. Peak fuel temperature must remain below incipient fuel melting conditions.
3. Mechanical energy generated as a result of (1) non-molten fuel-to-coolant interaction and (2) fuel rod burst must be addressed with respect to reactor pressure boundary, reactor internals, and fuel assembly structural integrity.
4. No loss of coolable geometry due to (1) fuel pellet and cladding fragmentation and dispersal and (2) fuel rod ballooning.

From conditions set forth in Sections 2.1.1 and 2.1.2, energetic ejection of fuel into the coolant is prevented by preserving the cladding integrity during high energy deposition pulses by staying below the cladding and fuel cal/g limits and below the fuel melt temperature.

Coolability for fuel rods undergoing DNB (DNBR failures) is established by limiting rod heatup during post critical heat flux (CHF). If the rod does not heatup enough to rupture, there are no coolability issues. For internal rod pressures above system pressure, rupture and significant ballooning are unlikely if the maximum cladding temperature is below [ ]. For internal rod pressures below system pressure, ballooning failures are not possible. For this sample problem, coolability is maintained by precluding PCMI failures, maximum total enthalpies above 150 cal/g, fuel melt, and maximum cladding temperatures greater than [ ].

2.3 Radiological Consequences

The radiological consequence evaluation associated with the postulated REA is defined outside of this methodology. A conservatively low estimate of the allowed failures of 4.3 percent of the rods in the core is used for this sample problem. The radiological consequences could be more severe for failed pins that experience high local energy depositions during an REA causing transient fission gas release. The formula in Section D of Reference 1 is used to increase the fission product gap activity for those rods that fail and is shown below.

$$TFGR = (0.2286 \times \Delta H) - 7.1419$$

where:

TFGR = Transient Fission Gas Release, percent (must be ≥ 0)

ΔH = Increase in prompt fuel enthalpy, Δcal/g

The gap activity of the axial node rod segments experiencing delta prompt fuel enthalpies greater than 31.2 cal/g ($\Delta H = 31.2$ when TFGR = 0) will increase by the

above equation. The radiological consequences will incorporate two relative source terms for rods that fail due to DNBR during the REA event. The radiological consequences can be simplified to a function of the equivalent number of rods failed and can be represented by the following equation.

$$EQP = F + FGRF \leq A$$

where:

EQP = Equivalent number of rods failed

F = Total number of rods failed due to DNBR

FGRF = Equivalent number of additional rods failed due to Transient Fission Gas Released from high Δcal/g

A = Maximum allowed number of rods that could fail due to only DNBR failures and stay within the dose limits.

For example, if the base release inventory for a fuel rod failure exceeding DNBR is 10 percent FGR and the enthalpy rise of the pin yields a TFGR of 5 percent, then for this fuel rod, the total fission gas release would be 15 percent. This amount of release is equivalent to 1.5 failures for the value of EQP for this pin rather than 1.0. This calculation would be repeated for all fuel rods that have an enthalpy rise greater than 31.2 Δcal/g. The sum of the individual rod EQPs is then compared against the value of A.

2.4 Licensing Criteria for Crystal River 3

The conditions in Table 2-1 define the limits to be met for Crystal River 3.

Table 2-1 REA Limits for Crystal River 3

Criterion Description	Limit
Peak radial average fuel enthalpy for initial core powers ≤5%	≤150 cal/g
Maximum energy deposition during prompt power pulse for initial core powers ≤5%	≤125 Δcal/g
Fuel Failure criterion for initial core powers > 5%	DNBR < Design Limit
Fuel Melt for all core power levels	= 0%
Maximum Cladding Temperature for all core power levels	[ ]
After power pulse, number of equivalent rods failed due to DNBR	≤ 4.3% *

Notes:

* Conservatively low estimate is assumed for sample problem.

3.0 COMPUTER CODE REQUIREMENTS

The use of a nodal 3-D kinetics solution with both T-H and fuel temperature feedback and a peak rod thermal evaluation model with an open channel T-H and fuel thermal model are required. The requirement for the computational codes is that they are qualified and approved by the U.S. NRC for time-dependent solutions.

In general, a fuel performance model will provide the thermal properties for the fuel, gap and clad. The 3-D neutronic solution with T-H feedback will calculate the core power and the local power distribution response to an ejected rod. This information will then be used by an open channel T-H and fuel thermal code to calculate the fuel enthalpy, the temperature distributions, and the DNBR for the peak rod in the core. If the peak rod fails due to DNBR, the open channel T-H code is also used to establish the power conditions at which a rod will fail to determine radiological consequences. A T-H system code is used to establish reactor system conditions with time such as pressure, flow, and inlet temperature. The boundary conditions and uncertainties used in the codes for the REA simulation are addressed in Section 4.0.

4.0 MODEL BOUNDARY CONDITIONS AND UNCERTAINTIES REQUIREMENTS

This section addresses the boundary conditions and uncertainties considered for the REA. The analysis can be divided into two parts, the plant transient analysis and the fuel rod transient analysis as defined in the Phenomenon Identification and Ranking Tables (PIRT) in Reference 3. For ease of reference the list of the phenomena, their importance ratio and knowledge ratio from Reference 3 is presented in Table 4-1 for the plant transient analysis.

A similar list is presented in Table 4-2 for fuel and cladding temperatures. Many of the items included in Table 3-3 in Reference 3 are not included in Table 4-2 because they are captured by a cal/g limit or have little relevance to a DNBR limit. The items that are categorized relative to "PCMI loading to cladding" effects are captured by the cal/g failure limit. The gap size, gas pressure, gas composition, gas distribution, fuel-cladding gap friction coefficient and rod volume are essentially captured in the context of gap conductance. The hydrogen concentration, hydrogen distribution, and spallation effects on the cladding are captured in the cal/g failure limit. Fast fluence, porosity, rim size, bubble size, and bubble distribution are captured by the fuel pellet conductivity and/or the cal/g limit. Therefore, these items are not included in Table 4-2.

Reference 3 states that the phenomena with importance ratios above 75 are important and those with knowledge ratios above 75 are well known. It also warns that parameters near the threshold should not necessarily be ignored. Additional parameters address impacts on DNBR since the scope of Reference 3 was primarily concerned with PCMI type failures and not DNBR. Each of the parameters are addressed with respect to the requirements for modeling relative to the need to bound, apply uncertainty, or to demonstrate a negligible consequence. This section provides a general discussion of the parameters that are to be examined and Section 7.0 examines the parameters with sensitivity calculations.

4.1 Plant Transient Analysis

The plant transient analysis is dominated during the first 5-10 seconds (less than the loop time) by the core kinetics, nodal fuel temperatures, and nodal T-H conditions. Inlet temperature, core pressure, and flow are relatively constant during an REA so that the 3-D core kinetics can be used with, or independently of, a system T-H code. The results and dependencies of a 3-D kinetics solution are identical to a point kinetics solution for uniform changes to a core. The difference in the two solutions is the local weighting of the changes that occur, which become very important during an REA. Therefore, many of the dependencies of the parameters from the point kinetics models remain applicable to 3-D kinetics. Since a static reactivity calculation provides a 3-D weighting of the core effects, standard static methods to calculate reactivity coefficients, delayed neutron fractions, and rod worths can be used to evaluate the initial conditions for the sensitivities. This section is a review of the parameters listed in Table 4-1 relative to 3-D kinetics and other effects that could impact the results.

4.1.1 Maximum Ejected Rod Worth

The maximum ejected rod worth is a limiting parameter and is the driver for the event. It is integral to the neutronic nodal simulator solution through the input of the initial insertion of the rod bank(s) and the control rod cross sections. The worth is not a direct input and is calculated using standard static methods with moderator temperature and fuel temperature held constant. The worth depends on fuel cycle design, cycle lifetime, and initial xenon conditions. The initial conditions are required to be a reasonable representation of the limiting conditions allowed by Technical Specifications that maximize the worth. In addition, an uncertainty is applied that is equal to or greater than the approved uncertainty value. Additional conservatisms can be applied to bound future fuel cycle designs.

4.1.2 Rate of Reactivity Insertion

Rate of reactivity insertion is not rated as an important parameter for prompt critical rod ejections. A sensitivity calculation is performed to confirm the impact for the range of conditions analyzed.

4.1.3 Moderator Feedback

Moderator feedback (i.e., Moderator Temperature Coefficient, (MTC)) is not rated as an important parameter relative to the power pulse. However, the MTC does affect the power after the pulse, which can affect DNBR. The MTC is not a direct input to the neutronics computer code and is required to be adjusted to represent an uncertainty.

4.1.4 Fuel Temperature Feedback

The fuel temperature feedback (i.e., Doppler Temperature Coefficient, (DTC)) terminates the prompt critical power excursion and is an important parameter. The DTC is calculated using standard static methods with moderator temperature held constant. The DTC is dependent upon core design and cycle lifetime. The magnitude of DTC is conservatively reduced by the uncertainty.

4.1.5 Delayed Neutron Fraction

For a given reactivity insertion, the sensitivity of total delayed neutron fraction (β_{eff}) is addressed from a point kinetics viewpoint. The β_{eff} determines the rate of neutron flux change from an initial static condition. The higher the reactivity relative to β_{eff}, the faster the flux increases. For reactivity insertions less than β_{eff}, a higher reactivity will increase the prompt jump and decrease the subsequent doubling time. When the reactivity insertion exceeds β_{eff}, the core becomes critical on prompt neutrons and the doubling time can decrease by more than an order of magnitude. For step reactivity insertions as with an REA, a low β_{eff} results in higher core powers. Therefore, the β_{eff} is lowered by the uncertainty for the cases where fast increases are limiting.

4.1.6 Reactor Trip Reactivity

For prompt critical excursions, the power excursion is terminated by the DTC and the core returns to a much lower power level. Also, the excore high flux trip is reached shortly after the rod is ejected. After the DTC terminates the pulse, the core power flattens with time until the rods are inserted from the reactor trip. The reactor trip reactivity reduces the core power to shutdown conditions. The Phenomena Importance Ranking Tables (PIRT) analysis correctly rates reactor trip reactivity as zero importance for the prompt power pulse. However, the severity of the departure from nucleate boiling (DNB) response may be affected by the timing of the power reduction due to the insertion of the rods. The trip reactivity sensitivity could be important for the "at power" cases where a trip limits the amount of time the core is at elevated powers and can limit the core damage due to potential DNBR failures. The timing of the trip is also important relative to the excore response of the detectors to the asymmetric flux caused by the ejected rod. As with the ejected rod worth, the trip reactivity is not an input quantity to the 3-D kinetics calculations. The reactivity effects of the rods are dynamically calculated based on their position with time. It can be adjusted by changing the amount of banks inserted prior to the accident, the control rod cross sections, and the trip time parameters. The sensitivity of the trip reactivity to the "at power" events is used to determine the level of conservatisms required.

4.1.7 Fuel Cycle Design

Most of the fuel cycle design dependencies are captured by examining the beginning of cycle (BOC) and end of cycle (EOC) behavior on ejected rod worth, β_{eff}, DTC, MTC, and peaking. The fuel cycle design can also influence the proximity of the high burnup rods to the ejected rod location. When burnup dependent limits are used, a lower ejected rod worth in the proximity of high burnup assemblies could be more limiting than a higher worth rod in the proximity of lower burnup assemblies. More than the maximum ejected rod location is evaluated for burnup dependent limits if they are used. These fuel cycle design elements are addressed in Section 7.1.5.

4.1.8 Heat Resistances and Transient Cladding to Coolant Heat Transfer

The heat resistances and transient cladding to coolant heat transfer are not viewed as sensitive parameters to the ejected rod event and sensitivity calculations are used to confirm this conclusion. The heat resistances comprise the thermal conductivity of the fuel and cladding, and the gap conductance. Nominal gap conductance values can vary by more than a factor of ten for an open gap between the fuel pellet and cladding versus a closed gap.

4.1.9 Heat Capacities

The heat capacity is rated as an important parameter in Reference 3. The heat capacity determines how much the fuel temperature increases as the energy is deposited into the fuel; therefore, the energy deposited is proportional to the heat capacity and the temperature increase. For prompt critical power excursions, the point kinetics equations can be approximated by the following analytical equation representing the energy deposition:

$$ED = \frac{2(\rho - \beta) \cdot C_p}{DTC}$$

where:

ED = Energy Deposition

ρ = Step Reactivity Change

β = Beta Effective

C_p = Heat Capacity of the Fuel

DTC = Doppler Temperature Coefficient

This equation shows the dependence of the energy deposition on heat capacity. If the temperature is the parameter of interest, then the delta temperature reached from an energy deposition with no heat loss can be represented as follows:

$$\Delta T = ED / C_p$$

where:

ΔT = Temperature rise

Substituting the first equation yields:

$$\Delta T = \frac{2 \cdot (\rho - \beta)}{DTC}$$

The temperature increase from the power excursion with a step change in reactivity is not a function of heat capacity of the fuel when controlled by Doppler. For slow transients near static conditions ($\rho << \beta$), the fuel temperature is dominated by the heat resistance of the rods. Therefore, for fuel temperature predictions, heat capacity is not an important parameter.

Reference 4 is considered a standard for defining heat capacity for UO_2. The variation of the UO_2 heat capacity is only a function of temperature. As long as the heat capacity is used consistently in analysis codes and in the experiments that were used to set the limits, consistent results are obtained. No error estimate or special treatment is used for the UO_2 heat capacity.

4.1.10 Fractional Heat Deposited in Pellet

The fraction of heat deposited in the coolant can affect the relative amount of direct heating of the water and the fuel. The different prompt temperatures of the water and the fuel can result in different feedback between the MTC and DTC during a power pulse. The direct heating of the coolant could have an impact on the results since MTC can vary from small positive to large negative values from BOC to EOC conditions,

respectively. A constant fraction of direct heating of the coolant is used throughout the transient because it has few or no dependencies upon other core parameters. A sensitivity calculation is used to determine its importance.

4.1.11 Pellet Radial Power Distribution

The pellet radial power distribution could affect the rate of energy transferred from the fuel pellet to the coolant or it could affect the weighting of the pellet temperature distribution on the DTC. This power profile has very weak dependencies on other core parameters. A sensitivity calculation is used to determine its importance.

4.1.12 Rod Peaking Factors

The rod peaking factors are important relative to the weighting of the local powers to the overall core reactivity as well as the local energy deposition during the power pulse. As with the ejected rod worth, the rod peaking is not an input quantity to the 3-D kinetics calculations. If the peaking factors increased, the local fuel temperatures would increase so that the Doppler response would lower the core power. Therefore, the peaking factors that are used in the kinetics calculation are best estimate and the peaking factors for the fuel rod thermal model are conservatively increased by the expected uncertainties.

4.1.13 Neutron Velocities

Since the dominant fission reactions occur with thermal neutrons, the thermal neutron velocities determine the rate at which the neutrons multiply. The mean generation time in point kinetics is calculated based on the neutron velocities. The impact of neutron velocities on the REA energy deposition is negligible because the energy deposition in the first equation in Section 4.1.9 is not a function of mean generation time. However, the pulse width is roughly inversely proportional to the thermal neutron velocity and narrow pulse widths could become more important when evaluating potential coolability concerns when PCMI failures occur. Since this methodology shows that energy deposition is below the cal/g for PCMI failure criteria for M5™, the neutron velocity is not a key parameter.

4.1.14 System T-H Conditions

The kinetics solution can be affected by changes in inlet temperature, pressure, and flow. The longer the transient is modeled (greater than 5 seconds) the more the system T-H conditions can influence the neutronic kinetic solution. It is expected that prompt critical excursions will not be affected by the system T-H conditions since the maximum power deposition and maximum fuel temperatures are reached in less than a second. Non-prompt excursions may require modeling for more than a few seconds. Sensitivity calculations are performed to assess these impacts.

4.2 Fuel Rod Transient Model for Fuel and Cladding Temperatures and DNBR

The fuel and cladding temperatures are dominated by the initial temperatures and the energy deposition versus time. Similar to the previous section, inlet temperature, core pressure, and flow are relatively constant and the fuel rod transient model can be used independently of a system T-H code. The discussion in this section is a review of the parameters listed in Table 4-2 relative to the fuel rod transient model for fuel and cladding temperatures. Additional parameters address impacts on DNBR since the scope of Reference 3 was primarily concerned with PCMI type failures and not DNBR.

4.2.1 Pellet and Cladding Dimensions

Pellet and cladding dimensions are considered important and well known. Nominal dimensions and application of the uncertainty for manufacturing allowances are appropriate. Approximations of the full core geometry model surrounding the limiting rod can affect the results. These approximations are shown to be appropriate for the REA analysis.

4.2.2 Burnup Distribution

The local rod radial burnup distribution is rated as a relatively low importance parameter and a homogenized pellet is acceptable.

4.2.3 Cladding Oxidation

The cladding oxidation is rated as a relatively low importance parameter and can be modeled on a best estimate basis or ignored.

4.2.4 Power Distribution

The power distribution is assumed to be the radial pellet power distribution and is weighted as an important parameter. The conditions that do change during a REA transient do not affect the radial pellet power profile. The radial pellet power profile is a strong function of pellet burnup and uranium enrichment. These two conditions are not affected by transient behavior. The burnup determines the amount of plutonium created in the rim of the pellet from U-238 resonance absorptions. At high burnups, the rim power can be twice as high as the average pellet power. The initial enrichment also has an effect, but it is less pronounced. Initially, the higher enrichment has a slightly higher surface power because of the higher self shielding of thermal flux. As the plutonium is created on the rim, the plutonium power fraction is less in a higher enrichment pellet, and the surface power is smaller than a lower enriched pellet at the same burnup. The initial enrichment and burnup for the pellet are initial conditions for the transient and the pellet radial power profile remains fixed during the transient. A typical or bounding fuel performance power history from an approved fuel performance code can provide this information and is acceptable for the REA. Sensitivity calculations are used to define the impact of this parameter.

4.2.5 Initial Coolant Conditions

Initial coolant conditions for inlet temperature, flow and pressure are defined by the initial power level and operational mode. These parameters are already defined conservatively for other safety analyses. Existing methods are applicable.

4.2.6 Transient Power Specification

The transient core power and peaking factors are defined by the results generated from the plant transient analysis, which also includes the initial power distributions. The

uncertainties applied to the REA power distributions are consistent with the current uncertainties applied for $F_{\Delta H}$ and F_Q for other accidents. Initial distributions are representative of the worst conditions allowed by Technical Specifications. The uncertainties of the power peaking factors are addressed.

4.2.7 Heat Resistances in Fuel, Gap, and Cladding

A typical or bounding fuel performance power history from an approved fuel performance code can provide the heat resistances in fuel, gap, and cladding, and is acceptable for the REA. Sensitivity calculations are used to define the bounding conditions. Decreased thermal conductivity can increase the maximum fuel temperature but reduce the heat flux which increases DNBR. Therefore, two calculations modeling the limiting direction of the resistances are needed. One is used for maximum fuel temperature prediction and the other to predict MDNBR.

4.2.8 Transient Cladding-to-Coolant Heat Transfer Coefficient

The importance of the cladding to coolant heat transfer coefficient for prompt critical power excursions is rated of little importance. However, because the present methodology treats DNBR as a fuel failure criterion, transient cladding-to-coolant heat transfer becomes an important parameter. Transient heat transfer and critical heat flux (CHF) are not as well understood as static CHF. In general, the application of the static heat transfer, CHF, and failure when exceeding MDNBR is considered conservative for rapidly changing conditions that is supported by Reference 7. Therefore, the use of existing approved T-H codes, CHF correlations, and MDNBR cladding failure criterion is considered acceptable.

4.2.9 Heat Capacities of Fuel and Cladding

The heat capacity of UO_2 is primarily dependent upon temperature. Therefore, the local rod model requirement for heat capacity is the same as that used in the plant transient model. Section 4.1.9 addresses the heat capacity as a non-critical parameter for REA when predicting temperatures and no uncertainty is needed.

4.2.10 Coolant Conditions

The transient water temperatures, local flows, and pressure are important to estimate fuel and cladding temperatures and DNBR of the fuel rods. An approved T-H computer code with time dependent capability is used with the approved uncertainties defined for licensing.

4.2.11 System T-H Conditions

The inlet temperature, core flow, and system pressure can affect the fuel rod transient analysis. The longer the transient is modeled (greater than 5 seconds) the more the system T-H conditions can impact the transient fuel rod model. Prompt critical excursions will not be impacted by the system T-H conditions because the maximum power deposition and maximum fuel temperatures are reached in less than a second. Non-prompt excursions may require modeling for more than a few seconds and the impact of plant conditions on the overall results is evaluated.

4.3 Time Dependent Analysis

The sensitivity of the time dependent calculations to time step meshing is addressed.

4.4 Failure Analysis

There are many ways to count the number of rod failures. The failure criteria defined for this methodology in Section 2.1.3 is used. Rod by rod explicit analysis is acceptable. Rod by rod explicit analysis models the power versus time of every rod and counts each rod that has a DNBR less than the design limit as failed. Also, setting a conservative value for $F_{\Delta H}$ and F_Q and counting any rod above either value as a rod failed is acceptable.

Section 1.C.iv of Reference 1 requests examination of DNB failure propagation due to ballooning. Since the peak radial average fuel enthalpy is less than 150 cal/g and the maximum cladding temperature is less than [ ], ballooning failure is precluded. In addition, the DNB propagation impact on fuel failure for dose calculations is assessed. Exceeding a 95/95 tolerance/confidence limit on DNBR is conservative as a

failure criterion. If the number of rods is statistically counted, only 5 percent or less of the rods having powers equal to the criteria would be failed. The 5 percent of the rods that are at the failure criterion is far less than assuming all the rods failed as defined by this methodology. Therefore, no additional DNBR propagation of failures needs to be considered for dose.

Table 4-1 PIRT Plant Transient Analysis

Subcategory	Phenomenon	IR*	KR**
Calculation of power history during pulse (includes pulse width)	Ejected control rod worth	100	100
	Rate of reactivity insertion	61	88
	Moderator feedback	38	93
	Fuel temperature feedback	100	96
	Delayed-neutron fraction	95	96
	Reactor trip reactivity	0	96
	Fuel cycle design	92	100
Calculation of rod fuel enthalpy increase during pulse (includes cladding temperature)	Heat resistances in high burnup fuel, gap, and cladding (including oxide layer)	58	67
	Transient cladding-to-coolant heat transfer coefficient	56	64
	Heat capacities of fuel and cladding	94	90
	Fractional energy deposition in pellet	4	93
	Pellet radial power distribution	63	88
	Rod-peaking factors	97	100

Notes:
* Importance Ratio IR>75 Important
**Knowledge Ratio KR<75 Not completely understood

Table 4-2 PIRT Fuel Rod Transient Analysis for Fuel and Cladding Temperatures

Subcategory	Phenomenon	IR*	KR**
Initial conditions	Pellet and cladding dimensions	91	96
	Burnup distribution	55	89
	Cladding oxidation	46	73
	Power distribution	100	89
	Coolant conditions	93	96
	Transient power specification	100	94
Fuel and cladding temperature changes	Heat resistances in fuel, gap, and cladding	75	77
	Transient cladding-to-coolant heat transfer coefficient (oxidized cladding)	50	58
	Heat capacities of fuel and cladding	88	93
	Coolant conditions	85	88

Notes:
* Importance Ratio IR>75 Important
**Knowledge Ratio KR<75 Not completely understood

5.0 CRYSTAL RIVER 3 REA METHODOLOGY

This methodology is the same as the methodology described in Reference 5 except that it is applied to Crystal River 3. A bounding sample problem analysis is presented in the following sections to demonstrate the process, computer codes, boundary conditions, uncertainties, and results for the REA event for Crystal River 3. The computer codes that are used are described in Section 6.0. Section 7.0 describes the boundary conditions and uncertainties that are applied to the specific analyses. Section 8.0 provides the sample problem results. This methodology also provides in Section 9.0 the static conditions that a future cycle must meet for this analysis to remain valid. A cycle specific analysis can be repeated for those cycle parameters that do not meet the REA design parameters or a complete re-analysis can be performed to meet more challenging fuel designs.

5.1 Overall Code Calculational Flow for the Ejected Rod Accident Evaluation

As stated in Section 3.0, the primary computer models needed are a fuel performance code, a 3-D neutronic kinetic solution with thermal feed back, an open channel T-H code, and a T-H system code. The computer codes used to demonstrate the applicability of this methodology are COPERNIC[2], NEMO-K[6], LYNXT[7], and RELAP5/MOD2[8,9], respectively. The calculational flow of these codes and data process linkages is presented in Figure 5-1. COPERNIC calculations are run to obtain gap conductance tables for both NEMO-K and LYNXT. The fuel property correlation equations from COPERNIC are used in NEMO-K. The fuel property equations from COPERNIC are used to create fitting tables in LYNXT for conductivities and heat capacities for the clad and fuel.

The static option of NEMO-K is used to set initial boundary conditions for the ejected rod transient. The primary boundary conditions are ejected rod worth, DTC, MTC, β_{eff}, time-in-cycle, and power levels. The ejected rod transient is simulated with NEMO-K at each of the plant initial conditions of power and time in life (BOC and EOC). The core

power, $F_{\Delta H}$ for the peak pin of interest, and axial powers versus time are extracted from NEMO-K and processed to create inputs for LYNXT. The axial power shape data passed from NEMO-K model output to the LYNXT model input is converted to the axial elevation spacing required by LYNXT. The fuel rod powers supplied to LYNXT from NEMO-K are calculated from the $F_{\Delta H}$ power transient of the fuel assembly of interest and its neighboring assemblies. The powers are mapped to the LYNXT model geometry with an intra-assembly radial power distribution.

Two cases (i.e., [ ]) are run with LYNXT for each of the plant initial conditions. The results are reviewed relative to their respective limiting conditions, as discussed in Section 2.0. If the fuel temperature, clad temperature or enthalpy rise is above the limits listed in Table 2-1, the initial design conditions must be re-evaluated and the NEMO-K is rerun. If these parameters are acceptable relative to these limits at this point, the fuel rod failure census is compared against the maximum number of rods that may be failed for radiological release consequences as discussed in Section 2.3. If the fuel rod failure census is not acceptable during the first few seconds (prompt response), the initial design conditions must be re-evaluated and the NEMO-K is rerun.

If a reactor trip does not occur during the power pulse in the first few seconds, both the kinetic and static NEMO-K cases are run to bound the power versus time response. This power history information is passed to RELAP5/MOD2 to model the plant system response. Additional NEMO-K and RELAP5/MOD2 cases can be run to obtain a tighter coupling between the core response from NEMO-K and the system conditions from RELAP/MOD2. The time dependent response of the inlet temperature, flow, and pressure from RELAP5/MOD2 is input to LYNXT to obtain the fuel thermal response for times beyond approximately 5 seconds.

The fuel failure census is repeated for the conditions resulting after approximately 5 seconds. If the number of fuel rods considered failed is acceptable, this initial condition for power level and time in life is complete. If the number of fuel rods considered failed

exceeds the limit, the initial design conditions must be re-evaluated and the NEMO-K is rerun.

Figure 5-1 Calculational Flow Interfaces

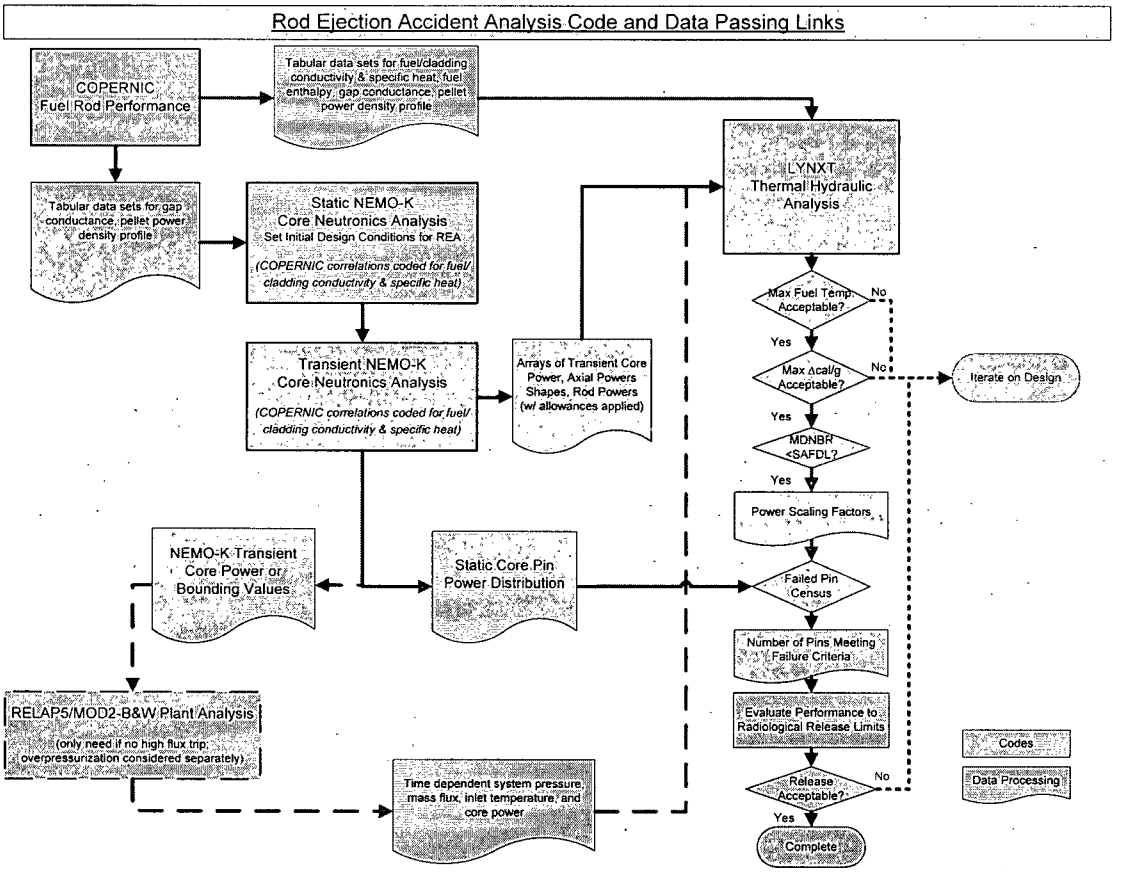

6.0 COMPUTER CODES

The computer codes used to demonstrate the applicability of this methodology are COPERNIC[2], NEMO-K[6], LYNXT[7], and RELAP5/MOD2[8,9]. Other approved computer codes which perform the same types of calculations are also acceptable. The only significant changes to this section relative to Reference 5 are the addition of clarifications based upon the responses to the requests for additional information and specific customization to Crystal River 3.

6.1 COPERNIC

COPERNIC is used to define the fuel and cladding thermal properties for both NEMO-K and LYNXT. These properties include the fuel and cladding thermal conductivity which includes oxide formation, the heat capacity for the fuel pellet and cladding, the radial power distribution in the fuel pellet, and the gap conductance. Fuel burnup affects the fuel conductivity, the pellet radial power profile, the gap conductance, and cladding oxide. The gap conductance is a complex function of the gap and surface temperatures, gap size (i.e., creep and thermal expansion), contact pressure, and fission gas content. To capture these effects in the downstream codes using a constant fuel geometry model, the gap conductance is interpolated from a table of gap conductance values [

] Repeating these calculations of gap conductance values at various burnup levels, a complete table is developed that captures the complex effects of burnup on the gap as well as the transient effects due to thermal expansion.

6.2 Plant Transient Model

The approved NEMO-K code is used as the plant transient model. It is a 3-D neutronic kinetics solution with time dependent fuel and coolant models and is not dependent upon LYNXT for fuel temperatures or moderator conditions. Benchmarks presented in

Reference 6 include three HZP and three HFP ejected rod code benchmarks and confirm that NEMO-K is applicable for calculating core power and peaking response during an ejected rod event. This section provides an overview of the features added to NEMO-K and its applicability to Crystal River 3.

6.2.1 Trip Function

Crystal River 3 uses an excore power trip signal to sense severe RIAs and subsequently shutdown the core. This trip function requires two different models: excore detector signals and a control rod drop model. The excore detectors are located near the minor axis of each quadrant, which causes the excore signal response to differ from the core average value when an asymmetric rod is ejected. These signals are compared to the trip values. Once the criteria for trip are reached (2/4 logic when trip signal is exceeded), a time delay is employed before the control rods are moved. The rod position with time in NEMO-K is defined by the safety analysis control rod drop position versus time from an input table. The physical models for the excore signals and the dropping of the control rods are discussed in the following sub-sections.

6.2.1.1 *Excore Detector Model*

Reactor protection systems typically measure the excore power detector signals and trip when predefined limits are exceeded. These excore detectors measure the fast flux exiting the reactor core and are a measure of the actual reactor conditions. These excore detector signals are simulated by using the NEMO-K assembly powers multiplied by weighting factors to translate the incore conditions to the excore signals. As demonstrated in Reference 6, a simple weighting of the peripheral locations closest to the excore detector provides good simulated results compared to the actual results in an operating reactor when an asymmetric control rod is dropped.

The excore detector model in NEMO supports a top and bottom detector at four radial locations. Detector response is computed by:

$$E_n^{T/B} = C_n^{T/B} \cdot F\left(T_n^{T/B}\right) \cdot \left[\sum_{j=1}^{J} W_j \cdot \sum_{k=1}^{K} D_k^{T/B} \cdot P_{jk}\right] \cdot P_{th}$$

where:

$E_n^{T/B}$ = top or bottom excore response in terms of percent power for radial detector *n*

$C_n^{T/B}$ = top or bottom excore response calibration factor for radial detector *n*

$F\left(T_n^{T/B}\right)$ = top or bottom excore response correction function for coolant temperature compensation for radial detector *n*

W_j = weighting factor for the assembly *j* contribution to the excore detector response

$D_k^{T/B}$ = weighting factor for the axial level *k* contribution to the top or the bottom detector response

P_{jk} = normalized power density for assembly *j* at axial level *k*

P_{th} = percent thermal power

The calibration factor represents the actual calibration performed at the plant when the excore detectors are periodically normalized to the measured thermal power. The calibration factor is either input or calculated by NEMO-K, if requested. For the requested calibration, the detectors are calibrated to core power using a static case that is run before the transient. The temperature correction factors and the radial and the axial weighting factors are inputs to the code.

6.2.1.2 *Control Rod Drop*

Rod movement during a scram is characterized by several distinct conditions:

- An initial acceleration period.
- Free fall from above the deceleration region.

- Deceleration due to flow restrictions.
- Free fall within the deceleration region.
- Stop at the bottom position.

The NEMO-K implementation models the movement for each rod or bank regardless of its initial position before scram. This leads to two different possible starting conditions:

- Rods that begin above deceleration region.
- Rods that begin at the top of or within the deceleration region.

When rod movement begins from a trip actuation, NEMO-K drops the rods or banks from their current height to the fully inserted position. The position versus time of a rod or bank depends upon the initial position prior to the trip. [

] This control rod drop model allows the rods to fall from any initial position in a manner consistent with the safety analysis assumptions.

6.2.2 *Adiabatic cal/g Edit*

An edit is provided that calculates the change in pellet enthalpy during a transient. The method integrates the change in rod segment power produced (relative to the beginning of the transient) over each timestep. The total energy deposited is the change in enthalpy. This method conservatively estimates the cal/g as defined for RIA criterion because it neglects the energy lost from the fuel rod by heat transfer to the coolant. This definition provides a useful means of identifying the relative impact of different conditions in two or more NEMO-K transients.

6.2.3 *Adjustment Factors*

In NEMO, there are four types of adjustment factors that can be used to account for uncertainty and conservative allowances. These adjustment factors are multipliers on the following parameters:

- Fuel conductivity
- Gap conductance
- Cross section changes due to fuel temperature variation (Doppler adjustment)
- Cross section changes due to control rod insertion (rod worth adjustment)

For the first three parameters the multipliers are applied to every node location. The control rod multiplier can be applied by bank or assembly location. These multipliers are factors that can be applied to examine sensitivities or to formulate a limiting case with uncertainties and/or conservative allowances.

6.2.4 *Pellet Weighted Temperature for DTC*

The cross sections are generated for NEMO-K using a flat pellet temperature profile. The pellet temperature distribution can vary significantly with time during an REA. For a pellet with a temperature distribution, a simple approach is to use volume averaging to

obtain the effective temperature for the cross sections. Another common method uses a weighting of the centerline and surface temperatures as shown below:

$$T_{eff} = T_S \cdot wt_{SC} + T_{CL} \cdot (1 - wt_{SC})$$

where:

T_{eff} = the effective flat temperature

T_S = the fuel surface temperature

T_{CL}= the fuel centerline temperature

wt_{SC} = the weighting factor for the surface/centerline formula

For example, Reference 10 uses this formulation with a weighting factor of 0.7. The disadvantages of this formulation are that it uses only two temperatures of the pellet and that it is based on the typical radius squared variation of the fuel pellet temperature at static conditions. An improved weighting method is employed in NEMO-K [

]

The relationship for the effective temperature (T_{eff}) has been validated with the computer code APOLLO2 described in BAW-10228PA, (Reference 11). The reactivity and U-238 capture rate of several snapshot fuel temperature distributions at steady state conditions and those temperatures expected during a Reactivity Initiated Accident (RIA) event were examined with APOLLO2. Calculations were repeated with a uniform

fuel temperature until the reactivity and U-238 capture rates were equivalent to the non-uniform temperature distributions. This uniform temperature was defined as the effective temperature and compared to the values predicted by Rowland's formula and the new T_{eff} formula. Fifteen cases were run for each temperature distribution, which spanned burnups from 0 to 60 GWD/MTU and U-235 enrichments from [ ] weight percent (w/o). Results showed that Rowland's formula resulted in nearly the same temperature as the new T_{eff} formula for steady state cases, and that both agreed with the APOLLO2 effective temperature. For the transient fuel temperature cases, the new T_{eff} definition showed substantial improvement reducing the mean prediction error of T_{eff} from a range [ ] K for the Rowlands formula down to a range of [ ] K. Both models had about a [ ] K standard deviation. The APOLLO2 temperature solution was benchmarked to Monte Carlo N-Particle (MCNP) transport code calculations. In addition, the new T_{eff} method was compared in Table 7-5 to an average temperature formulation and was found to yield slightly more limiting results than a simple average weighting.

6.2.5 NEMO-K Summary

Some of the results from Reference 6 that are pertinent to the REA are summarized to illustrate the accuracy of NEMO-K to a fine mesh reference solution. Table 6-1 shows the current NEMO-K results for each of the six rod ejection benchmark cases. These results are comparable to Table 4-5 in Reference 6. The six cases include a HZP (x1) and a HFP (x2) rod ejection with three different core geometries (where x is A, B, or C). As stated in Reference 6, the agreement between NEMO-K and the reference solution is excellent. The only item that stands out in the table is case B2, where the time of the peak is predicted to be 0.10 seconds rather than 0.12 seconds as the reference solution. Although this is a large percentage difference, the absolute difference is small considering the relatively flat peak core power in this transient as shown in Figure 6-2.

Additionally, Figure 6-3 through Figure 6-5 show the power distribution comparisons for case A1 at initial, peak core power, and 5 seconds during the transient, respectively.

These figures correspond to Figures 4-17, 4-18, and 4-19 in Reference 6. As shown in the figures, NEMO-K agrees with the reference PANTHER solutions.

Figure 6-6 and Figure 6-7 show power distribution results that have not been previously published with NEMO-K for cases C1 and C2, respectively. These figures show the assembly planar power at a fixed height along the major axis at maximum transient core power. This dimensional slice includes the ejected rod location at B08. The power density values are normalized to the maximum value in this slice. The figures show excellent agreement between NEMO-K and the reference solution. The results demonstrate that NEMO-K accurately models REA time dependent phenomena and is applicable for the methodology presented.

6.3 Transient Fuel Rod Model

The fuel rod model in LYNXT[7], an approved code, is used as the transient fuel rod model. Changes to the core thermal-hydraulic code LYNXT are implemented in the fuel rod modeling for the REA analysis. This section contains a brief overview of the approved fuel rod model as well as the changes in the fuel rod model made for the REA and other static and transient fuel rod modeling applications.

6.3.1 General Overview of Existing LYNXT Fuel Rod Models

The approved fuel rod model in LYNXT is based on a two-dimensional conduction equation with a radial and optional axial dependence. The solution is based on the orthogonal collocation method where the solution locations within the fuel and cladding are determined based on the collocation order. Two fuel rod models exist in LYNXT as approved by the U.S. NRC:

- Constant Gap/Constant Properties (CG/CP) – This is the same model in COBRA-IV-I[12], which served as the basis for LYNXT. The fuel-to-cladding gap dimension remains invariant throughout the modeled event as do all the thermal properties, with the exception of the fuel thermal conductivity which can optionally be modeled using a third order temperature dependence.

- Variable Gap/Temperature Dependent Properties (VG/TDP) – This fuel rod model is based on the thermal and mechanical properties of the TAFY[13], TACO[14], and TACO2[15] fuel performance codes. The VG/TDP fuel rod model allows the fuel and cladding dimensions to change during the event due to temperature and pressure difference effects (i.e., pressure difference between coolant and internal fuel rod pressure), based on the TAFY, TACO, and TACO2 models. The VG/TDP fuel rod model uses the same gap conductance model from TAFY, TACO, and TACO2 with the gas inventory at the start of the event being invariant throughout the event. The LYNXT VG/TDP model allows the radial power profile data from the three fuel performance codes to be used as an optional input, which is held invariant during the modeled event.

6.3.2 Enhancements to the Fuel Rod Models

The enhancements to the approved LYNXT fuel rod models increase the number of solution locations in the fuel pellet and increase the modeling flexibility of the fuel rod model (including the cladding). Increasing the number of solution locations in the fuel allows the fuel rod model to more accurately represent various radial power profiles across the fuel pellet, including those with the peak radial power in the outer portions of the fuel pellet. Expanding the modeling capability allows various fuel performance codes, such as (but not limited to) TACO3[16] or COPERNIC[2], to be used as the basis of a LYNXT time dependent analysis. The enhancements use the same fuel and cladding energy equations and solution process as the CG/CP and VG/TDP models (defined in Equations 2-6 through 2-13 for the energy equations and Equations 2-117 through 2-125 for the solution process in Reference 7), but use input property values for the pellet, gap, and cladding instead of the code specific values relative to TAFY, TACO, and TACO2.

The maximum number of solution locations in the cylindrical fuel is increased from 6th order collocation in Reference 7 to 20th order collocation (the number of solution locations in the fuel pellet equals the collocation order plus one). The additional solution locations are available for the enhanced fuel rod model and the approved CG/CP and

VG/TDP fuel rod models. Table 6-2 contains the collocation locations, both the cylindrical and planar data up to 6th order collocation are from Figure 2-5 of Reference 7, as well as the additional 8th, 10th, 12th, 16th, and 20th order radial locations in the fuel pellet. The planar data is unchanged from COBRA-IV-I[12].

The enhancements to the fuel rod model to expand the modeling capability allow the various temperature dependent properties and radial power profile characteristics used in the fuel/cladding energy equation calculations to be based on a number of potential fuel performance codes. The enhancements provide a fuel rod model that is based on the following parameters being invariant during the modeled event:

- Fuel Dimensions - Thermal and lateral pressure changes to the geometry are not modeled. Gap conductance is allowed to change in a transient [

  ]

- Cladding, gap, and fuel properties dependent on parameters other than temperature, such as pressure difference across the cladding.

- Gas inventory during the event - This is consistent with the VG/TDP model.

- Radial power profile - This is consistent with the VG/TDP model.

The new fuel rod model is called the Constant Gap/Temperature Dependent Property (CG/TDP) model because the fuel-to-cladding gap dimension is invariant and various thermal properties may be temperature dependent.

The CG/TDP model allows the input of the following temperature dependent properties, in tabular form:

- Thermal conductivity for the fuel and/or cladding

- Specific heat for the fuel and/or cladding

- Gap conductance
- Fuel enthalpy

The fuel rod thermal properties' tabular input to LYNXT for the LYNXT Constant Gap/Temperature Dependent Properties (CG/TDP) option are input as a pair of temperature and thermal property values repeated for the range of temperatures modeled. The properties are the fuel thermal conductivity, fuel specific heat, cladding thermal conductivity, and cladding specific heat. The gap conductance property is input as a [ ].

Additionally, the fuel enthalpy can be input as a function of fuel temperature in order for LYNXT to determine the total enthalpy and change in enthalpy at the radial locations in the fuel pellet. The attribute of the radial pellet power profile is input as a function of radial position. The radial pellet power shape is an important attribute for determining the steady state and transient temperature distributions at different burnup conditions.

6.3.3 LYNXT Benchmark Review

The LYNXT thermal equations have not changed; only the user inputs to those equations have changed. Therefore, the validation of the code equations remains valid. This subsection reviews the past qualification of the code and provides some example cases with the new input options to illustrate the new coupling of inputs.

6.3.3.1 *Past Qualification*

The benchmarks for the CG/CP and VG/TDP fuel rod models included:

- Analytical solution of the fuel and cladding with the gap conductance assumed as negligible.
- Power ramp comparisons to TACO (Reference 14).
- Non-crossflow transient fuel temperature and DNBR code, RADAR[17], using the four pump coastdown and the four pump locked rotor transients.

- Sensitivity studies using the hot full power ejected rod (HFPER) event.

The Reference 7 CG/CP and VG/TDP benchmark cases indicated the following in terms of the maximum difference:

- Agreement between the CG/CP LYNXT fuel rod model and the analytical solution was within 0.5 percent on the fuel centerline temperature.

- Agreement between the VG/TDP LYNXT fuel rod model (initialized to 102 percent rated power with TACO) and TACO over a power ramp range from 60 to 135 percent rated power was within 2 percent on centerline temperature and 4 percent on fuel surface temperature for BOL conditions.

- Agreement between the VG/TDP LYNXT fuel rod model and the RADAR fuel rod model for the transients was within 3 percent on the fuel centerline temperature, within 4.5 percent on the radial average temperature, and 2.5 percent on the transient minimum DNBR (MDNBR). These comparisons are based on BOL conditions.

The fuel rod model benchmark cases for LYNXT, based on Reference 7, confirm that the VG/TDP LYNXT fuel rod model is capable of predicting consistent results with fuel performance codes (limited to TAFY, TACO, and TACO2). The CG/CP and VG/TDP fuel rod models are capable of predicting the fuel temperatures, cladding temperatures and DNBR from other transient fuel performance and DNBR codes such as RADAR over a wide range of static and transient events typically encountered in plant operations.

These benchmarks are repeated with the new LYNXT version which produced equivalent results (within roundoff). In addition, several cases were repeated with the higher collocation orders and with the CG/TDP fuel option which produced equivalent results. Therefore, the conclusions made for LYNXT in Reference 7 remain valid for the CG/TDP fuel option.

6.3.3.2 *LYNXT-to-COPERNIC Example Cases*

The LYNXT to COPERNIC models are designed to investigate the performance of the LYNXT CG/TDP fuel rod model using the tabular fuel thermal properties compared to the COPERNIC full detailed capability model. The CG/TDP LYNXT fuel rod model is compared to COPERNIC (Reference 2) using a representative rod ejection transient starting at HZP and HFP conditions. Even though COPERNIC is not approved for fast transients like REA, this comparison highlights any significant differences between LYNXT and a more precise treatment of the fuel rod thermal parameters. These calculations were repeated for both BOL and EOL burnup-based fuel rod conditions. The CG/TDP LYNXT inputs for these rod ejection cases are thermal properties (including gap conductance) and radial/axial power profiles based on static COPERNIC calculations. In addition to any temperature dependence, the COPERNIC-based LYNXT inputs consider the burnup effects, the uranium enrichment, the porosity of the fuel, and the oxide thickness on the cladding. The same transient boundary conditions for power, $F_{\Delta H}$, axial shape, and cladding outer wall temperature versus time are used in both the COPERNIC and LYNXT transient analyses. The modeling assumptions used for the LYNXT to COPERNIC transient model comparison are listed below:

- A model of a single fuel rod with the same pellet radial power profile.
- Uniform power distribution in the axial direction to allow a single axial node to be compared.
- Same power history transient for the fuel. Time dependent inputs for LYNXT were linearly interpolated between no more than 101 input values. COPERNIC uses step values with a significantly finer mesh.
- Constant outer wall cladding temperature (set by creating nearly infinite heat transfer coefficient).

- Fuel pellet mesh—COPERNIC used 5 equal area nodes each with 4 equal area sub-nodes. LYNXT used ten collocation points for twelve radial temperature values.

- Cladding Mesh—COPERNIC used 4 equal radial area nodes. LYNXT used two collocation radial points.

- Constant burnup profile within the fuel pellet so that fuel rod thermal properties are nearly the same.

- Fuel and cladding thermal properties (conductivity, specific heat, gap conductance)—COPERNIC uses inherent functions of the computer code fuel performance correlations. LYNXT uses tables of properties as a function of temperature.

The following four example cases are performed for LYNXT and COPERNIC:

- HZP/EOL – Based on EOL burnup conditions (60 GWD/MTU) for HZP transient boundary conditions.

- HFP/EOL – Based on EOL burnup conditions for HFP transient boundary conditions.

- HZP/BOL – Based on BOL burnup conditions (2.5 GWD/MTU) for HZP transient boundary conditions.

- HFP/BOL – Based on BOL burnup conditions for the HFP transient boundary conditions.

The transient comparisons of the fuel surface, fuel radial average, fuel centerline, fuel maximum, and the cladding maximum temperatures for the four different cases are presented in Figure 6-8 through Figure 6-27 as illustrated in the following table.

Condition	Fuel temperature				Cladding maximum temperature
	Surface	Average	Centerline	Maximum	
HZP/EOL	Figure 6-8	Figure 6-9	Figure 6-10	Figure 6-11	Figure 6-12
HFP/EOL	Figure 6-13	Figure 6-14	Figure 6-15	Figure 6-16	Figure 6-17
HZP/BOL	Figure 6-18	Figure 6-19	Figure 6-20	Figure 6-21	Figure 6-22
HFP/BOL	Figure 6-23	Figure 6-24	Figure 6-25	Figure 6-26	Figure 6-27

Table 6-3 contains a numerical summary for the LYNXT and COPERNIC comparisons for each of the four transient cases when transient time steps are the same in both codes. At each common time point in the two computer code simulations, the ratio of the respective fuel and cladding temperature results from the two codes is calculated. The ratio is the COPERNIC result divided by the LYNXT Constant Gap/Temperature Dependent Property (CG/TDP) result. For each of the four transients, the average, standard deviation, maximum, and minimum of the ratios during the transient simulation are calculated and tabulated in Table 6-3. The sample size reported is the number of common time points during the transient.

With the exception of the HZP/EOL fuel surface temperatures in the 0.15 to 0.20 second time frame, the maximum difference between the transient COPERNIC and LYNXT CG/TDP fuel temperatures is less than [ ] percent. During this 0.05 second interval for HZP/EOL, which represents the time of the neutron power spike due to the rod ejection, the differences between the COPERNIC and the CG/TDP LYNXT fuel surface temperatures are [

]. This difference in the gap conductance is for a short duration and has little impact on the maximum fuel temperature comparisons, which are within [ ]

percent. The maximum difference in the maximum cladding temperatures between COPERNIC and LYNXT is within [ ] percent, with LYNXT predicting higher temperatures than COPERNIC. Since this LYNXT model tends to yield higher peak cladding temperatures and accurately predicts peak fuel temperatures, this model with the gap conductance fitting tables is acceptable to predict fuel melt and minimum DNBR conditions for REA.

6.3.4 LYNXT Conclusions

Three different fuel rod models are available in LYNXT (i.e., CG/CP, VG/TDP, and CG/TDP). These models are summarized in Table 6-4. The enhancements used to form the CG/TDP model provide LYNXT the ability to use thermal properties and other conditions from any fuel performance code, such as (but not limited to) TACO3 (Reference 16) or COPERNIC (Reference 2). The CG/TDP fuel rod model allows LYNXT to mimic the behavior of various fuel performance codes without the need to implement each of the various fuel performance code models and properties within LYNXT. The CG/TDP model allows the specification of the following, based on input:

- Temperature dependent thermal properties for the fuel and cladding
- Gap conductance based on the [ ]
- Radial power profile across the fuel pellet

The limitations of the CG/TDP LYNXT fuel rod model are as follows:

- Cladding, gap, and fuel dimensions are invariant throughout the event.
- Cladding, gap, and fuel properties are only temperature dependent.
- Cladding, gap, and fuel properties apply throughout the event.
- Radial power profile is invariant throughout the event.

- Gas inventory during the event is invariant.

The last two limitations are also limitations of the VG/TDP fuel rod model.

Three different types of cases to verify that the CG/TDP fuel rod model is accurately predicting the results of various fuel performance codes are as follows:

- Analytical benchmark (same as in Reference 7).
- Original fuel performance code benchmarks using a variable gap conductance fuel rod model (same as in Reference 7).
- Example cases with COPERNIC.

The code comparisons indicate that the CG/TDP fuel rod model predicts the known solution (analytical or from a fuel performance code) to within [ ] percent, based on the input gap conductance table accurately predicting the fuel performance code gap conductance behavior. As the burnup increases and the power excursion gets larger it becomes [ ]. For these higher burnups and large power excursions, the difference between the CG/TDP LYNXT local fuel temperature predictions and COPERNIC is [ ], with LYNXT producing higher temperatures. Even with these differences for short durations, the maximum difference in the maximum fuel temperature is less than [ ] percent. Therefore, this model with the gap conductance fitting tables is acceptable to predict fuel melt and minimum DNBR conditions for REA analyses.

6.4 System T-H Model

The plant transient model uses a constant pressure, inlet temperature, and flow model. A system T-H model is needed to model the trip functions, primary and secondary systems to address those conditions that may change pressure, inlet temperature and/or flow during an REA. RELAP5/MOD2[8,9] is used for non-LOCA safety analyses

and is also used to estimate changing plant conditions during an REA. The only significant change to this model for REA simulations is to turn off the point kinetics model and substitute the power versus time obtained from NEMO-K.

Table 6-1 NEACRP Kinetic Results

	NEMO-K	Ref	Diff	% Diff
A1				
Maximum Core Power Fraction	1.223	1.179	0.044	3.7
Core Power Fraction @ 5 sec	0.200	0.196	0.004	2.0
Time of Maximum Power	0.550	0.560	-0.010	-1.8
Fuel Temperature at Max Power	294.7	294.5	0.200	0.1
Fuel Temperature @ 5 sec	325.1	324.3	0.800	0.2
A2				
Maximum Core Power Fraction	1.082	1.080	0.002	0.2
Core Power Fraction @ 5 sec	1.036	1.035	0.001	0.1
Time of Maximum Power	0.1	0.1	0.000	0.0
Fuel Temperature at Max Power	544.6	546.5	-1.900	-0.3
Fuel Temperature @ 5 sec	553.0	554.6	-1.600	-0.3
B1				
Maximum Core Power Fraction	2.431	2.441	-0.010	-0.4
Core Power Fraction @ 5 sec	0.324	0.320	0.004	1.3
Time of Maximum Power	0.520	0.517	0.003	0.6
Fuel Temperature at Max Power	301.4	301.4	0.000	0.0
Fuel Temperature @ 5 sec	350.3	349.9	0.400	0.1
B2				
Maximum Core Power Fraction	1.062	1.063	-0.001	-0.1
Core Power Fraction @ 5 sec	1.038	1.038	0.000	0.0
Time of Maximum Power	0.10	0.12	-0.020	-16.7
Fuel Temperature at Max Power	542.1	544.1	-2.000	-0.4
Fuel Temperature @ 5 sec	550.0	552.0	-2.000	-0.4
C1				
Maximum Core Power Fraction	4.735	4.773	-0.038	-0.8
Core Power Fraction @ 5 sec	0.148	0.146	0.002	1.4
Time of Maximum Power	0.268	0.268	0.000	0.0
Fuel Temperature at Max Power	298.2	297.9	0.300	0.1
Fuel Temperature @ 5 sec	316.1	315.9	0.200	0.1
C2				
Maximum Core Power Fraction	1.074	1.071	0.003	0.3
Core Power Fraction @ 5 sec	1.031	1.030	0.001	0.1
Time of Maximum Power	0.1	0.1	0.000	0.0
Fuel Temperature at Max Power	544.5	546.4	-1.900	-0.3
Fuel Temperature @ 5 sec	551.8	553.5	-1.700	-0.3

Table 6-2 Cylindrical and Planar Geometry Collocation Points for LYNXT

Cylindrical geometry

N = 2	N = 3	N = 4	N = 5	N= 6
0.393765	0.297637	0.238965	0.199524	0.171220
0.803087	0.639896	0.526159	0.444987	0.384810
	0.887502	0.763931	0.661797	0.580504
		0.927491	0.833945	0.747443
			0.949455	0.877060
				0.962780

[ ]

Planar Geometry

N = 2	N = 3
0.285232	0.209299
0.765055	0.591700
	0.871740

Notes:

1. All collocation points are normalized, based on fuel pellet/plate outer surface.
2. The point, based on a normalized location, of 1.0 is a collocation point for all orders. This represents the fuel surface.
3. N denotes the collocation order.

Table 6-3 LYNXT and COPERNIC Transient Temperature Ratio Comparisons

Comparison parameter	Fuel temperature				Cladding maximum temperature
	Surface	Average	Centerline	Maximum	
HZP EOL					
Average					
Std. dev.					
Maximum					
Minimum					
Sample size					
HFP EOL					
Average					
Std. dev.					
Maximum					
Minimum					
Sample size					
HZP BOL					
Average					
Std. dev.					
Maximum					
Minimum					
Sample size					
HFP BOL					
Average					
Std. dev.					
Maximum					
Minimum					
Sample size					

Notes:

1. The data is based on (COPERNIC result) / (LYNXT CG/TDP result).
2. "Std. dev." is the standard deviation of the data about the average. Sample size is the number of transient time steps.

Table 6-4 LYNXT Fuel Rod Model Options

Fuel/cladding parameter	CG/CP	VG/TDP	CG/TDP
Collocation orders	See Note 1	See Note 1	All values in Table 6-2
Fuel thermal conductivity	Constant or user-supplied third order polynomial	TAFY, TACO, TACO2 property	User-supplied function of fuel temperature
Fuel specific heat	Constant	Temperature-dependent function	
Cladding thermal conductivity		TAFY, TACO, TACO2 property	User-supplied function of cladding temperature
Cladding specific heat		Temperature-dependent function	
Fuel-to-cladding gap dimension		Variable	Constant
Gap conductance		TAFY, TACO, TACO2 model	User-supplied function of [ ]
Radial power profile	Uniform	User-supplied as a function of fuel pellet radial location	User-supplied as a function of fuel pellet radial location
Fuel enthalpy	Not available	Not available	User-supplied function of fuel temperature

Notes:

1. The collocation orders in Reference 7 are 2, 3, 4, 5, and 6 (cylindrical). The potential collocation orders were expanded to include all the locations in Table 6-2.
2. In the CG/TDP fuel rod model the input of each of the user-supplied functions is optional and if used is supplied in tabular form.

Figure 6-1 Sample Scram Position Versus Drop Time

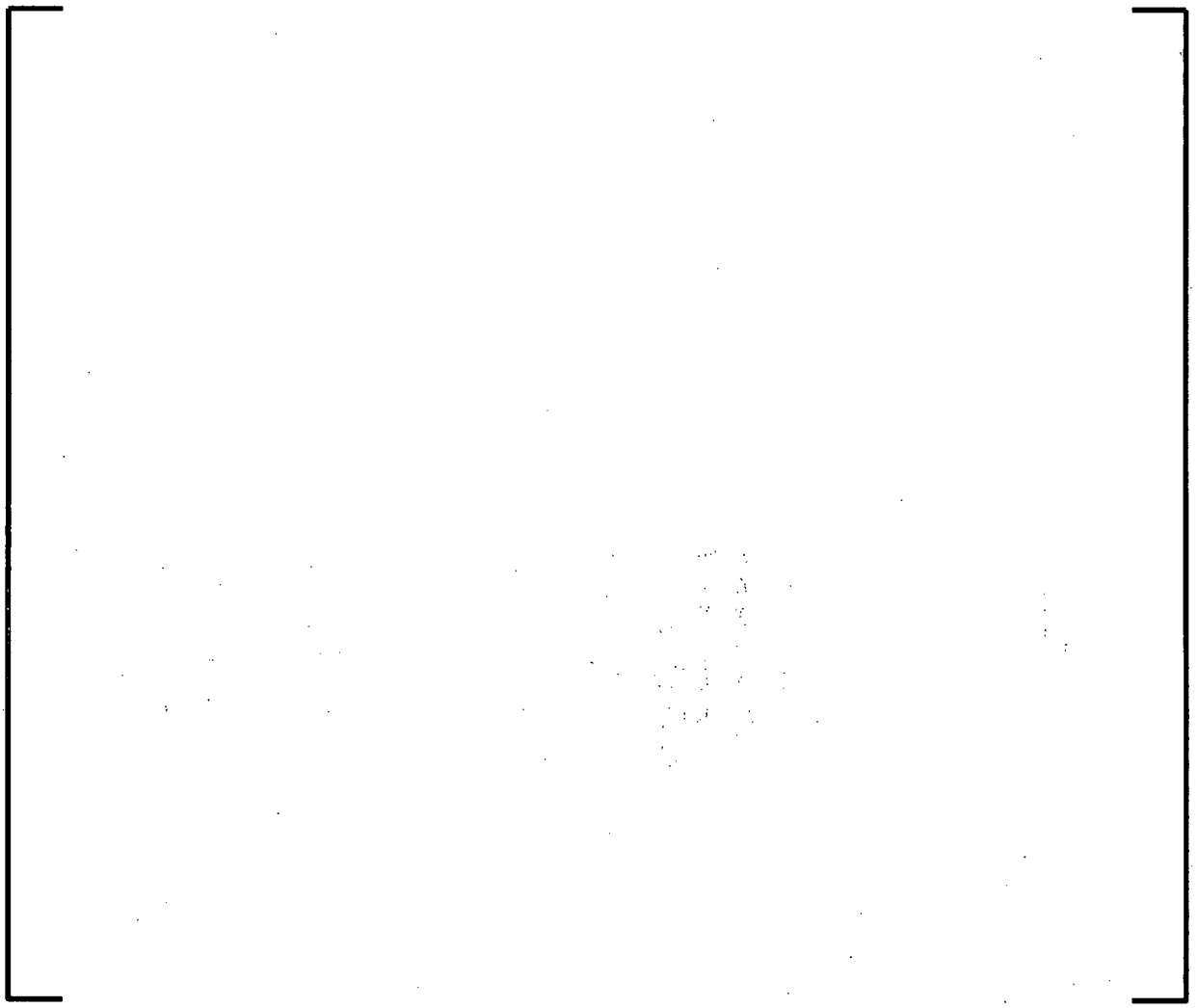

Figure 6-2 Core Power Fraction – Case B2

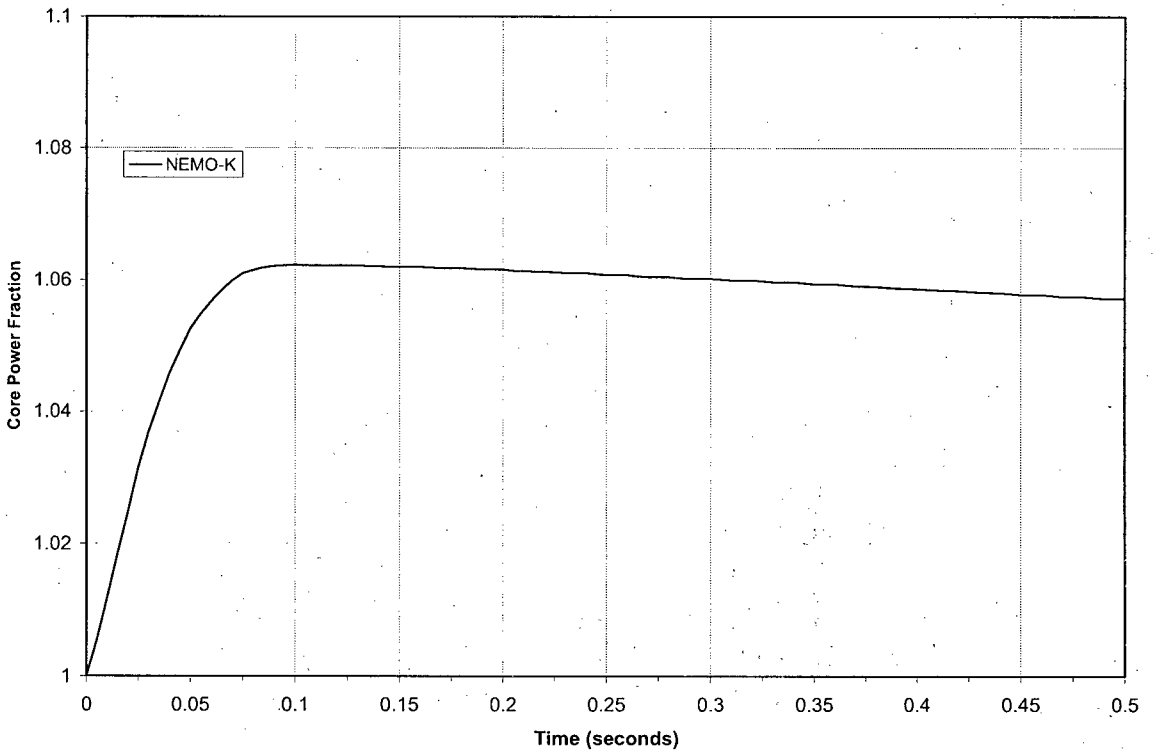

Figure 6-3 Power Distribution at Initial Conditions – Case A1

1/8th Core Assembly Power Map at Plane 6

PANTHER

				0.293	0.354		
			0.752	0.533	0.497	0.285	
		0.545	0.757	0.393	0.380	0.206	
	0.964	0.867	1.000	0.745	0.301	0.294	0.226
0.533	0.793	0.575	0.945	0.951	0.527	0.214	0.285

NEMO-K

Nodal Layer Peak		2.372		0.284	0.353		
			0.752	0.532	0.496	0.284	
		0.530	0.757	0.382	0.380	0.200	
	0.965	0.868	1.000	0.745	0.292	0.293	0.225
0.518	0.794	0.559	0.945	0.950	0.527	0.207	0.284

DIFFERENCE (N-P)

STD	0.006			-0.009	-0.001		
			0.000	-0.001	-0.001	-0.001	
		-0.015	0.000	-0.011	0.000	-0.006	
	0.001	0.001	0.000	0.000	-0.009	-0.001	-0.001
-0.015	0.001	-0.016	0.000	-0.001	0.000	-0.007	-0.001

Figure 6-4 Power Distribution at Maximum Core Power – Case A1

1/8th Core Assembly Power Map at Plane 6

PANTHER

				0.128	0.150		
			0.362	0.242	0.214	0.120	
		0.316	0.390	0.188	0.169	0.088	
	0.790	0.562	0.540	0.371	0.140	0.126	0.093
1.000	0.778	0.390	0.513	0.474	0.248	0.093	0.117

NEMO-K

Nodal Layer Peak		4.357		0.124	0.149		
			0.362	0.242	0.213	0.119	
		0.307	0.391	0.183	0.169	0.085	
	0.790	0.562	0.540	0.371	0.136	0.126	0.093
1.000	0.778	0.379	0.513	0.474	0.248	0.090	0.117

DIFFERENCE (N-P)

STD	0.003			-0.004	-0.001		
			0.000	0.000	-0.001	-0.001	
		-0.009	0.001	-0.005	0.000	-0.003	
	0.000	0.000	0.000	0.000	-0.004	0.000	0.000
0.000	0.000	-0.011	0.000	0.000	0.000	-0.003	0.000

Figure 6-5 Power Distribution at 5 Seconds – Case A1

1/8th Core Assembly Power Map at Plane 6

PANTHER

				0.143	0.168		
			0.392	0.266	0.239	0.135	
		0.333	0.417	0.205	0.188	0.099	
	0.802	0.581	0.569	0.397	0.153	0.142	0.106
1.000	0.785	0.403	0.540	0.505	0.269	0.104	0.134

NEMO-K

Nodal Layer Peak		4.554		0.139	0.169		
			0.392	0.266	0.239	0.135	
		0.323	0.417	0.199	0.188	0.096	
	0.802	0.582	0.570	0.397	0.149	0.142	0.106
1.000	0.785	0.392	0.541	0.505	0.270	0.101	0.134

DIFFERENCE (N-P)

STD	0.003			-0.004	0.001		
			0.000	0.000	0.000	0.000	
		-0.010	0.000	-0.006	0.000	-0.003	
	0.000	0.001	0.001	0.000	-0.004	0.000	0.000
0.000	0.000	-0.011	0.001	0.000	0.001	-0.003	0.000

Figure 6-6 Comparison of Radial Power at Max Power – C1

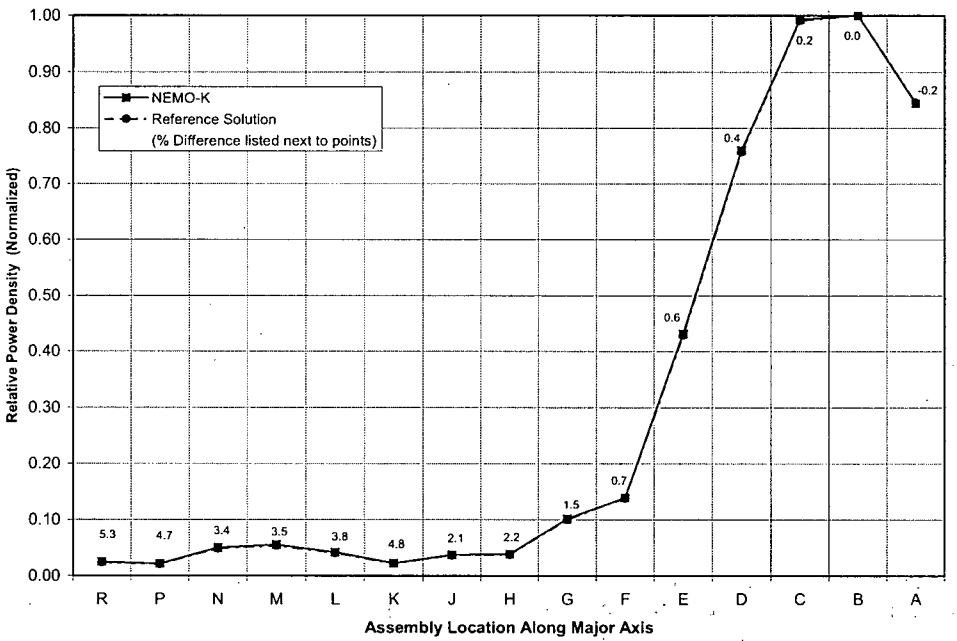

Figure 6-7 Comparison of Radial Power at Max Power – C2

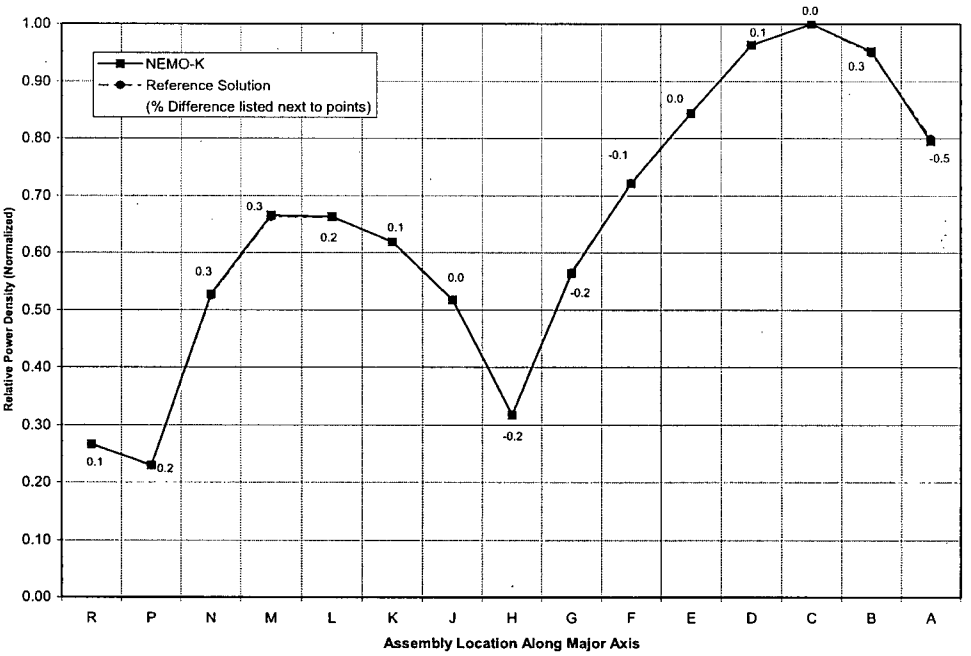

Figure 6-8 HZP/EOL Transient Fuel Surface Temperature

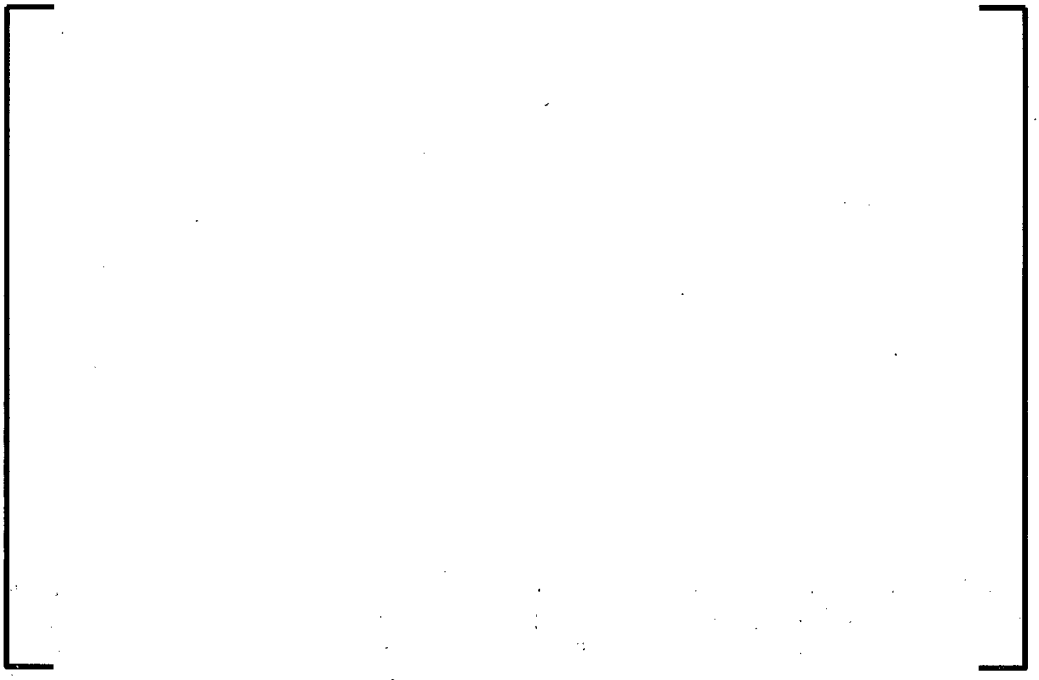

Figure 6-9 HZP/EOL Transient Fuel Average Temperature

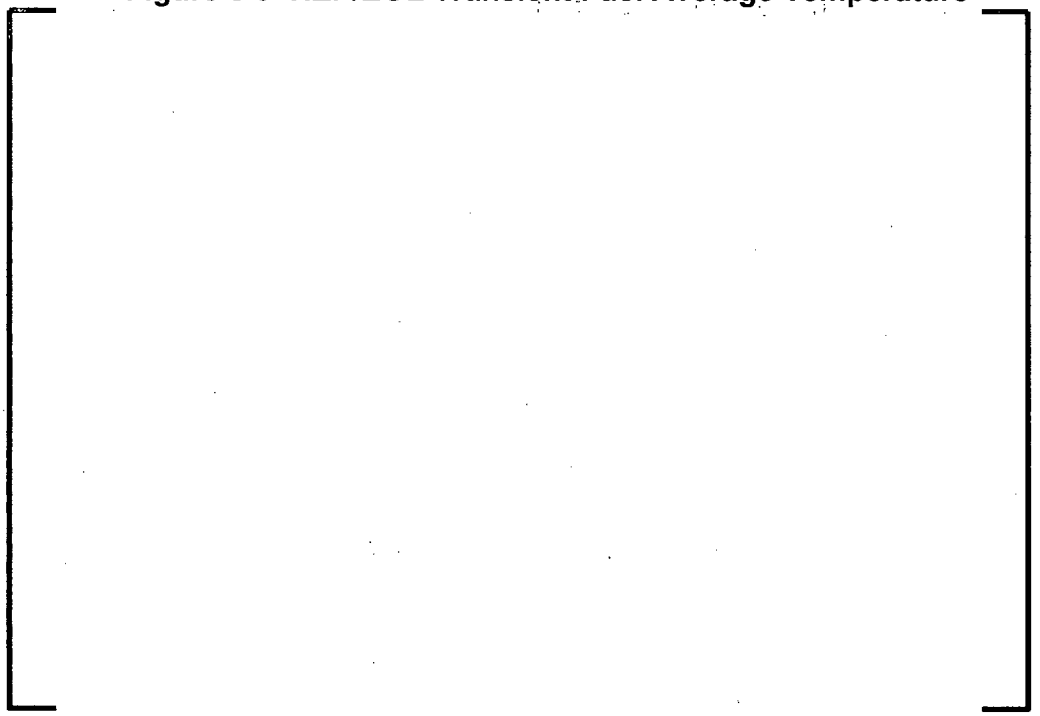

Figure 6-10 HZP/EOL Transient Fuel Centerline Temperature

Figure 6-11 HZP/EOL Transient Fuel Maximum Temperature

Figure 6-12 HZP/EOL Transient Cladding Maximum Temperature

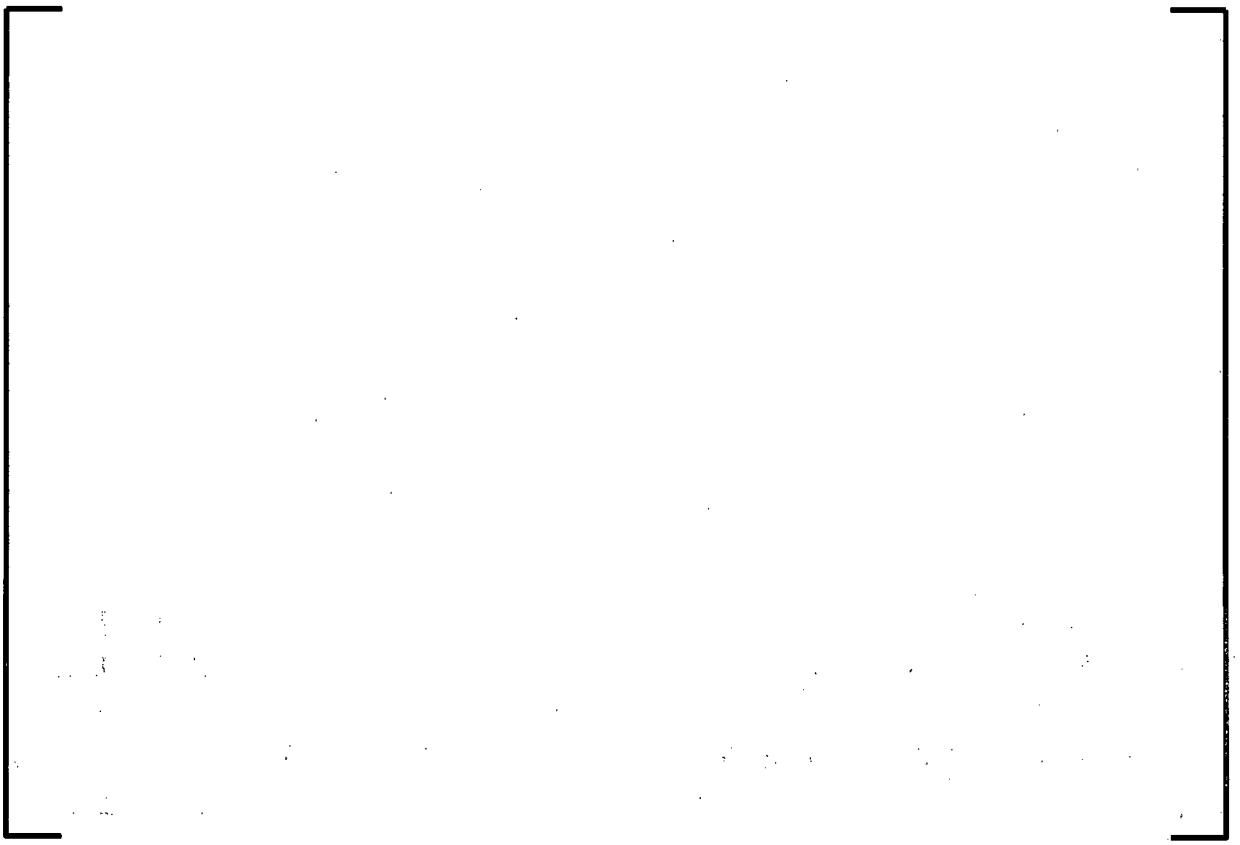

Figure 6-13 HFP/EOL Transient Fuel Surface Temperature

Figure 6-14 HFP/EOL Transient Fuel Average Temperature

Figure 6-15 HFP/EOL Transient Fuel Centerline Temperature

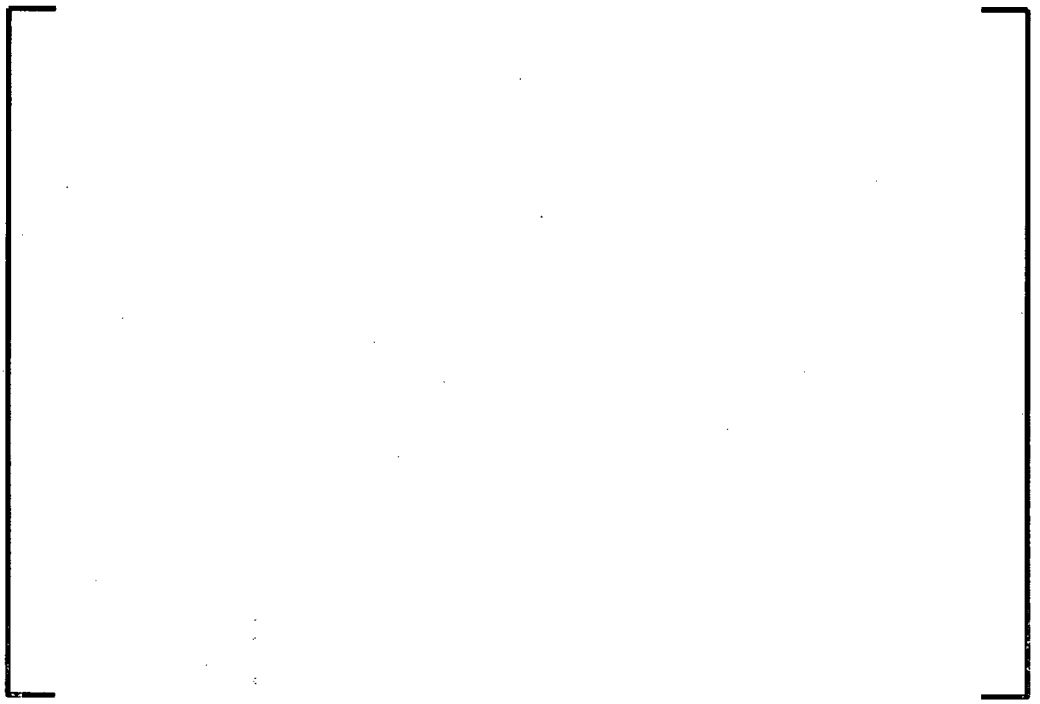

Figure 6-16 HFP/EOL Transient Fuel Maximum Temperature

Figure 6-17 HFP/EOL Transient Cladding Maximum Temperature

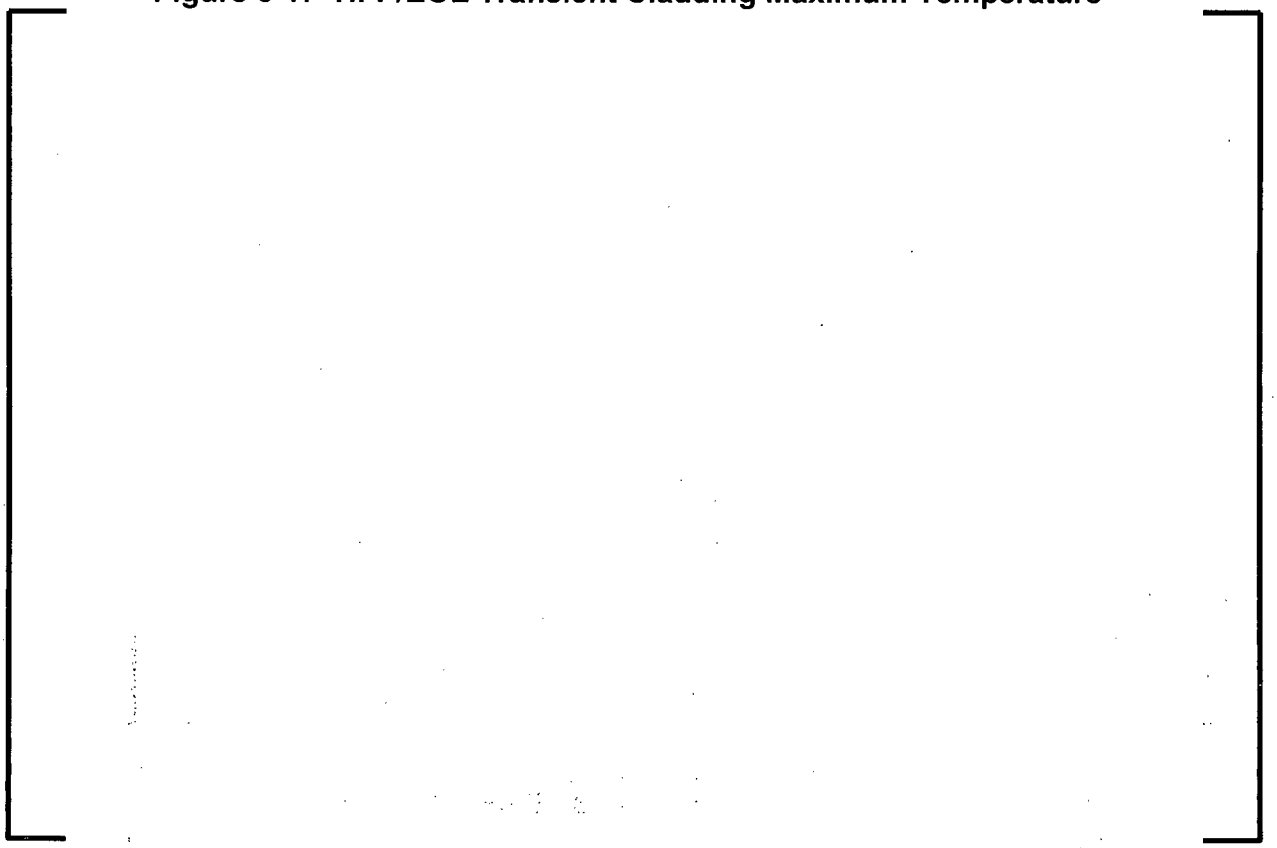

Figure 6-18 HZP/BOL Transient Fuel Surface Temperature

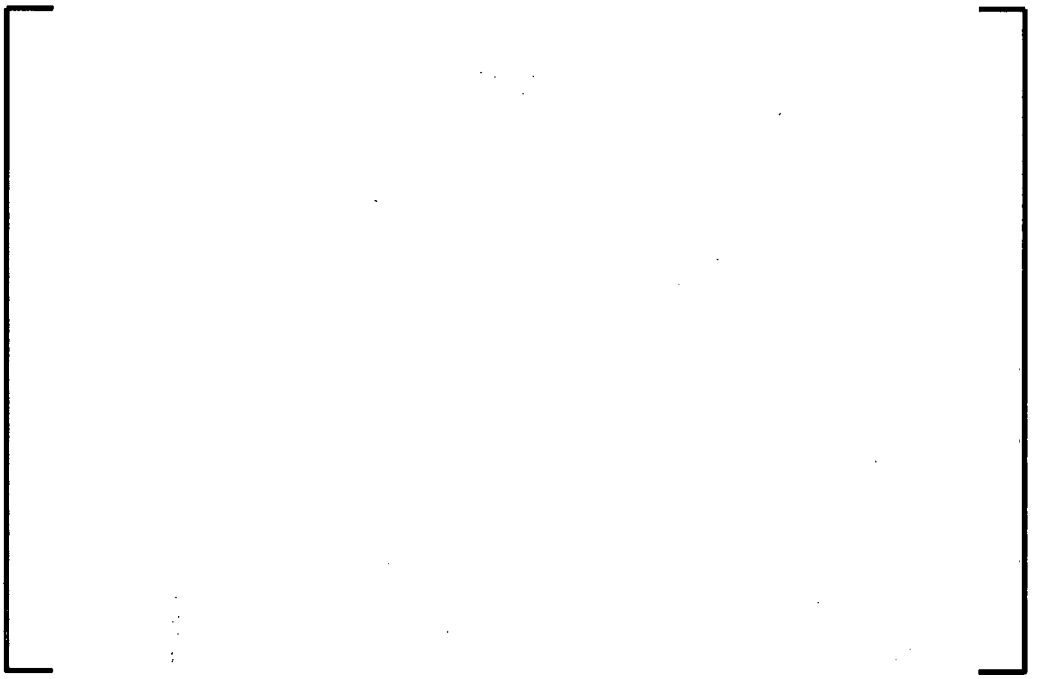

Figure 6-19 HZP/BOL Transient Fuel Average Temperature

Figure 6-20 HZP/BOL Transient Fuel Centerline Temperature

Figure 6-21 HZP/BOL Transient Fuel Maximum Temperature

Figure 6-22 HZP/BOL Transient Cladding Maximum Temperature

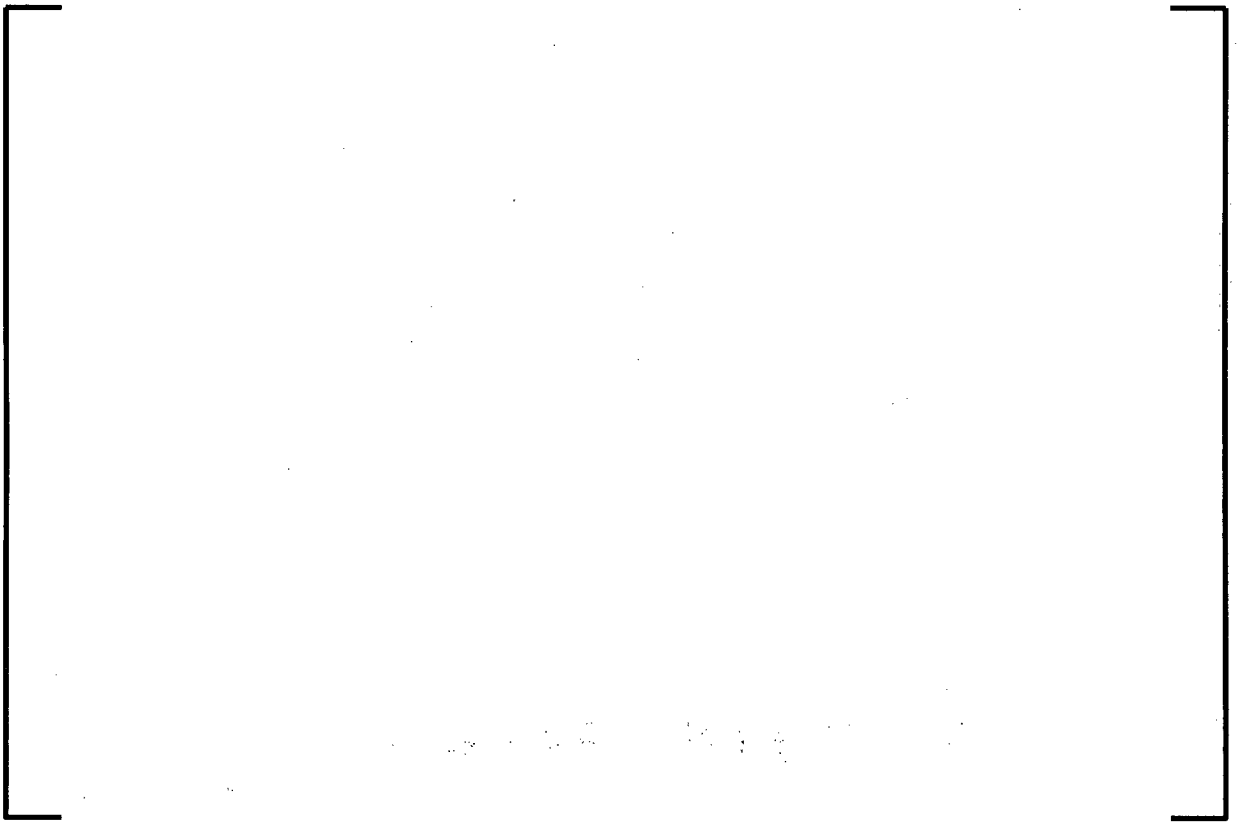

Figure 6-23 HFP/BOL Transient Fuel Surface Temperature

Note that the slight slope discontinuities of the LNYXT results are caused by the slope discontinuity at a fit point when using linear interpolation of the gap conductance table values.

Figure 6-24 HFP/BOL Transient Fuel Average Temperature

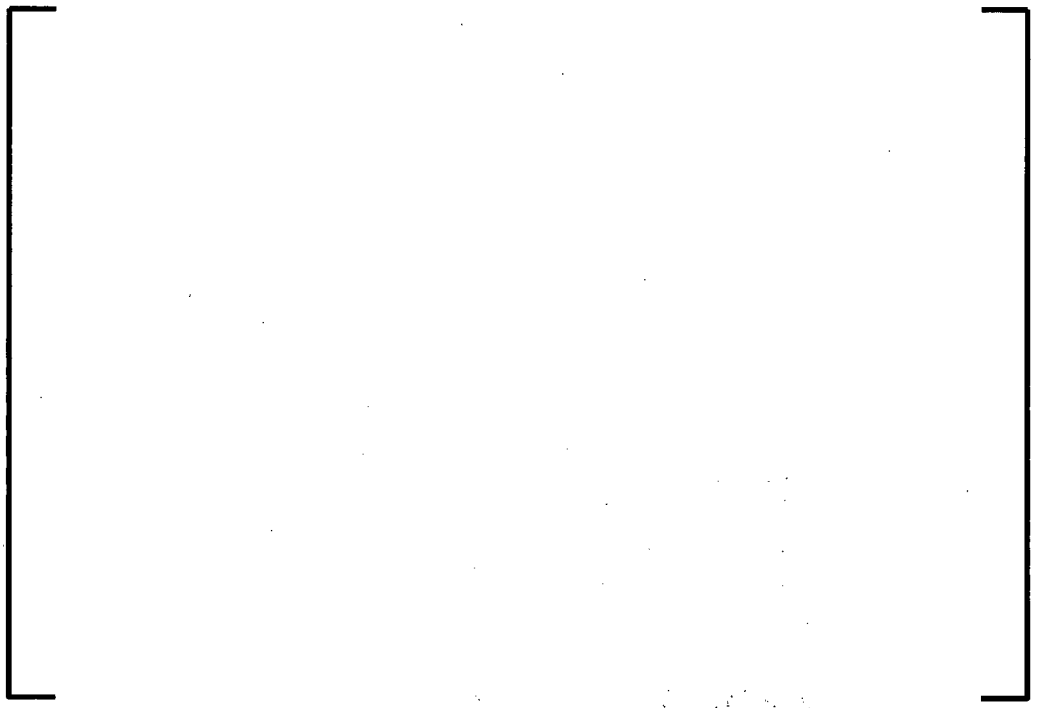

Figure 6-25 HFP/BOL Transient Fuel Centerline Temperature

Figure 6-26 HFP/BOL Transient Fuel Maximum Temperature

Figure 6-27 HFP/BOL Transient Cladding Maximum Temperature

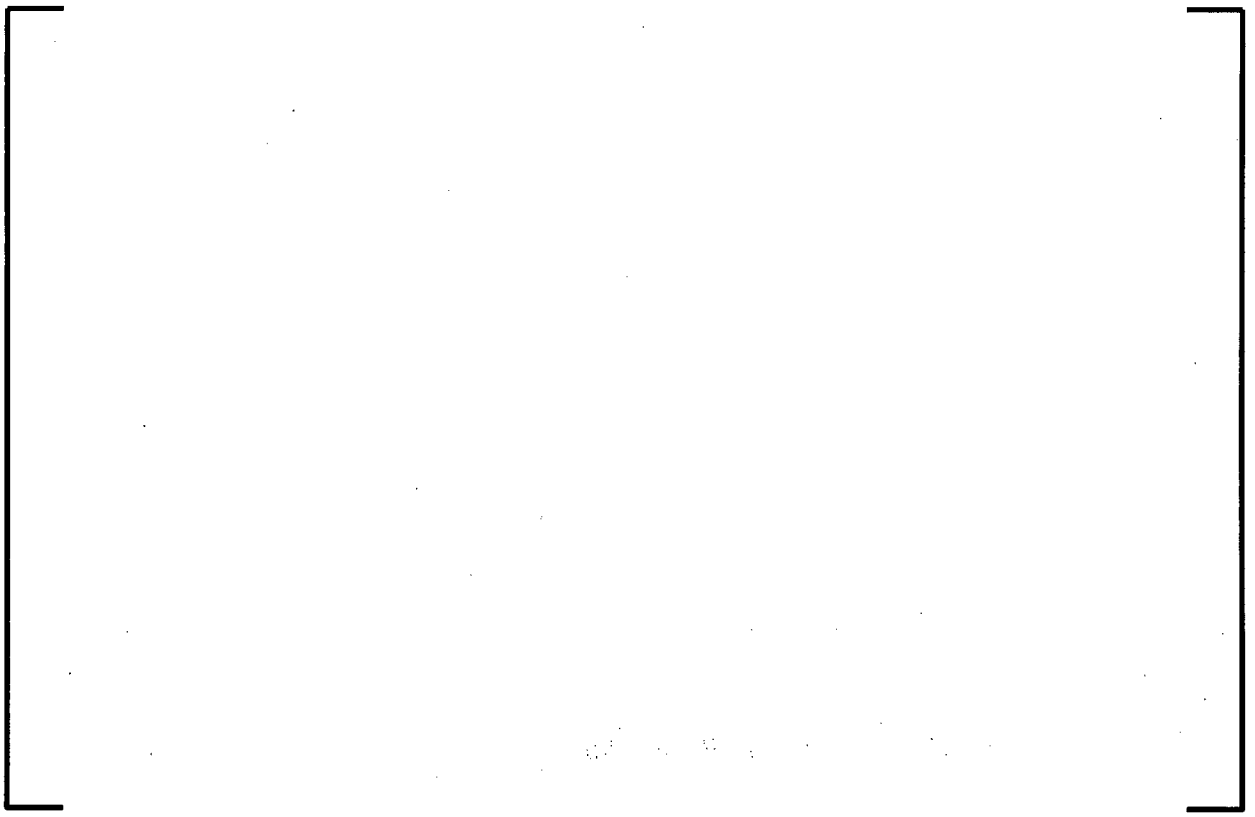

Note that the slight slope discontinuities of the LNYXT results are caused by the slope discontinuity at a fit point when using linear interpolation of the gap conductance table values.

7.0 APPLICATION OF BOUNDARY CONDITIONS AND UNCERTAINTIES

This section discusses the REA analysis boundary conditions and uncertainties for the plant transient model, the fuel rod model, and the failure analysis. The minimum requirement is to analyze/bound the limits of operation from HZP to HFP and from BOC to EOC. The Crystal River 3 vessel average temperature versus power level is shown in Figure 7-1. Since DNBR is one of the main failure criteria and it can be sensitive to the coolant temperature, the core powers of 0, 20, and 100 percent (i.e., at the transition temperatures) are analyzed to demonstrate where the limiting conditions occur relative to initial power level. In this sample problem, there are no discontinuous behaviors with cycle burnup and maximum MTC occurs at BOC, hence BOC and EOC conditions are adequate to bound the operation of the plant. If boundary conditions are introduced that are not continuous with burnup, intermediate cycle burnup discontinuities could be analyzed to justify these conditions. For example, if the rod position limit is desired to be different at BOC versus EOC, then an MOC case at the more restrictive condition could be defined and analyzed to justify the change.

7.1 NEMO-K Boundary Conditions and Uncertainties

The treatment of the NEMO-K boundary conditions and uncertainties is addressed in this section. The sensitivity calculations for the parameters which have conservatisms and/or uncertainties are presented to illustrate the conservatisms in the calculations. The application of conservatisms and uncertainties of the ejected rod worth, MTC, DTC, β_{eff}, fuel cycle design, and rod power peaking is addressed in the following sections. In general, the values for these parameters are set to bound the range of best estimate values adjusted by the uncertainty for the parameter and by an allowance for future cycles in the limiting direction.

7.1.1 Ejected Rod Worth

The uncertainty for the ejected rod worth is 15 percent for NEMO-K. This uncertainty is consistent with the currently employed methods that use NEMO[18]. The initial rod position prior to rod ejection and the change in fuel assembly cross sections due to the presence of control rods can be conservatively changed to bound the cycle-to-cycle variation of the observed ejected control rod worths and the uncertainty of 15%. The rod position limit for Crystal River 3 for the REA analysis is shown in Figure 7-2.

The Design and the REA Analysis Conditions for BOC and EOC at HFP and HZP are shown in Table 7-1. The range of calculated ejected rod worths for the example cycles 18, 19, and 20 at the EPU conditions are calculated for nominal HFP xenon at the rod position limits. The next row of information in Table 7-1 contains the cycle 20 calculated values with abnormal xenon distribution (power skewed to the top of the core) increased by the ejected rod worth uncertainty. The third row contains the bounding analysis values in NEMO-K for the REA example analysis. This data structure is repeated for MTC, DTC, and β_{eff} as discussed below.

7.1.2 MTC

A 2 pcm/°F uncertainty is used. The MTC uncertainty of 2 pcm/°F has been used as the acceptance criterion for current licensed cores. NEMO comparisons to measurement results support a value lower than 2 pcm/°F. The values in Table 7-1 for HZP are generated at zero xenon to maximize MTC for the cycle 18, 19, and 20 data.

7.1.3 DTC

A DTC uncertainty of 10 percent is used. A 10 percent uncertainty was determined based on the underprediction of the Doppler Power Coefficients (DPC) compared to measurements. Table 7-2 lists the DPC predictions to measurements for NEMO from Reference 19 and for NEMO using the fuel temperature model with T_{eff} from Section 6.2.4. The predictions of these models underestimate the measured magnitude of the DPC by approximately 20 percent with either model. The DPC is proportional to the Doppler Temperature Coefficient (DTC) with the proportional constant being the ratio of

the fuel temperature change to the percent power change. The bias could be from either the DTC or the fuel temperature predictions. These benchmarks are performed at beginning of cycle (BOC) for a cycle 1 core which has less than 6 EFPD of irradiation. Because the fuel properties for fuel with zero burnup are well characterized, it is unlikely that every pin in the core is biased low in the fuel temperature predictions. Therefore, a significant portion of underprediction in the DPC magnitude is probably due to the DTC component of the DPC. Having a lower prediction for the magnitude of the DTC is conservative for the ejected rod application due to a resultant lower negative reactivity feedback. Due to this conservatism and the 10 percent additional uncertainty, sufficient conservatism exists in the model, and no variation of the uncertainty is assessed as a function of burnup.

7.1.4 β_{eff}

A β_{eff} uncertainty of 5 percent is used that is obtained from Reference 20.

7.1.5 Fuel Cycle Design

Twenty four month core designs for cycles 18, 19 and 20 are used to define the bounding initial conditions. The base REA analysis model uses cycle 20. The proximity of the fuel to the ejected rod location will affect the local cal/g. Since the limits are not burnup dependent (see Section 2.1.1) and the MDNBR is evaluated for the full range of burnups (see Section 7.2.6), only the maximum ejected rod worth is investigated to determine the maximum power response of the peak assembly. Table 7-1 lists the nominal range of the key parameter values and the REA analysis values at BOC and EOC for both HZP and HFP for the available core designs.

A point kinetics model has very few inputs and the applicability to core designs has been demonstrated by using conservative reactivity core coefficients. Reference 5 demonstrated that 3-D kinetics can be used in a similar fashion for two quite different core designs and yield similar results to each other. Therefore, future cycle results can be compared to these results to verify the applicability of this analysis for Crystal River 3.

7.1.6 Transient Power and Rod Power Peaking

The example uncertainties and peaking allowances that are used for the REA analyses are shown in Table 7-3. These values are consistent with values employed for the safety analysis of other events. The $F_{\Delta H}$ and F_Q uncertainty components are combined appropriately and determined to be [ ] percent on $F_{\Delta H}$ and [ ] percent on F_Q for 100% power. These uncertainties are only be applied to the fuel rod model.

7.1.7 Base Analysis Conditions

The base analysis conditions for the other parameters listed in Section 4.1 are listed in Table 7-4.

7.1.8 Sensitivity Calculations for Plant Transient Calculations

Table 7-5 provides a list of parameters, the range of transients sampled, and the estimated range of sensitivity in terms of estimated power differences from Reference 5. The difference in core power, core power times peaking factor ($F_{\Delta H}$ and F_Q), and/or maximum adiabatic cal/g (see section 6.2.2) are compared at the time of peak power and after the pulse has flattened out. The largest of the range of results are tabulated. When more than one "Δ Case Conditions" is listed within a row, all of the listed changes were made in the input to obtain a single output sensitivity for each transient examined. The first sensitivity case is the base model with the uncertainties removed on ejected rod worth, β_{eff}, DTC, and MTC. The results can be significantly different for a prompt critical rod ejection calculation versus a non prompt critical rod ejection. The prompt critical excursion at EOC HZP has approximately [ ] percent conservatism or a delta of [ ] cal/g over the first second. The BOC HZP ejected rod worth is not prompt critical and is not as limiting as a higher initial power. Therefore, the BOC 25 percent power transient is used to replace the sensitivities of the analysis for BOC HZP. The BOC 25 percent power case has between [ ] percent conservatism. The HFP cases have the least conservatism [ ] depending on the time of the comparison. The minimum conservatism at peak power is [ ] percent. The smaller

value corresponds to the near static condition at greater than 5 seconds. The trend of decreasing conservatism as power increases is expected. The uncertainties are applied to maximize the resultant power change for a given reactivity insertion and the full power cases have the smallest change for the ejected rod worth.

For the remaining studies it is shown that [

] In general, the conclusions drawn from these results are applicable to Crystal River 3. Because the Crystal River 3 HZP cal/g is higher than that reported in Reference 5, those sensitivities are shown in Table 7-6 for the HZP cases. It can be seen in this table that the same trends are seen in the Crystal River 3 specific HZP cases as shown in Table 7-5. It is therefore concluded that the sensitivities generated in Reference 5 are applicable to the results presented in this report. If in future analyses, the cal/g of the analysis significantly exceeds the cal/g presented herein, the HZP sensitivity cases would need to be repeated for those conditions.

7.2 LYNXT Boundary Conditions and Uncertainties

The treatment for the LYNXT boundary conditions and uncertainties demonstrates which parameters need to be modeled and what conservatisms and uncertainties are applied. The application of boundary conditions and uncertainties for the pellet and cladding dimensions (geometry), cladding oxidation, radial pellet power distribution, coolant conditions, transient power, heat resistances, transient coolant heat transfer coefficient, and transient coolant conditions is addressed in the following sections.

7.2.1 Pellet and Cladding Dimensions (Geometry)

The LYXNT geometry model used for the rod ejection accident analysis is based upon a model used for the majority of the thermal-hydraulic and MDNBR evaluations. The model is developed to be consistent with the methods and geometries described in Reference 7. The LYNXT core model uses a $1/8^{th}$ symmetric model with [

] Figure 7-3 shows the baseline geometry for the radial layout of LYNXT model, which is constant for each axial node.

The geometry model for the temperature and enthalpy calculations within the fuel rod is based on the nominal dimensions for all cases. Engineering hot channel factors on the local heat flux and enthalpy rise are used to account for the off nominal dimensions and other manufacturing tolerances not covered by the power factors applied to NEMO-K peak rod powers.

Axially, the overall cladding length for the coolant heat transfer model is extended beyond the active fuel length to 155 inches to account for the lower and upper gas plenums.

7.2.2 Cladding Oxidation

The thermal conductivity of a zirconia corrosion layer on the cladding is lower than the M5™ cladding. The LYNXT code does not currently allow two regions of cladding properties to be used, but the decrease in the effective cladding thermal conductivity can be modeled with the CG/TDP property sets. To determine the impact of a maximum anticipated oxide thickness of 40 µm on DNBR and temperatures, a sensitivity calculation was performed using a cladding conductivity reduced to 66 percent of the nominal temperature dependent values. The study was run on the BOC

HFP rod ejection cases. The results showed that the peak cladding temperatures increased by less than [ ] and the peak fuel temperatures increased by less than [ ]. The timing of the DNBR response was minimally impacted and results indicated similar DNBR values. For the evaluation of the spectrum of rod ejections, the cladding conductivity properties with no oxide thickness are used in order to provide consistent predictions of the MNDBR.

7.2.3 Radial Pellet Power Distribution

The pellet radial power profile is primarily a function of burnup and initial enrichment. These two conditions are not affected by transient behavior. The burnup determines the amount of plutonium created in the rim of the pellet from U-238 resonance absorptions. At high burnups, the rim power can be twice as high as the average pellet power. The initial enrichment also has an effect, but it is less pronounced. Initially, the higher enrichment has a slightly higher surface power because of the higher self shielding of thermal flux. As the plutonium is created on the rim, the plutonium power fraction is less in a higher enrichment pellet, and the surface power is smaller than a lower enriched pellet at the same burnup. The initial enrichment and burnup for the pellet are initial conditions for the transient and the pellet radial power profile remains fixed during the transient. Section 7.2.6 addresses the effects of the radial power profile by examining enrichment and burnup sensitivities.

7.2.4 Coolant Conditions

The coolant boundary conditions used in the LYNXT models are the system pressure, inlet coolant temperature, and inlet mass flux. For the system pressure, the core exit pressure is used. This is adjusted downward by 65 psia to account for uncertainties in the measurement of the pressure. The minimum thermal design volumetric flow is reduced by [ ] percent for the core bypass to obtain the inlet mass flux boundary condition for the core. This inlet mass flux is reduced by 2.5 percent to account for uncertainties in the measurement of the flow. An additional local reduction in the inlet mass flux is applied to the bundle of interest. This provides a low value estimate of the

inlet mass flux. The inlet temperature and mass flux are determined by a heat balance performed in conjunction with the coolant average temperature as a function of power level. The inlet temperature is increased by 2 °F to account for uncertainties in the measurement of the temperature. The vessel average coolant temperature as a function of the core power is given in Figure 7-1. For transients less than 5-10 seconds, these thermal boundary conditions are held constant. For longer duration transients, time varying inputs may be used. Boundary conditions generated with RELAP5/MOD2 are evaluated to estimate the thermal performance for the 20 percent power case and the HFP cases for both BOC and EOC.

7.2.5 Transient Power

Each fuel rod node is assigned time dependent normalized axial power shapes and radial peaking factors. The fraction of core power is also assigned a time dependent array of values. These are used to approximate the relative global and local heating rates as determined by the NEMO-K neutronics calculations within the number of time-step limitations of the LYNXT code. For DNBR performance, one assembly of the core is considered to be the "assembly of interest." A detailed channel analysis is performed for the peak rod from this assembly. The transient axial shape factors are taken to be that of the fuel assembly of interest and are used for the entire core.

The rod powers for the 13 fuel rod nodes in the assembly of interest are conservatively assumed for this analysis to have [

]

No sensitivities are performed because this is a conservative model.

7.2.6 Heat Resistances in Fuel, Gap and Cladding

A representative approach is used to treat the heat resistances of the fuel and gap. The effect of the cladding resistance is addressed in section 7.2.2. A single uranium enrichment at the extreme burnups is evaluated. Sensitivity calculations are presented for burnup, uranium enrichment, and gadolinia content to illustrate the analysis conditions.

A typical EOC HZP power excursion from Reference 5 is presented for 2.0 and 5.0 w/o U_{235} at two different burnup conditions to determine the uranium enrichment and burnup sensitivity. The two different burnup conditions are maximum gap (near BOL) and end of life. [ ] The practical maximum burnup for a 2.0 and 5.0 w/o U_{235} pellet is estimated to be 50 and 70 GWD/MTU, respectively. The MDNBR performance is shown in Figure 7-4 for these cases. [

] This is due to higher gap conductance values and higher pellet rim power peaking. Calculations are performed with 5.0 w/o U_{235} fuel at 2.5 and 50 GWD/MTU burnup levels for the BOC cases and 20 and 70 GWD/MTU burnup levels for the EOC cases in order to bound the potential burnup thermal property states of the fuel rods.

Fuel loaded with gadolinia has a lower thermal conductivity than pure UO_2. The higher the gadolinia content, the lower the thermal conductivity of the fuel pellet. This increases the fuel temperatures of the gadolinia fuel if operated at the same LHGR as a UO_2 fuel rod. However the gadolinia rods typically have low maximum powers because

of lower fuel uranium enrichments and parasitic neutron absorption by the residual gadolinium isotopes. To determine if the analysis can be performed using only UO_2 properties, a sensitivity calculation is run on the Crystal River 3 BOC HFP power excursion with gadolinia loadings of 3 w/o and 8 w/o gadolinia. The gadolinia rods are run with the same power history as the pure UO_2 rod and with the maximum power level anticipated for a gadolinia loaded rod. [

]

Figure 7-5 shows the peak fuel temperatures for 0, 3, and 8 w/o gadolinia loadings. When the transient temperatures for gadolinia fuel are calculated with the power reduction factors, the maximum temperatures during the transient are bounded by the maximum UO_2 temperature. Because the UO_2 rod bounds the temperatures, the LYNXT calculations use the [

]

7.2.7 Coolant Heat Transfer Coefficient and Transient Coolant Conditions

Minimum flow is used and if the local DNBR is less than the design limit, the heat transfer correlation conservatively switches from Dittus-Boelter to include consideration of the inception of film boiling and post-CHF conditions. The DNBR design limit used for this sample problem is [ ] (Reference 21).

For the short duration scenarios (i.e., 0-5 seconds), the coolant boundary conditions are assumed constant and only the power distribution history is modeled. For the events that do not have an excore high flux trip (usually occurs within the first 2 seconds), coolant boundary conditions from RELAP5/MOD2 calculations using the NEMO-K core power history instead of the point kinetics are used to further degrade the LYNXT transient boundary conditions for the calculation of the thermal performance of the fuel rods.

7.3 Fuel Melt Limit

The UO_2 melting temperature is a function of burnup. The best estimate melt temperature is adjusted downward by a [

] The limiting centerline fuel melt (CFM) temperature is represented by the following equations from Reference 2 (Equation 12-3, pg 12-7):

[ ]

where:
T_{LC} = *reduced melt temperature, C*
T_{LF} = *reduced melt temperature, F*
Bu = *pellet burnup, GWD / tU*

For very fast transients, when the maximum pellet temperature may be close to the rim, the melting temperature limit must also account for local burnup levels being higher than the pellet average. During pellet irradiation, the radial pellet power distribution shifts from [ ] the pellet average power on the rim. So at the point of maximum pellet average burnup, the ratio of the rim burnup to the average burnup will be no higher than [ ]. This factor is used conservatively to lower the fuel melt limit for these regions. Using 70 GWD/MTU as the maximum average pellet burnup, the maximum rim burnup is no larger than [

]. The peak fuel temperature can not exceed this temperature.

7.4 Failure Boundary Conditions

For a core that has a peak rod exceeding the DNBR criterion for powers greater than 5%, a fuel census will be performed. The minimum DNBR Design Limit criterion used for this sample problem is [ ].

The most accurate approach to perform the census of fuel rod failures would be to obtain the rod by rod power distributions versus time from the neutronics 3-D kinetics

model and pass them to a thermal-hydraulic code to evaluate MDNBR. This would require an extensive analysis for each cycle to evaluate failures. Instead, a simplified approach to counting fuel rod failures based upon static calculations is defined and used for the methodology.

For an ejected rod transient at power, the thermal performance of the fuel rod is dependent upon the initial pre-ejection condition and the time dependent post-ejection power versus time. The higher the initial power, the less energy that can be deposited in a transient before MDNBR is reached. Conversely, the lower the initial power, the higher the energy that can be deposited before thermal limits are reached. For an ejected rod transient starting at zero power, the thermal performance of the fuel rod is solely dependent upon the time dependent post-ejection power versus time.

The initial fuel rod power distribution in the core is a static condition and is readily available from a neutronics calculation, in this case from the NEMO-K code. The static power distribution post-ejection without thermal reactivity feedback, commonly used for point kinetics, is also readily available. The time dependent power peaking in the core with thermal feedback has been examined to establish that a correlation exists between the static model and the kinetics model.

The Beginning of Cycle (BOC), Hot Full Power (HFP) case from Reference 5 is used as an example to illustrate the method. The number of failures for the Crystal River 3 sample problem is provided in Section 8.4. The relationship between the [

] is provided for this example in Figure 7-6. For each assembly the [

]. For the [

]. The fuel assemblies with low [ ] values are excluded from Figure 7-6 for clarity.

As shown in Figure 7-6, there is a linear relationship (monotonically increasing) for the fuel rods in the core so that a one-to-one correlation can be made between the [

]

[

]

Example Calculation

[ ] assemblies are used to represent the range of radial/axial power behavior during the transient. These assemblies are chosen over a range of [ ] with the corresponding highest [ ]. Assemblies [ ] are chosen for the fuel rod failure census. The [ ] for these assemblies are shown in Figure 7-6. In this BOC HFP example, the N05 fuel assembly has the highest [ ].

The transient power histories for the chosen assemblies/rods, including appropriate uncertainties, are analyzed with the thermal-hydraulic code LYNXT. The power versus time response of the assembly is iteratively scaled up or down by a multiplier until the DNBR reaches the design limit. The multipliers determined for the [ ] fuel assemblies of this example are provided in Table 7-7. For this example, the data in the column labeled "Multiplier" in Table 7-7 are the multipliers for the respective assemblies.

For example, any fuel rod that has a pre-ejection $F_{\Delta H} \geq$ [ ] that has a transient power history shape like assembly [ ] will fail. A similar relationship applies to the [ ] fuel assemblies.

[

] The values for the fuel assemblies used in the example are provided in Table 7-8. These multipliers behave linearly as shown in Figure 7-9. Since both correlations are linear, interpolation between the initial $F_{\Delta H}$ values can be used to obtain the $F_{\Delta H}$ or F_Q that would fail the fuel rod.

The pre-ejection fuel rod power is available for fuel rods in the core from the static calculation. The static post ejection failure limit for $F_{\Delta H}$ and F_Q are interpolated from the [ ] available values. If the fuel rod has a post ejection $F_{\Delta H}$ or F_Q greater than equal to the respective limit interpolated from its initial $F_{\Delta H}$, the fuel rod is assumed failed. This process is repeated for each analyzed power level. For the BOC HFP case, the number of pins estimated to be below the MDNBR design limit in the first few seconds of the transient (prompt response) is 0.3 percent.

For the cases that do not trip, as in the HFP BOC case, the core continues to operate in a near steady state neutronic condition so that a failure census is needed to account for the system degradation with time. The pressure slowly degrades due to primary coolant leakage through the assumed hole left by the ejected rod. Since this is a near steady state neutronic problem, the initial power distribution is no longer relevant; only the current power distribution contributes to the heat flux. The process of finding the $F_{\Delta H}$ and F_Q values that exceed the DNBR limit is repeated with LYNXT based on the pressure, flow, and inlet temperature provided by RELAP5/MOD2 and the steady state peaking from NEMO-K. For the HFP static case at BOC, the peak assembly power is scaled in LYNXT until it reaches the MDNBR design limit. The values of $F_{\Delta H}$ and F_Q for this case become the failure criteria for each rod in the core. Any pin exceeding the $F_{\Delta H}$

or F_Q failure criteria is assumed failed. The number of pins estimated to be below the DNBR design limit is 7.2 percent for this illustration from Reference 5.

This failed fuel rod census is performed for the at power transients where the fuel rod conditions reach the MDNBR design limit threshold for the potential of fuel failure. The MDNBR of the bounding peak fuel rod can exceed the design limit threshold by a small amount and still yield no failures for a particular core design. The peak pin includes a [ ] to bound cycle to cycle variations. However, the actual core power distribution that is used for the census only applies the uncertainties with no allowance for cycle to cycle variation. Without this conservatism, the peak pin analysis can reach the DNB threshold and can have no fuel failures estimated.

Table 7-1 Design and REA Analysis Conditions

Parameter		Unc[1]	BOC, HZP	BOC, HFP	EOC, HZP	EOC, HFP
Ejected Rod Worth (pcm)	Cycles 18-20[2]	-	397 to 431	35 to 36	315 to 327	45
	Cycle 20	+15%	473	59	362	69
	REA Analysis	-	715	60	741	73
MTC (pcm/°F)	Cycles 18-20[2]	-	-4.0 to -3.5	-8.2 to -7.5	-20.9 to -20.8	-34.5
	Cycle 20	+2	-2.0	-6.2	-18.8	-32.5
	REA Analysis	-	+2.5	-2.0	-14.5	-26.0
DTC (pcm/°F)	Cycles 18-20[2]	-	-1.56	-1.26 to -1.25	-1.73 to -1.72	-1.45
	Cycle 20	-10%	-1.40	-1.13	-1.55	-1.31
	REA Analysis	-	-1.30	-1.00	-1.40	-1.20
Beta Effective (10^{-5})	Cycles 18-20	-	663 to 664	660 to 661	539 to 540	537 to 538
	Cycle 20	-5%	630	627	513	511
	REA Analysis	-	580	580	480	480

Notes:

1. Unc = Uncertainty to be applied to nominal conditions.
2. Single values means that all three cycles had the same value.

Table 7-2 Doppler Power Coefficient Comparisons to Measured

Power Level, %	Measured DPC, pcm/%full power	NEMO with TACO3 Average Fuel Temperature DPC (% Difference {(M P)/M*100%})	NEMO with COPERNIC dynamic fuel rod model and Teff DPC (% Difference {(M-P)/M*100%})
30	-13.6	-11.1 (-18%)	[ ]
50	-12.7	-10.4 (-18%)	[ ]
75	-11.6	-9.2 (-21%)	[ ]

Table 7-3 Crystal River 3 Peaking Uncertainties

F_Q Uncertainty*	%
Nuclear	4.8
HCF	[ ]
Rod Bow	[ ]
Assembly Bow	[ ]
LBP/Gad	[ ]
Core Power	0.4
Total SRSS	[ ]
$F_{\Delta H}$ Uncertainty*	%
Nuclear	3.8
HCF	[ ]
Rod Bow	[ ]
Assembly Bow	[ ]
LBP/Gad	[ ]
Core Power	0.4
Total SRSS	[ ]

* For F_Q there are additional multiplicative peaking penalties of [ ] for grid depression and 7.36% and 15% for Quadrant Power Tilt (QPT) for Powers>60 and $\leq$60, respectively. For $F_{\Delta H}$ the same QPT penalties are also included.

Table 7-4 Base NEMO-K Analysis Conditions

Parameter	Definition of Value	Value
Rate of reactivity insertion	Milliseconds for full ejection	100
Reactor trip reactivity	Multiplier to the delta cross section for control rods that are initially withdrawn	[ ]
Heat resistances fuel, gap, and cladding		Nominal
Transient cladding-to-coolant heat transfer coefficient		Nominal except no voiding assumed
Heat capacities of fuel and cladding		Nominal
Fractional energy deposition in pellet	Unitless	0.973
Pellet radial power distribution	Enrichment of fuel from which the distribution is used	5.0 w/o
Fuel Temperature Model		New T_{eff}

Table 7-5 Plant Transient Sensitivity Calculations Summary

Parameter	Δ Case Conditions	Range of Evaluation	% difference (Δ /base-1) *100% [a]	Comments
Ejected rod worth, DTC, β_{eff}, and MTC	-15% ejected rod worth 10% increase in Doppler magnitude (Multiplier of ~1.10) 5% increase in β_{eff} -2 pcm/°F MTC	BOC 25 BOC HFP EOC HZP EOC HFP	[	]
Rate of Reactivity Insertion	0.1 to 0.2 sec for full length ejection	BOC 25 BOC HFP EOC HZP EOC HFP		
Reactor Trip Reactivity	9% increase in trip worth Base analysis is 9% less than nominal	BOC 60 EOC HZP		
Power Peaking	13%	Not tested in plant model		
Heat Resistances and Transient cladding to Coolant Heat Transfer				
Fuel conductivity,	-20% change in Fuel conductivity (Multiplier of 0.80)	EOC HZP		
Gap Conductance	Gap conductance increased by 100% (Multiplier of 2.0)	BOC 25 BOC HFP EOC HZP EOC HFP		
Coolant Heat Transfer	-4% flow assumed by fuel rod model	BOC 25 EOC HZP EOC HFP		]

Parameter	Δ Case Conditions	Range of Evaluation	% difference (Δ /base-1) *100% [a]	Comments
Others				
Fractional Heat Deposited in Fuel	0.974 to 0.966	BOC 25 BOC HFP EOC HZP EOC HFP	[	]
Pellet Radial Power Profile	5 w/o fuel to 2 w/o fuel	BOC 25 BOC HFP EOC HZP EOC HFP		
Neutron Velocities	+10%	BOC HFP EOC HZP EOC HFP		
Time step	Flux Δt 2x Fuel Δt =4x Moderator Δt =4x	BOC 25 BOC HFP EOC HZP EOC HFP		
Number of Fuel Rod Nodes	15 to 20 fuel nodes 3 to 5 cladding nodes	BOC HFP EOC HZP EOC HFP		
Effective Temperature	New T_{eff} Weighting change to a pellet average temperature	BOC 25 BOC HFP EOC HZP EOC HFP		]

Notes:

[a] Negative values indicate that the base case yields more conservative results.

Table 7-6 Crystal River 3 Plant Transient Sensitivity Calculations Summary for Prompt Response

Parameter	Δ Case Conditions	Range of Evaluation	% difference (Δ /base-1) *100% [a]	Comments
Ejected rod worth, DTC, β_{eff}, and MTC	-15% ejected rod worth 10% increase in Doppler magnitude 5% increase in β_{eff} -2 pcm/°F MTC	BOC HZP EOC HZP	[	]
Rate of Reactivity Insertion	0.1 to 0.2 sec for full length ejection	BOC HZP EOC HZP		
Reactor Trip Reactivity	9% increase in trip worth Base analysis is 9% less than nominal	BOC HZP EOC HZP		
Power Peaking	Peaking Uncertainties in Table 7-3	Not tested in plant model		]
Heat Resistances and Transient cladding to Coolant Heat Transfer				
Fuel conductivity,	-20% change in Fuel conductivity	BOC HZP EOC HZP	[	]
Gap Conductance	Gap conductance increased by 100%	BOC HZP EOC HZP		
Coolant Heat Transfer	-4% flow assumed by fuel rod model	BOC HZP EOC HZP		]

Parameter	Δ Case Conditions	Range of Evaluation	% difference (Δ /base-1) *100% [a]	Comments
Others				
Fractional Heat Deposited in Fuel	0.973 to 0.966	BOC HZP EOC HZP	[	]
Pellet Radial Power Profile	5 w/o fuel to 4 w/o fuel	BOC HZP EOC HZP		
Neutron Velocities	+10%	BOC HZP EOC HZP		
Time step	Flux Δt=2x Fuel Δt =4x Moderator Δt =4x	BOC HZP EOC HZP		
Number of Fuel Rod Nodes	15 to 20 fuel nodes 3 to 5 cladding nodes	BOC HZP EOC HZP		
Effective Temperature	New T_{eff} Weighting change to a pellet average temperature	BOC HZP EOC HZP		

Notes:

[a] Negative values indicate that the base case yields more conservative results.

Table 7-7 BOC HFP Example Fuel Failure Census $F_{\Delta H}$ Threshold Determination

[ ]

Table 7-8 BOC HFP Example Fuel Failure Static Post-ejection $F_{\Delta H}$ and F_Q Threshold Determination

[ ]

Where:

mult = $F_{\Delta H}$ multiplier factor from Table 28-1 that brings the fuel rod to the MDNBR SAFDL
fdh0 = initial maximum $F_{\Delta H}$ of fuel rods in the selected fuel assembly
fdh1 = post-ejection maximum $F_{\Delta H}$ of fuel rods in the selected fuel assembly
fq1 = post-ejection maximum F_Q of fuel rods in the selected fuel assembly

Figure 7-1 Average Coolant Temperature with Power

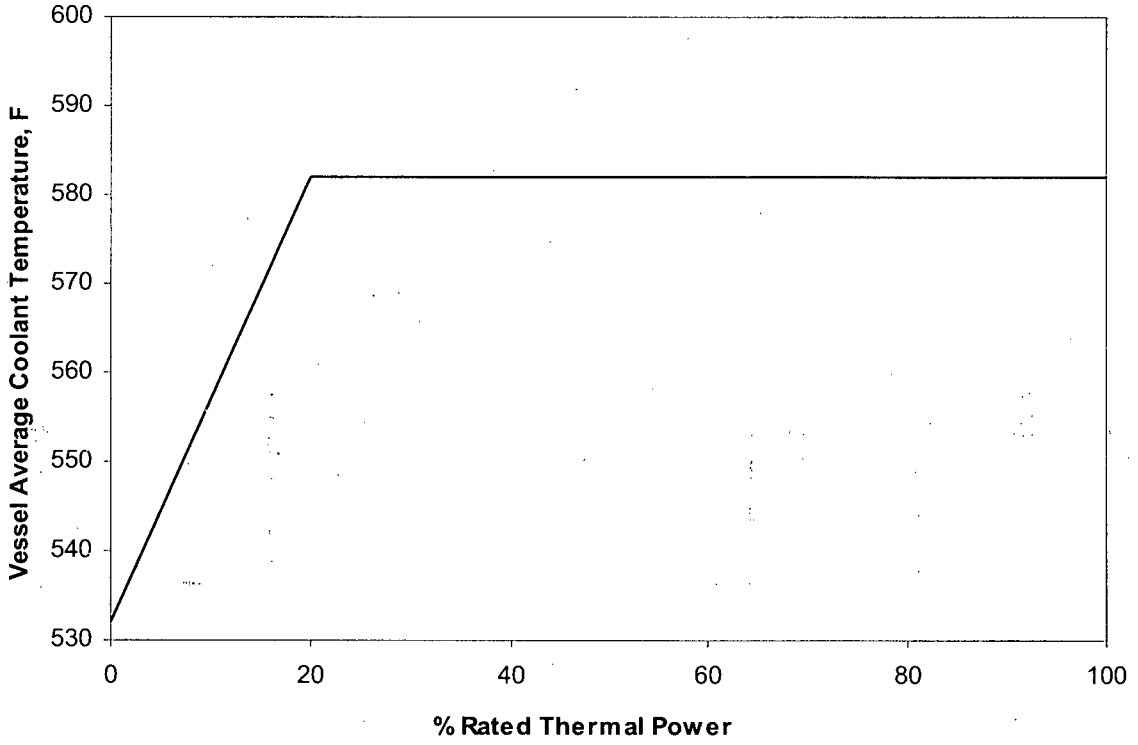

Figure 7-2 Rod Position Limits for REA Analysis

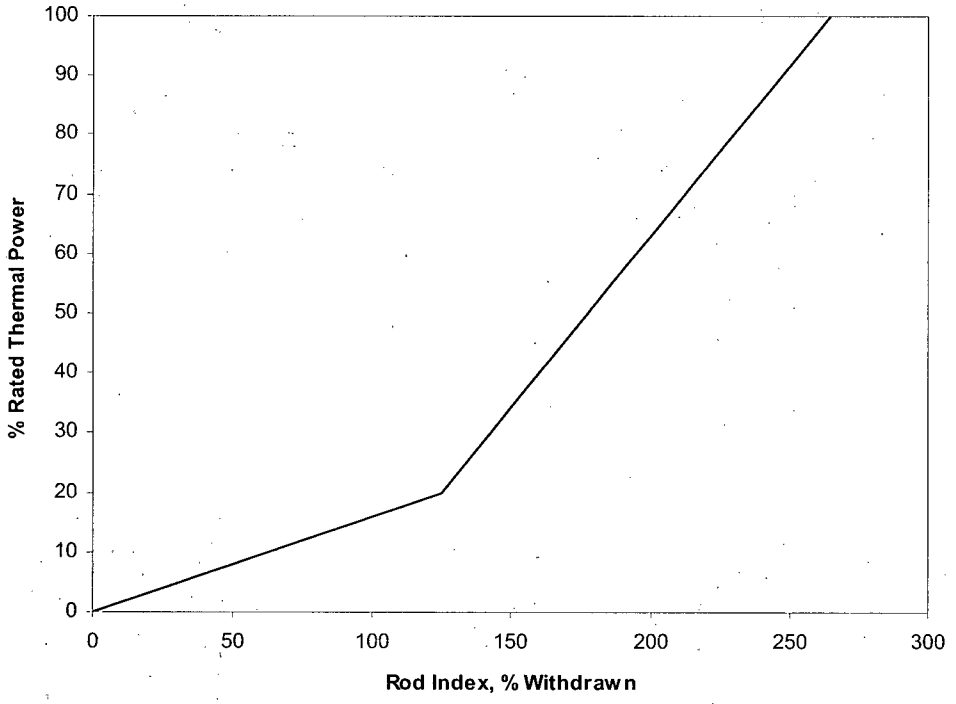

Figure 7-3 17-Channel LYNXT Model Diagram

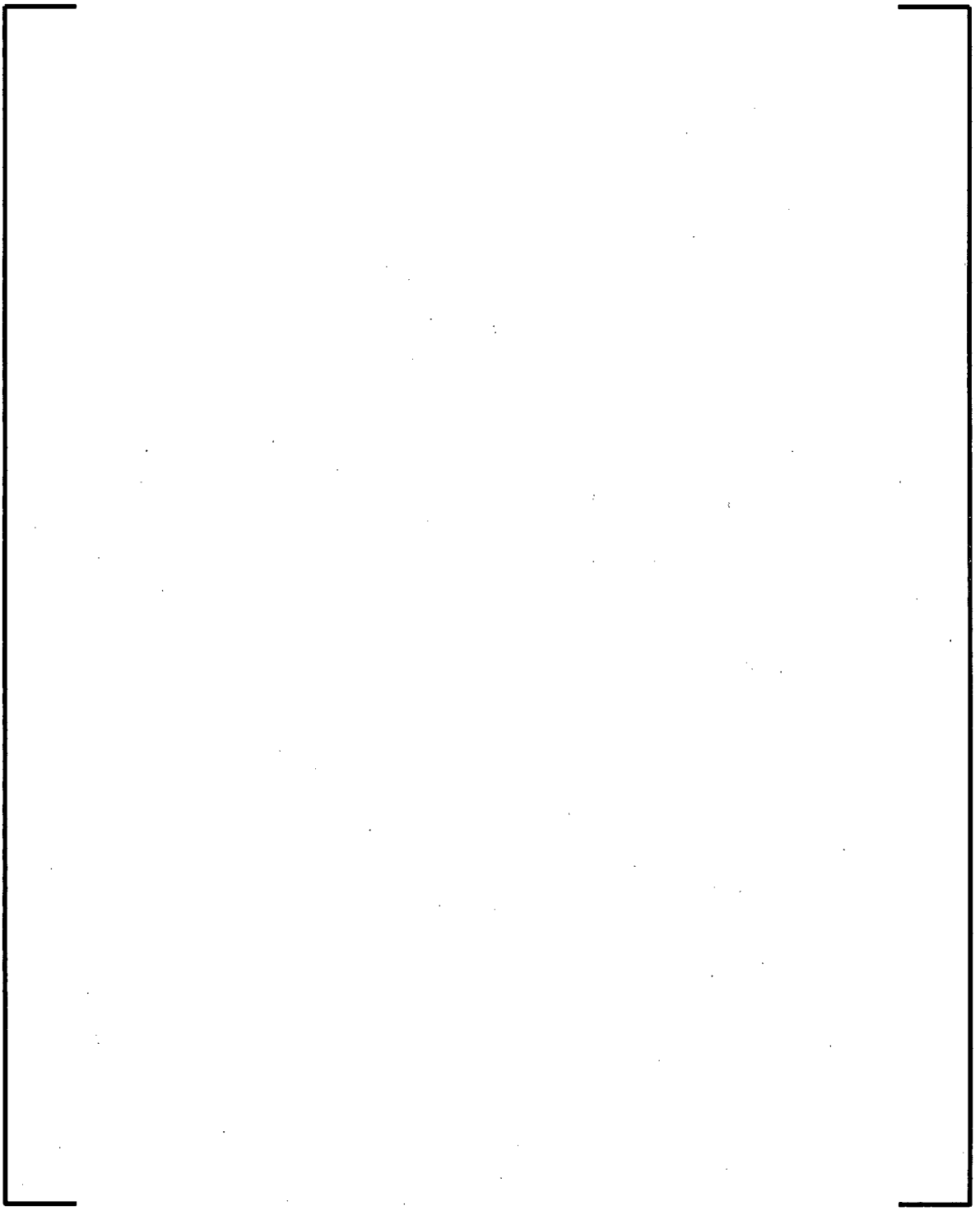

Figure 7-4 MDNBR Uranium Enrichment Response for EOC HZP

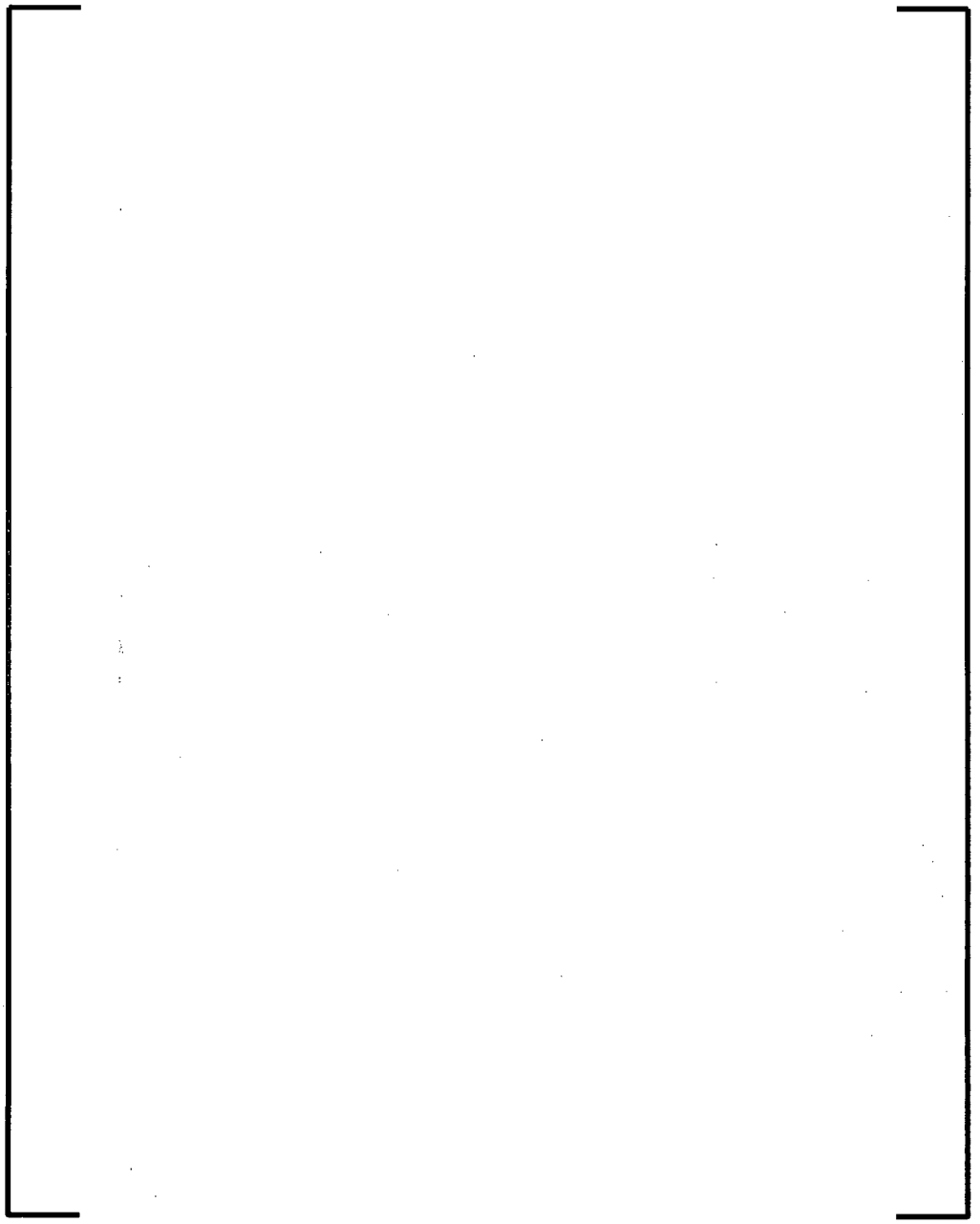

Figure 7-5 UO_2 and Gadolinia Fuel Temperatures for BOC HFP

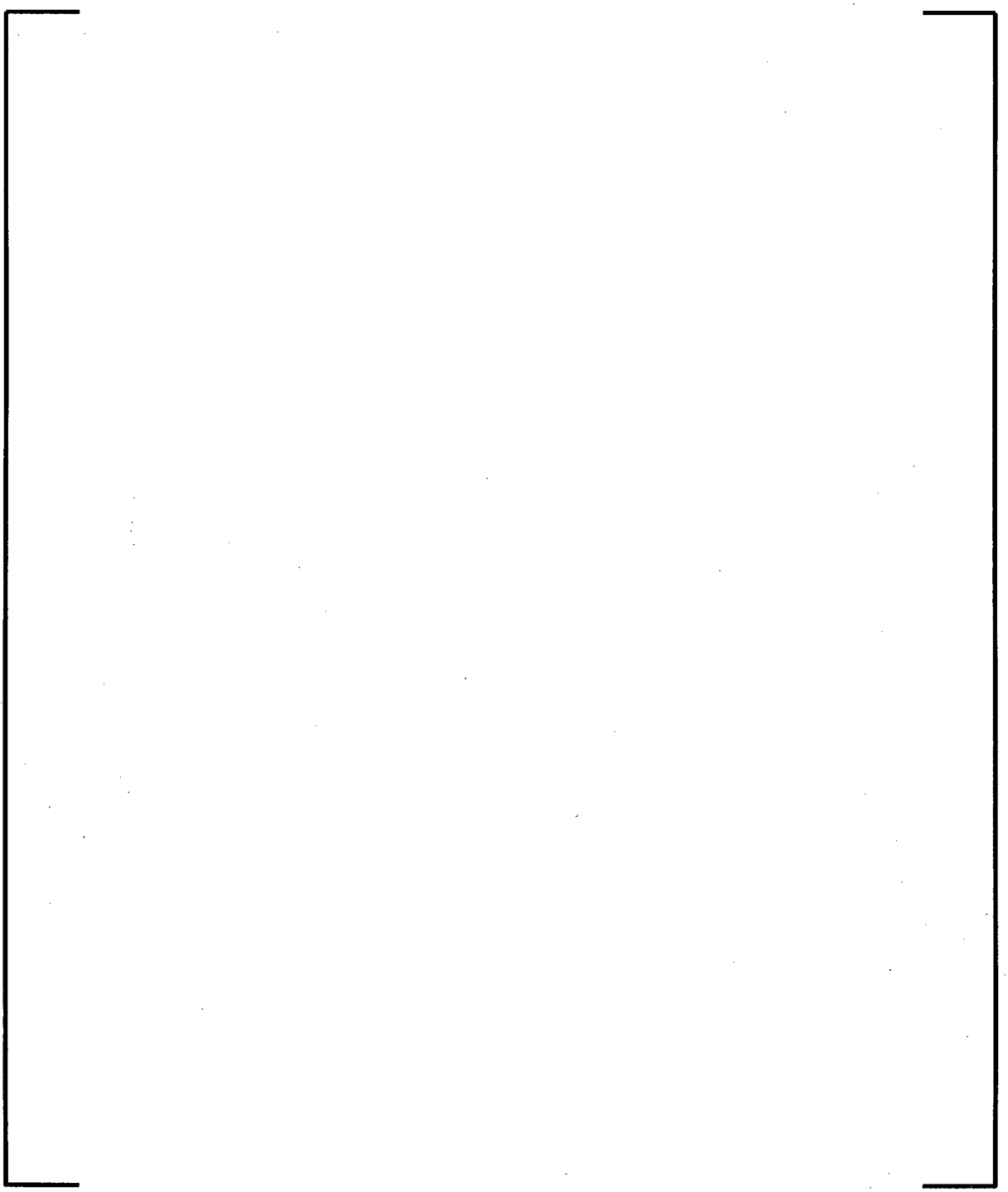

Figure 7-6 Transient Versus Static Peaking Ratios at 0.150 Seconds

Figure 7-7 Transient Versus Static Peaking Ratios at 0.044 Seconds

Figure 7-8 Transient Versus Static Peaking Ratios at 0.250 Seconds

Figure 7-9 Post-Ejection Static DNBR Limits

8.0 CRYSTAL RIVER 3 SAMPLE PROBLEM RESULTS

The Crystal River 3 sample problem results section contains the detailed results of this REA methodology. The trip functions that are used by this sample problem are shown in Table 8-1. The overall sequence of events for each of the transients is listed in an event timeline presented in Table 8-2 through Table 8-7.

8.1 NEMO-K Results

The transient simulations for 0, 20, and 100 percent power are performed at BOC and EOC. The results for core power, $F_{\Delta H}$ and F_Q are shown in Figure 8-1 through Figure 8-6. Because the ejected rod location starts at a lower power than the surrounding assemblies, it may be advantageous to perform an analysis for the ejected rod location and an analysis for the core peak. To illustrate, Figure 8-7 shows the nominal peaking from NEMO-K for the ejected rod and peak locations for the BOC HFP condition. For this particular example, the initial and time dependent core $F_{\Delta H}$ and F_Q values are higher than those of the ejected rod location and the extra analysis is not needed.

Core pressure, flow, and inlet temperature are held constant during these simulations. The 20 percent power and the HFP transient powers at BOC and EOC do not reach a high flux trip signal. Those conditions without a high flux trip require a RELAP5/MOD2 analysis, which is described in the following section.

8.2 RELAP5/MOD2 Evaluation

The RELAP5/MOD2 evaluation section reviews the consequences of using a constant pressure, inlet temperature and flow in NEMO-K and estimates its impact on the fuel rod model. For the plant model in NEMO-K, two conditions are reviewed:

- an increase in pressure due to the power insertion.
- operation without trip.

A calculation is performed to determine how an increase in pressure affects the core reactivity during the initial phase of the rod ejection. The power pulse after the ejection could cause an increase in the pressure if there is no hole in the primary system from the ejected rod. A maximum pressure increase of 40 psia is estimated. A power search is performed at EOC HFP at +40 psia. The temperature increase occurred after the peak power and would only affect the static power thereafter. The power difference is [ ].

For the condition of no trip with a leak in the primary, RELAP5/MOD2 calculations are performed to estimate the range of thermal conditions that could be reached for each case without a high flux trip. Two leak conditions are simulated as a full leak and a partial leak. The full leak area is defined as the inside diameter of the control rod flange (2.765") as the break diameter and applied to the top of the upper head volume. An intermediate break size (partial leak) is defined as the area of the control rod flange minus the area of the control rod lead screw. The simulations continue until a trip in the RELAP5/MOD2 model is reached. This simulation did not include any actions for the non-safety control systems that would tend to improve the situation. The RELAP5/MOD2 RCS pressure and inlet temperature results for 20 percent power and HFP at BOC are shown in Figure 8-8 and Figure 8-9, respectively. The RELAP5/MOD2 RCS pressure and inlet temperature results for 20 percent power and HFP at EOC are shown in Figure 8-10 and Figure 8-11, respectively. The REA simulations for the 20 percent and HFP initial conditions without a high flux trip are eventually predicted to trip on low RCS pressure, high RCS pressure, high RCS hot leg temperature, or variable low RCS pressure trip (VLPT).

These RELAP5/MOD2 simulations are performed with either a bounding power versus time or more coupled response between the RELAP5/MOD2 and NEMO-K conditions. For the bounding power approach, the duration is slow enough that the core is neutronically in near equilibrium with the thermal conditions. Rather than running this specific transient in NEMO-K, several static power searches are performed with the rod ejected at various thermal conditions from RELAP5/MOD2 to determine the limiting

power that may be reached after the initial ejection. These results are shown in Table 8-8. The maximum power and the time dependent range of thermal conditions from these cases are evaluated using the fuel rod model with LYNXT. For the coupled approach, the power history with time from NEMO-K is passed to the RELAP5/MOD2 simulation and the plant thermal boundary condition transient history (RCS pressure, core inlet temperature, and core inlet mass low rate) is passed to the NEMO-K simulation. The process is repeated until the results are adequately converged which is when the successive case power ratio to the previous case is between 0.995 and 1.005 (or a percent difference magnitude less than 0.5%). This process is used for the BOC 20% power simulation. The NEMO-K results from this process are shown in Figure 8-12. This figure shows the fraction of power (FOP), $F_{\Delta H}$, and F_Q with the RELAP5/MOD2 thermal hydraulic boundary conditions as inputs to NEMO-K (Core Exit Pressure, Core Inlet Temperature, Inlet Mass Flow Rate). There are two NEMO-K calculations performed with the RELAP5/MOD2 boundary conditions for a full leak break size (labeled "Full") and a partial leak break size (labeled "Partial"). The RELAP5/MOD2 results with the NEMO-K power simulations are shown in Figure 8-8.

8.3 LYNXT Results

The transient simulations are performed for 0, 20, and 100 percent power at BOC and EOC. The results for the MDNBR, peak fuel temperature, peak cladding temperature, and peak radially averaged enthalpy rise are shown in

Figure 8-13 through Figure 8-30.

The BOC 20 percent power, BOC HFP, EOC 20 percent power, and the EOC HFP transient simulations did not trip on high neutron flux. LYNXT models the RELAP5/MOD2 thermal boundary conditions as a function of time. The NEMO-K power results for the first 5 to 8 seconds are followed by a linear progression to the highest power predicted by the static NEMO-K cases. During the transient for the 20% power BOC case, the minimum DNBR for the peak power assembly does not exceed the design limit until after 8.3 seconds for the full leak and does not exceed the design limit

for the partial leak. After this point the post-CHF heat transfer mode is simulated causing the rapid rise in the peak cladding temperature. The 20% power EOC case did not exceed the MDNBR design limit.

For the BOC and EOC 100 percent power cases, the power level stabilizes at a power level to balance the reactivity. A conservative estimate of 106.4 percent for BOC and 104.0 percent for EOC is used in NEMO-K with no void reactivity feedback. For both BOC and EOC, the minimum DNBR for the peak power assembly rapidly drops below the DNBR design limit (before 10 seconds into the transient) and continues to degrade as the plant heats up and system pressure drops. The thermal boundary conditions continue to degrade and increase the peak fuel and cladding temperatures. The rate of increase reduces as the system approaches thermal equilibrium. The RELAP5/MOD2 model did not include the VLPT function, which would terminate the transient before the plant system trip on low pressure. The VLPT function is required to terminate the event to prevent the clad from reaching [ ]. In addition, it provides added protection in the event that the core achieves different powers, temperatures, and pressures than analyzed by the RELAP5/MOD2 by enabling the same relative DNBR protection. Based on this trip function applied to the RELAP5/MOD2 core conditions, a trip is estimated to occur for the HFP REA transients by 19 seconds for the full leak and 25 seconds for the partial leak.

The EOC HZP transient fuel pin reaches 34 Δcal/g as shown in Figure 8-24. The failure criterion for powers below 5 percent is 150 cal/g for the peak radial average enthalpy or 125 Δcal/g. The EOC HZP peak radial average enthalpy is less than 55 cal/g and the event is terminated due to the high flux trip and rods being inserted by 3.5 seconds.

Even though the DNBR design limit is exceeded for four of the evaluated cases, in no case did the peak fuel temperatures exceed the fuel melt limit for the expected higher burnup fuel [

]. The maximum temperatures calculated are 4231°F with the limiting fuel temperature case of BOC HFP partial leak at 25 seconds into the transient (time of

estimated VLPT trip event termination). The maximum cladding temperature was 1436 °F for with the limiting cladding temperature case of EOC HFP partial leak at 25 seconds into the transient (time of estimated VLPT trip event termination). The maximum prompt radially averaged fuel enthalpy rise determined for the entire spectrum of cases was less than 34 Δcal/g (EOC HZP) and a maximum integrated total enthalpy was less than 111 cal/g (EOC HFP).

8.4 Rod Census

The number of rods failed was estimated for BOC 20 percent, BOC HFP, and EOC HFP. For each transient, the rods may need to be counted for two different thermal conditions, the prompt response (i.e., 0-5 seconds) and the delayed response (i.e., greater than 5 seconds) when a high flux trip does not occur from the power pulse. The latter case reduces to a static case where the neutron power is in equilibrium with the thermal output of the core. None of the assemblies experienced a prompt enthalpy rise of more than 23 Δcal/g so that the fuel failure analysis does not need to consider the elevated dose requirements outlined in Section 2.3. In addition, none of the cases exceeded the fuel failure criterion during the power pulse so that only the delayed response needed to be considered for fuel failure census.

LYNXT cases are run for each condition to determine the power at which the limiting fuel rod has a MDNBR of [ ]. The $F_{\Delta H}$ and F_Q for this condition are used as the failure criteria. Any rod with an $F_{\Delta H}$ or F_Q exceeding this value is assumed failed. The cases with no trip (delayed response) can be treated simply as a static case and therefore, only one assembly of interest distribution is needed to define the limiting $F_{\Delta H}$ and F_Q prior to reaching the MDNBR. Table 8-9 contains the estimated rod failures for each of the transients.

8.5 Coolability Criterion

A limiting criterion in these simulations is the [ ] clad temperature limit for coolability. This high temperature limit is only approached after the pin is in DNB. The

fuel failure census is examined to determine if high burnup pins are in DNB. The census is repeated for all the cases with the peak pin in DNB with an artificial 5% increase in peaking to investigate the burnups of the pins that would be failed if the net effect of the event is 5 percent higher. The maximum pin burnup in the assemblies that contained pin failures is shown in Table 8-10. This demonstrates that all the BOC failures have burnups less than 31 GWD/MTU and all the EOC failures have burnups less than 33 GWD/MTU. The maximum pin pressure for pins with burnups below 33 GWD/MTU are typically less than system pressure and ballooning is not plausible. Therefore, the assumption of a [ ] clad temperature limit for coolability is conservative. Future applications may define alternative coolability criterion that have internal pin pressure and/or burnup constraints that use this methodology.

8.6 Summary Results

The overall REA results for the plant transient analysis and fuel rod model are shown in Table 8-11 and Table 8-12 for BOC and EOC, respectively. The maximum prompt Δcal/g is calculated at one pulse width after the peak. For those cases that have no discernable pulse, the value at 1.0 second is used. For all of the transients modeled that have fuel failures, the maximum Δcal/g is less than the threshold value (31.2 Δcal/g) to consider increased fission gas release and there is no fuel melt. Therefore, no equivalent pin failure adjustments are needed to the DNBR failures calculated. For all of the transients modeled there is no fuel melt and no cladding temperatures exceed [ ] prior to trip. The results are within the criteria listed in Table 2-1. The most limiting case for the number of fuel failures is the BOC 20 percent power case with the full leak size. This case is estimated to have 1.4 percent fuel failures.

Table 8-1 Trip Signal Parameters in Analysis

Trip Parameter	Analysis Limit	Sensor Scram Delay (seconds)
Excore High Flux, %RTP	112 (3/4 detectors[1])	0.42
Low RCS Pressure, psia	1893.95	0.61
High RCS Pressure, psia	2400.00	0.61
High Reactor Coolant Temperature, °F	620.00	5.67
Variable Low RCS Pressure, psia (T_{hot} is the RCS Hot Leg temperature)	$11.59*T_{hot}$-5049.46	5.67

Notes:

[1] Need 3 of 4 to trip in the model to conservatively account for 1 detector assumed failed and 2 of the remaining 3 detectors to sense a trip.

Table 8-2 Event Timeline for BOC HZP

Event	Time (seconds)
Ejection begins	0.000
Rod N12 fully ejected	0.100
High Flux Trip threshold reached	0.295
Peak Power reaches 285% power	0.305
Initial Minimum MDNBR/DL of 2.15 reached for 50 GWD/MTU properties	0.350
Prompt enthalpy rise of 21.1 Δcal/g	0.450
Scram control rods begin to insert	0.795
Scram control rods are fully inserted	3.195

Table 8-3 Event Timeline for BOC 20% Power

Event	Time (seconds)
Ejection begins	0.000
Rod N12 fully ejected	0.100
Peak Power reaches 111.3% power	0.137
Prompt enthalpy rise of 23.0 Δcal/g	1.00
Power drops to 43.7% power	38.3
MDNBR drops below limit for 2.5 GWD/MTU properties	8.4 – Full Leak N/A – Partial Leak
MDNBR drops below limit for 50 GWD/MTU properties	11.5 – Full Leak N/A– Partial Leak
Event terminated on • Full Leak: High RCS Hot Leg Temperature Trip Full leak reaches 43.7% power, 0.824 MDNBR/DL • Partial Leak: High RCS Pressure Trip Partial leak reaches 45.7% power, 1.001 MDNBR/CL	 39.3 – Full Leak 30.3 - Partial Leak

Table 8-4 Event Timeline for BOC HFP

Event	Time (seconds)
Ejection begins	0.000
Rod N12 fully ejected	0.035
Peak Power reaches 109.8% power	0.100
Prompt enthalpy rise of 6.3 Δcal/g	1.000
Power drops to 106.1 percent full power	6.90
MDNBR drops below limit for 50 GWD/MTU properties	11.0 – Full Leak 13.5 – Partial Leak
Trip initiated and control rods at 1/3 insertion based on VLPT trip setpoint • Full reaches 106.1% power, 0.929 MDNBR/DL • Partial reaches 106.2% power, 0.944 MDNBR/DL	 19.0 – Full Leak 25.0 – Partial Leak
RELAP is terminated on Low RCS Pressure Trip[1] • Full leak reaches 106.2% power • Partial leak reaches 106.3% power	 31.6 – Full Leak 49.8 – Partial Leak

[1] RELAP model does not have VLPT function and continues to run to these conditions.

Table 8-5 Event Timeline for EOC HZP

Event	Time (seconds)
Ejection begins	0.000
Rod N12 fully ejected	0.100
High Flux Trip threshold reached	0.205
Peak Power reaches 671% power	0.218
MDNBR drops below limit for 50 GWD/MTU properties	0.233
MDNBR increase above the limit for 50 GWD/MTU properties	0.300
Prompt enthalpy rise of 33.8 Δcal/g	0.350
Scram control rods begin to insert	0.705
Scram control rods are fully inserted	3.105

Table 8-6 Event Timeline for EOC 20% Power

Event	Time (seconds)
Ejection begins	0.000
Rod N12 fully ejected	0.100
Peak Power reaches 187.7% power	0.140
Prompt enthalpy rise of 17.4 Δcal/g	1.00
Power drops to 30.8% power	12.3
Trip initiated and rods at 1/3 insertion based on VLPT trip setpoint for partial leak Partial leak reaches 31.5% power, 1.263 MDNBR/DL	 56.0 – Partial Leak
• Full Leak event terminated on Low RCS Pressure: reaches 31.2 %power, 1.284 MDNBR/DL • RELAP is terminated for Partial Leak Event on High RCS Hot Leg Temperature: reaches 31.8 %power [1]	39.3 – Full Leak 90.6 – Partial Leak

[1] RELAP model does not have VLPT function and continues to run to these conditions.

Table 8-7 Event Timeline for EOC HFP

Event	Time (seconds)
Ejection begins	0.000
Rod N12 fully ejected	0.035
Peak Power reaches 113.9% power	0.060
Prompt enthalpy rise of 7.6 Δcal/g	1.000
Power drops to 104.0% power	6.90
MDNBR drops below limit for 50 GWD/MTU properties	9.20 – Full Leak 11.0 – Partial Leak
Trip initiated and rods at 1/3 insertion based on VLPT trip setpoint • Full reaches 104.0% power, 0.939 MDNBR/DL • Partial reaches 104.0% power, 0.949 MDNBR/DL	 19.0 – Full Leak 25.0 – Partial Leak
RELAP is terminated on Low RCS Pressure Trip[1] • Full leak reaches 104.0% power • Partial leak reaches 104.0% power	 29.0 – Full Leak 44.4 – Partial Leak

[1] RELAP model does not have VLPT function and continues to run to these conditions.

Table 8-8 Static Power Search

Core Condition	ΔPressure (psi)	Δ FOP
BOC HFP	0 to -300	-1%
EOC HFP	0 to -300	-5%
BOC 20%	0 to -300	~0%
EOC 20%	0 to -300	-4%

Table 8-9 Estimated Rod Failures

Core Condition	% Failed Rods in Census	
	Prompt	Static
BOC 20%	0	1.4
BOC HFP	0	1.2
EOC 20%	0	0
EOC HFP	0	0.0*

* Note: Although MDNBR [ ] for the conservative peak analysis to bound future cycles, the actual distribution did not result in any failures.

Table 8-10 Estimated Maximum Burnup of Rod Failures

Core Condition	Max Pin Exposure GWD/MTU
BOC HFP	0.2
BOC 20%	30.8
EOC HFP	32.7

Table 8-11 Ejected Rod Analysis Results for BOC

Parameter	Criterion	% Power Level		
		0	20	100
Rod Insertion Limit, % Withdrawn	-	0	125	265
Maximum Ejected Rod Worth, pcm	-	715	556	60
β_{eff}	-	0.0058	0.0058	0.0058
MTC, pcm/°F	-	2.5	0.0	-2.0
DTC, pcm/°F	-	-1.3	-1.24	-1.0
Initial F_Q	-	NA[a]	3.476	2.531
Maximum Transient F_Q	-	14.838	8.168	2.712
Initial $F_{\Delta H}$	-	NA[a]	2.272	1.710
Maximum Transient $F_{\Delta H}$	-	8.136	5.075	2.014
Maximum Neutron Power, FOP	-	2.85	1.11	1.10
Maximum cal/g	$\leq$ 150	50.9	101.9[b]	98.8[b]
Maximum Δcal/g, prompt	$\leq$ 125	21.1	23.0[b]	6.3[b]
Maximum Fuel Temperature, °F	< [ ]	1670	3804	4231
Maximum Cladding Temperature, °F	< [ ]	741	1353	1355
MDNBR/Limit for rod failure	$\leq$ 1.000	2.150[b]	0.824	0.929
Time of High Flux Trip (initiation of safety bank insertion), seconds	-	0.795	None	None
Equivalent nominal rods failed, %	$\leq$ 4.3	0.0	1.4	1.2

Notes:

[a] Not applicable since initial stored energy above the coolant temperature is zero.

[b] Criterion not applicable for these initial power levels

Table 8-12 Ejected Rod Analysis Results for EOC

Parameter	Criterion	% Power Level		
		0	20	100
Rod Insertion Limit, % Withdrawn	-	0	125	265
Maximum Ejected Rod Worth, pcm	-	741	535	73
β_{eff}	-	0.0048	0.0048	0.0048
MTC, pcm/°F	-	-14.5	-25.0	-26.0
DTC, pcm/°F	-	-1.4	-1.36	-1.2
Initial F_Q	-	NA[a]	5.374	2.250
Maximum Transient F_Q	-	27.21	11.761	2.835
Initial $F_{\Delta H}$	-	NA[a]	2.272	1.711
Maximum Transient $F_{\Delta H}$	-	7.703	4.581	2.076
Maximum Neutron Power, FOP	-	6.71	1.88	1.14
Maximum cal/g	$\leq$ 150	54.1	77.8[b]	111.0[b]
Maximum Δcal/g, prompt	$\leq$ 125	34	17.4[b]	7.6[b]
Maximum Fuel Temperature, °F	< [ ]	1675	3354	4013
Maximum Cladding Temperature, °F	< [ ]	1007	774	1436
MDNBR/Limit for rod failure	$\leq$ 1.000	0.917[b]	1.263	0.939
Time of High Flux Trip (initiation of safety bank insertion)	-	0.705	None	None
Equivalent nominal rods failed, %	$\leq$ 4.3	0.0	0.0	0.0

Notes:

[a] Not applicable since initial stored energy above the coolant temperature is zero.

[b] Criterion not applicable for these initial power levels

Figure 8-1 BOC 0% Power Transient

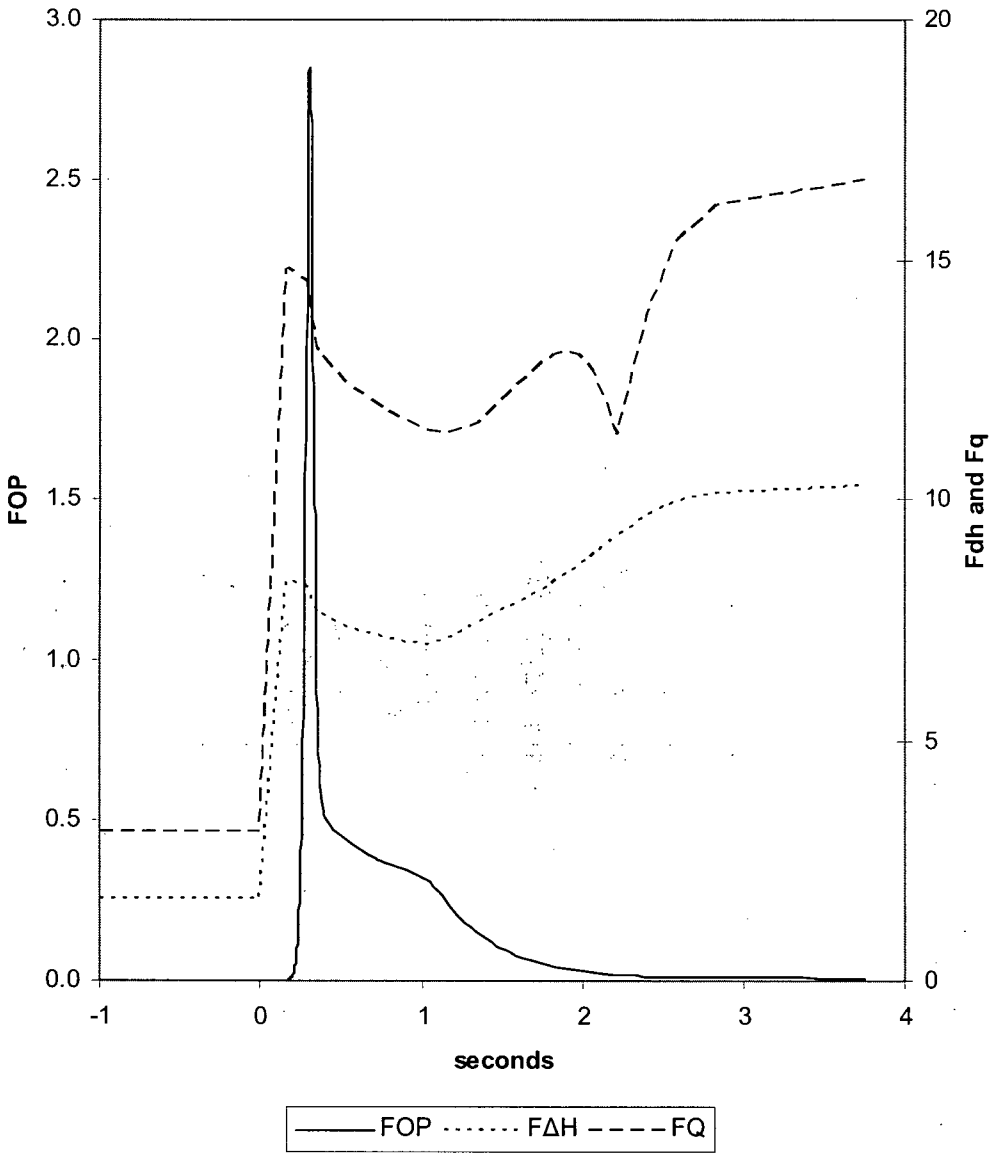

Figure 8-2 BOC 20% Power Transient

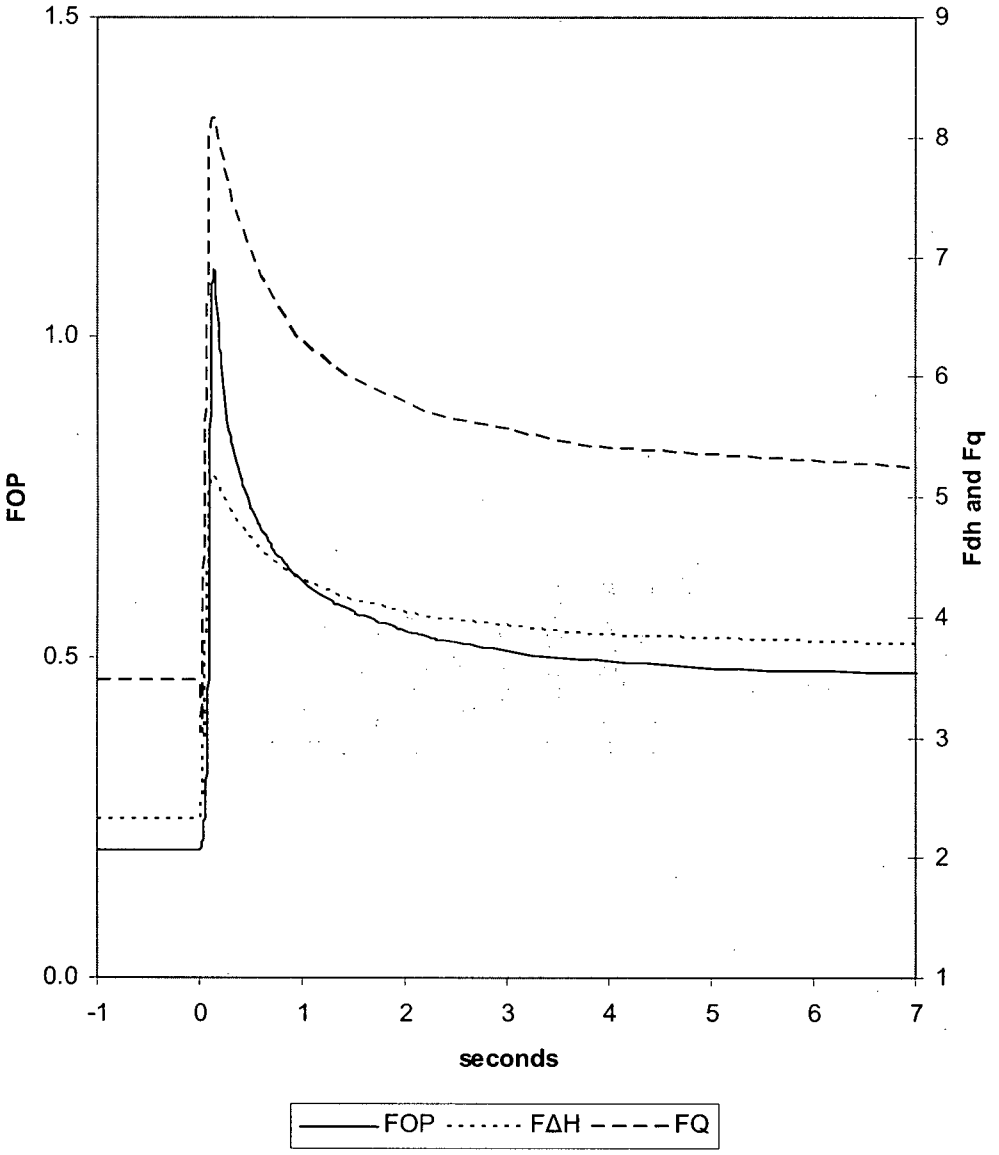

Figure 8-3 BOC 100% Power Transient

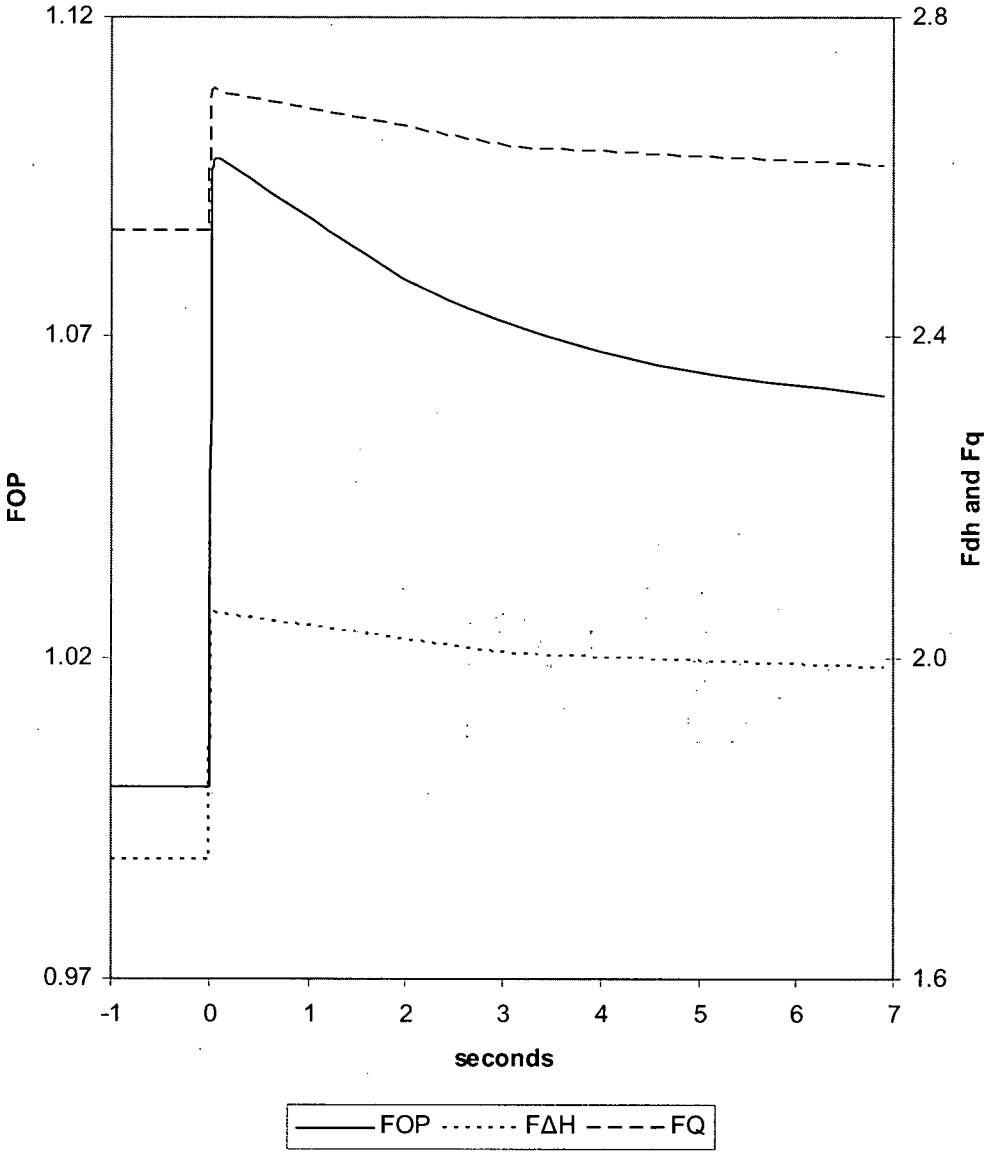

Figure 8-4 EOC 0% Power Transient

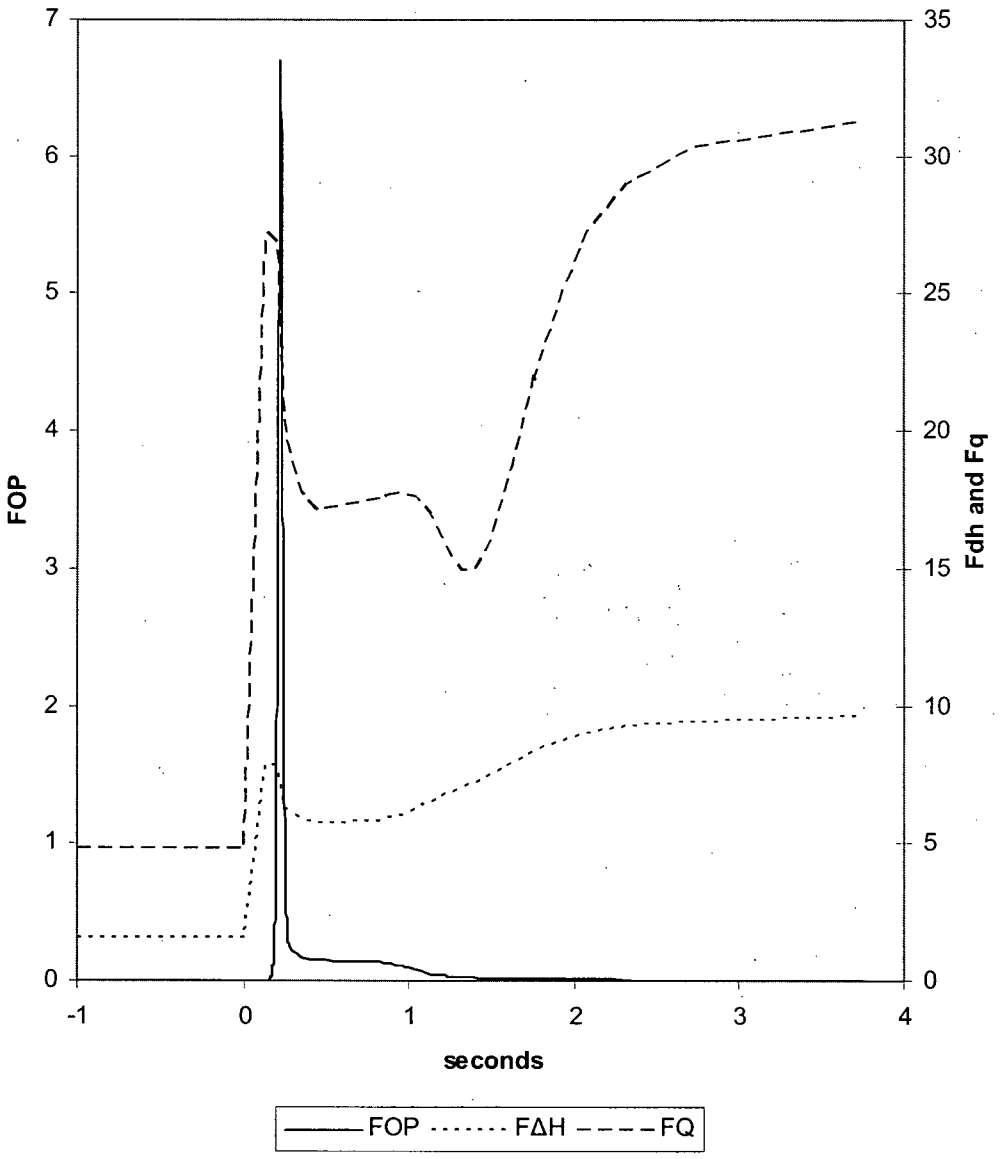

Figure 8-5 EOC 20% Power Transient

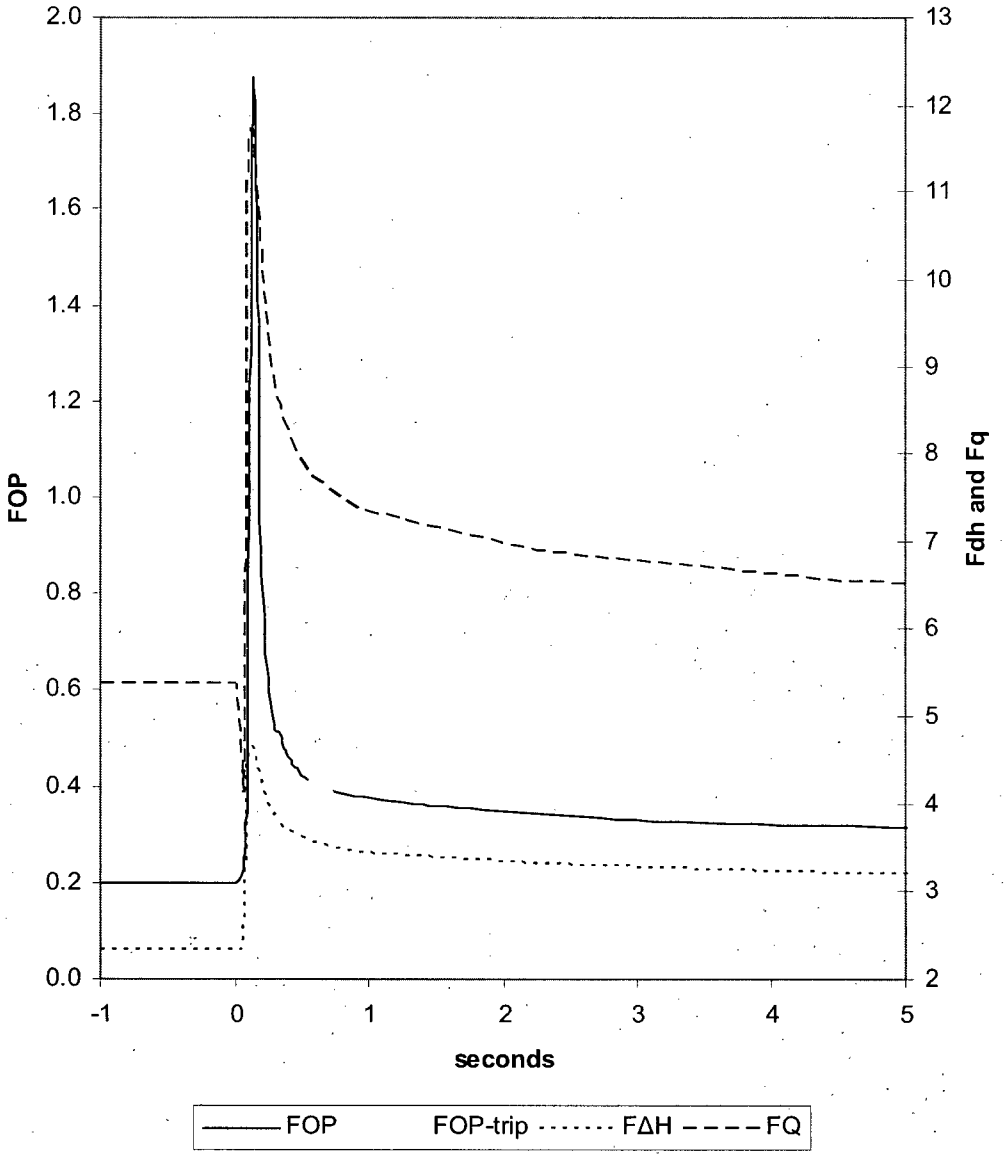

Figure 8-6 EOC 100% Power Transient

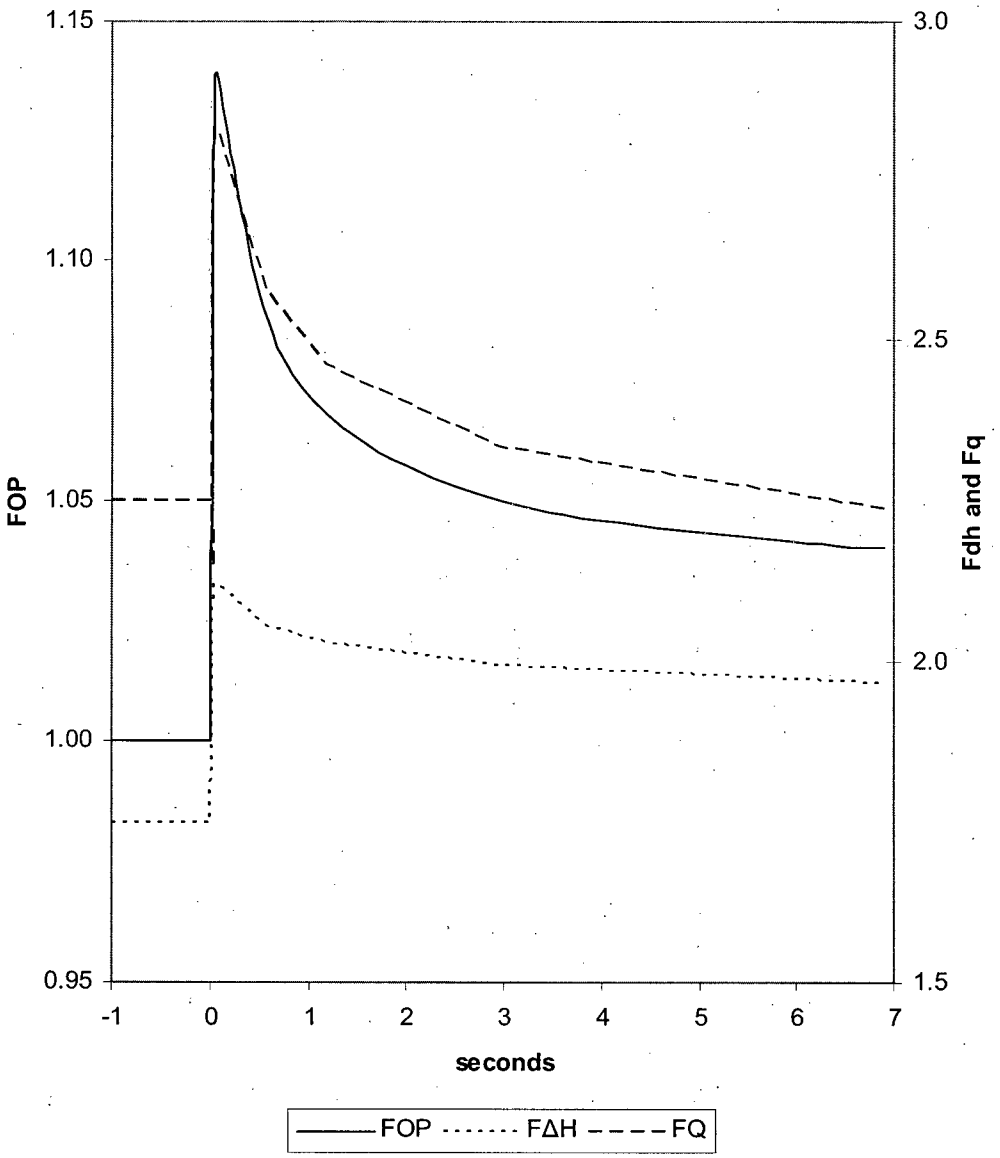

Figure 8-7 BOC 100% Power Transient for N12 Ejected

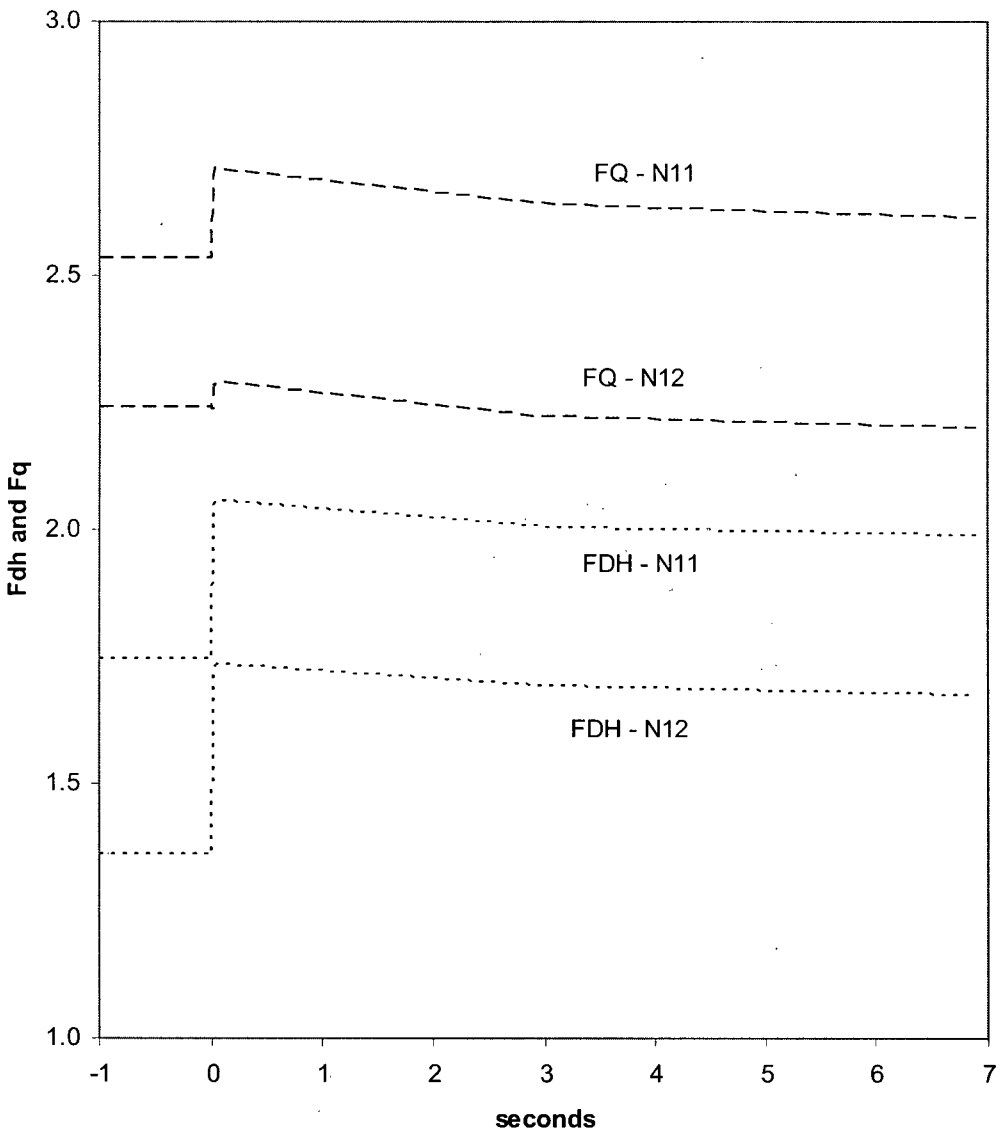

Figure 8-8 RELAP5/MOD2 Results for BOC 20% Power

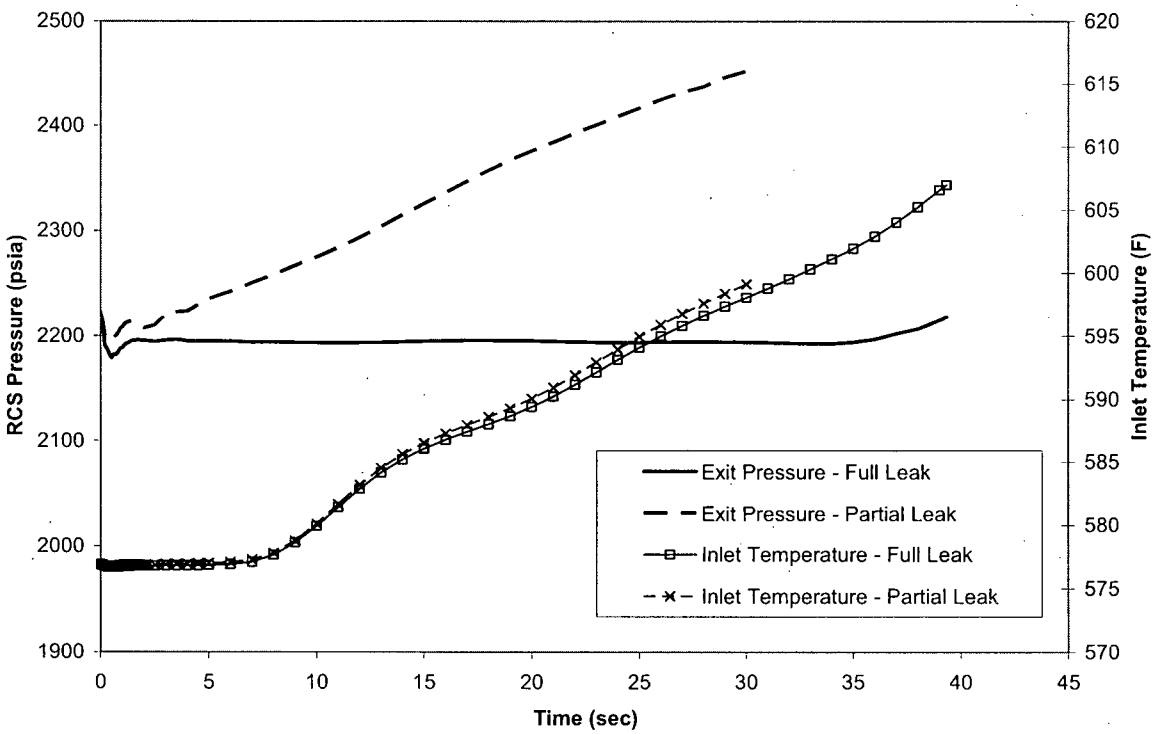

Figure 8-9 RELAP5/MOD2 Results for BOC HFP

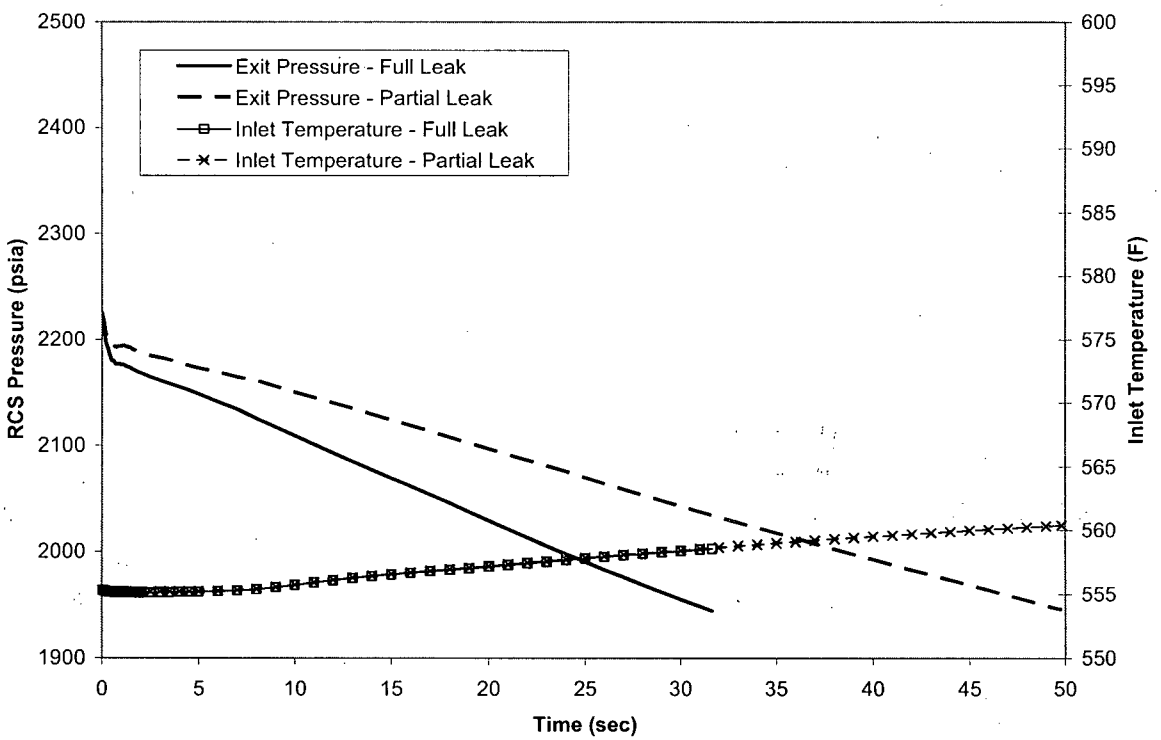

Figure 8-10 RELAP5/MOD2 Results for EOC 20% Power

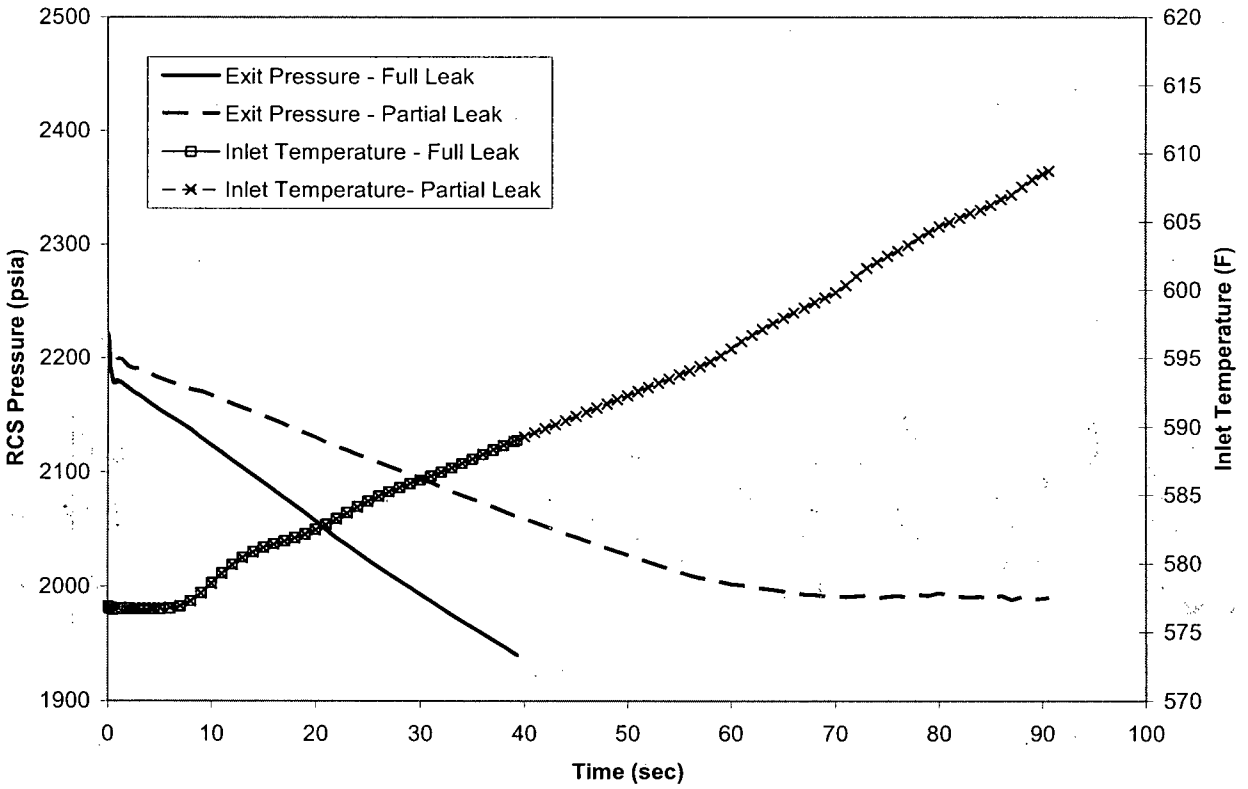

Figure 8-11 RELAP5/MOD2 Results for EOC HFP

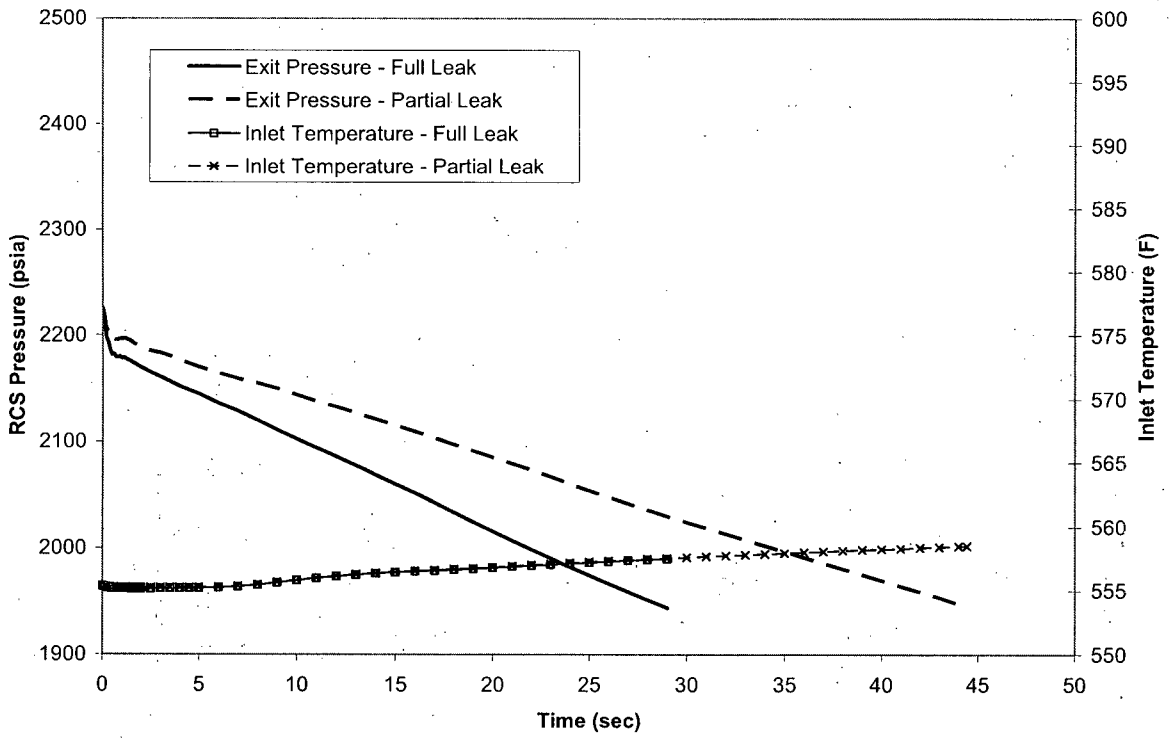

Figure 8-12 NEMO-K with RELAP5/MOD2 Conditions at BOC 20% Power

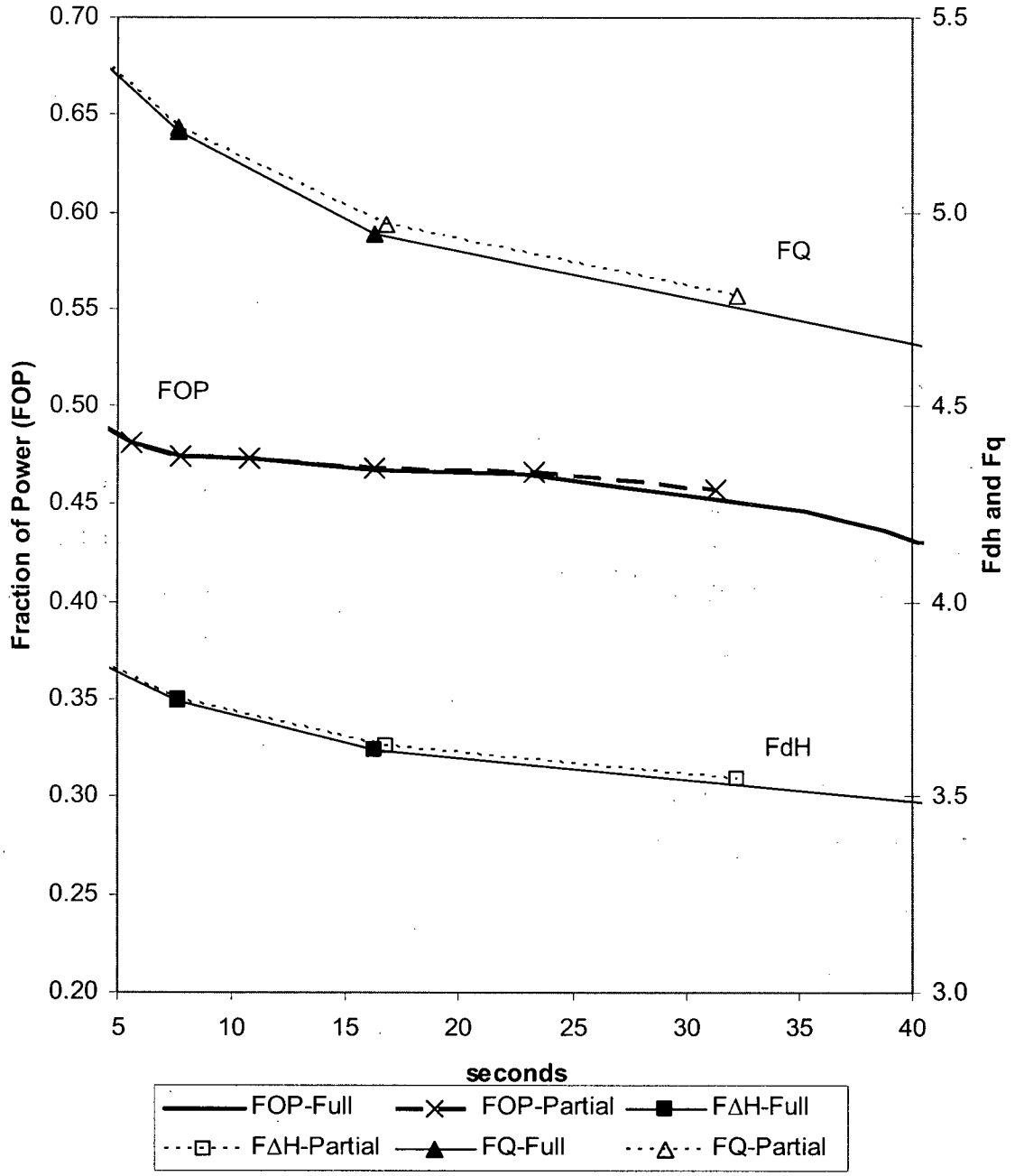

Figure 8-13 MDNBR for BOC HZP

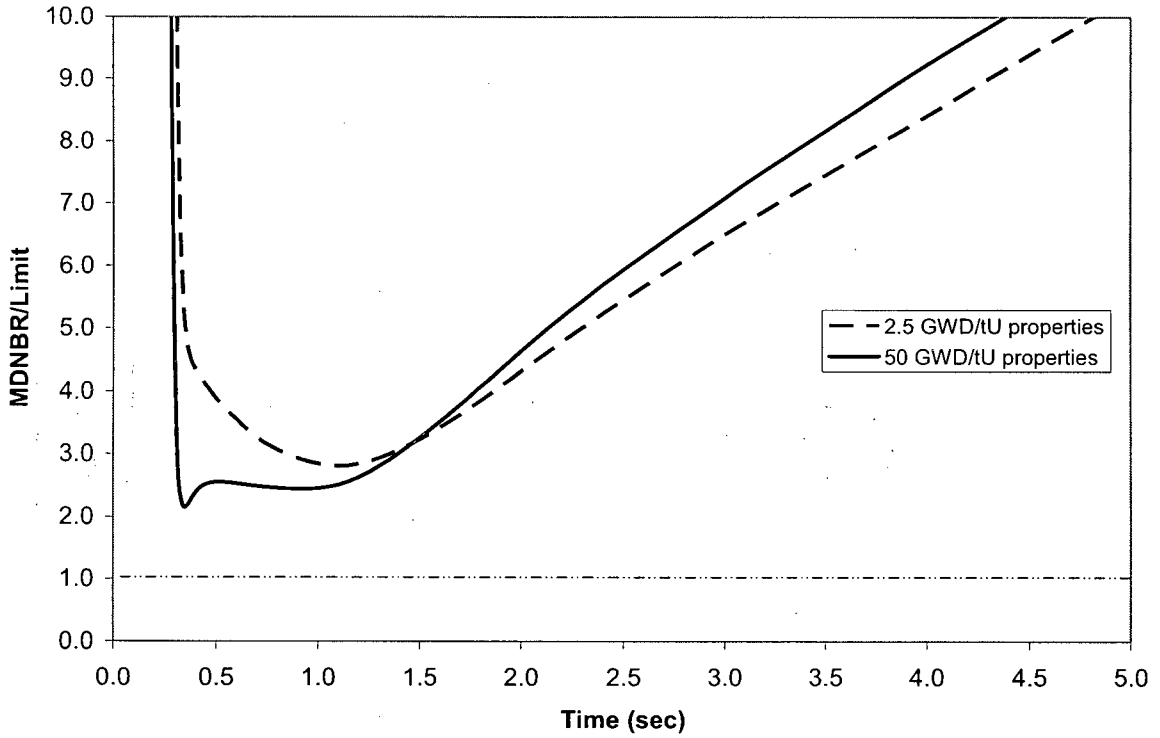

Figure 8-14 Fuel and Cladding Temperatures for BOC HZP

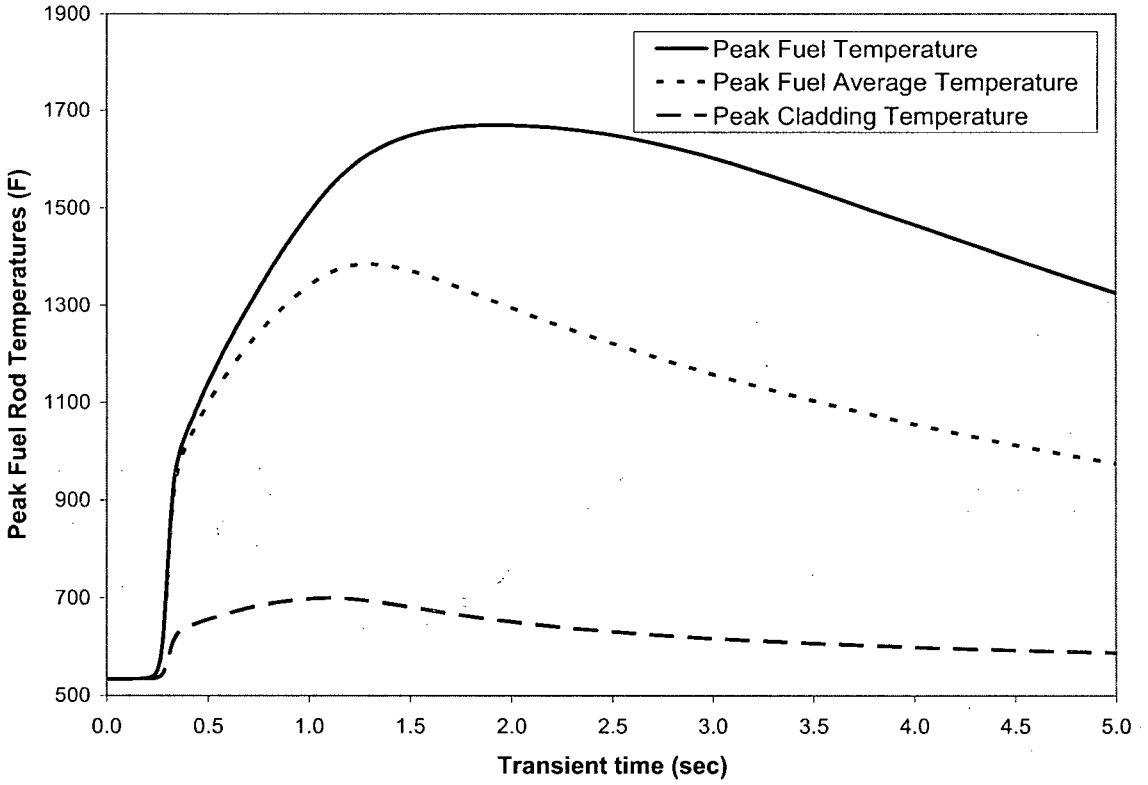

Figure 8-15 Peak Enthalpy Rise for BOC HZP

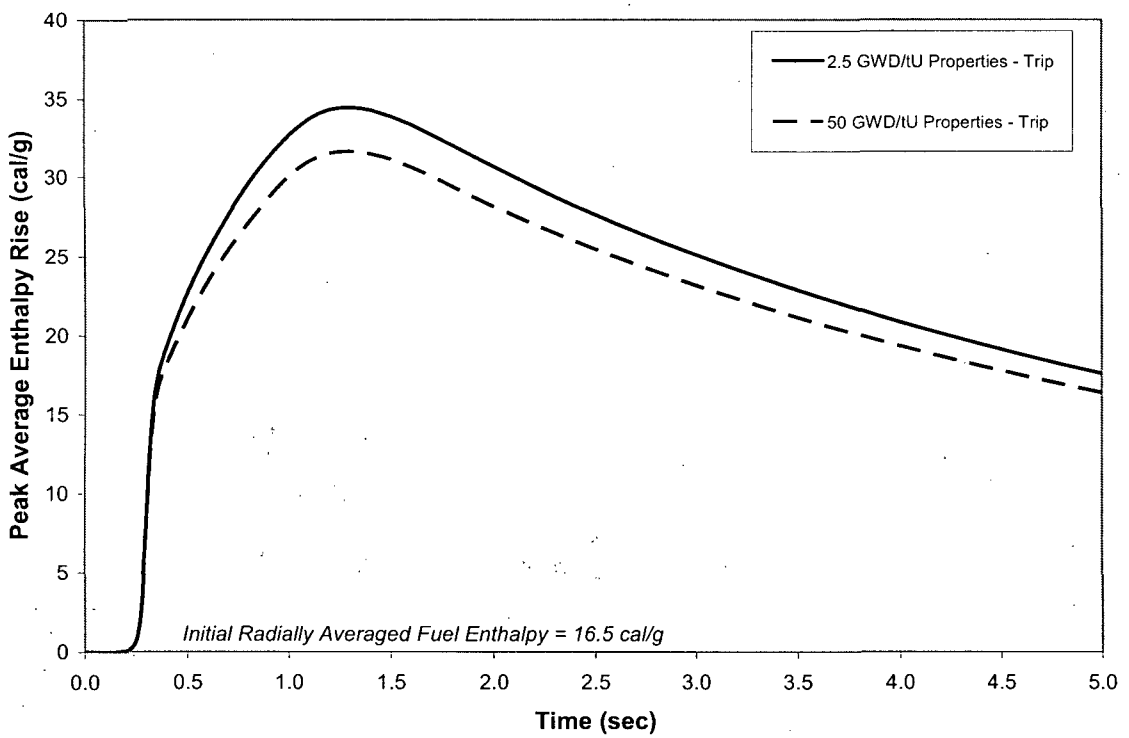

Figure 8-16 MDNBR for BOC 20% Power

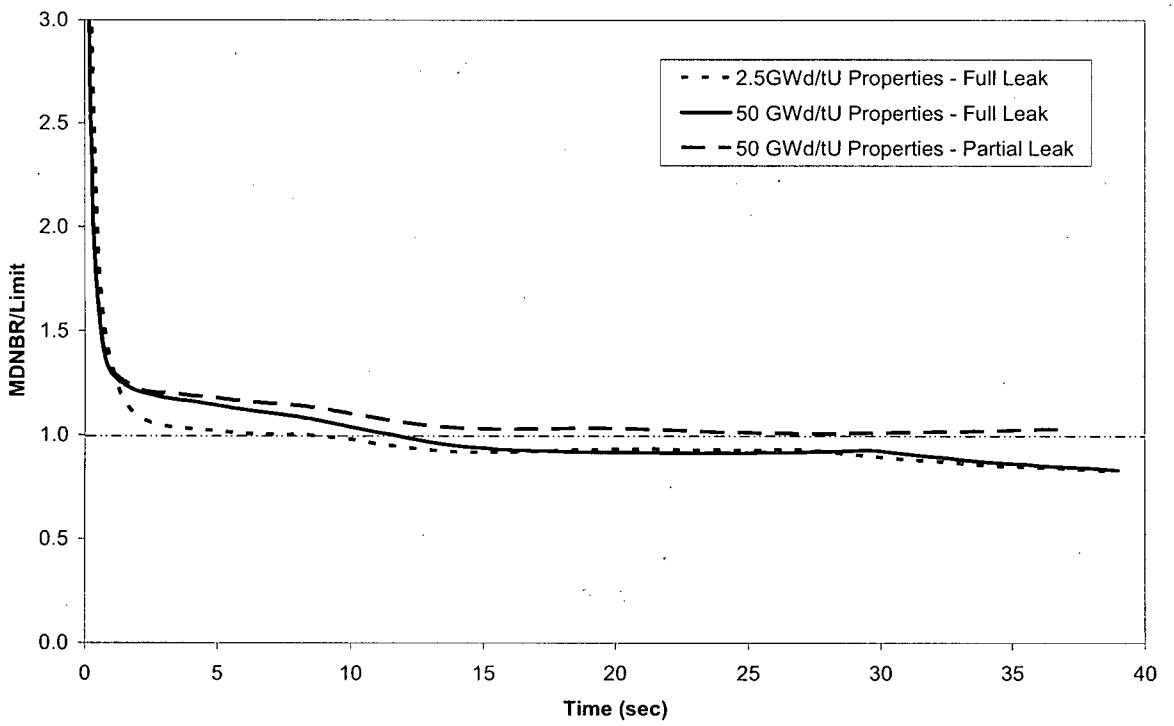

Figure 8-17 Fuel and Cladding Temperatures for BOC 20% Power

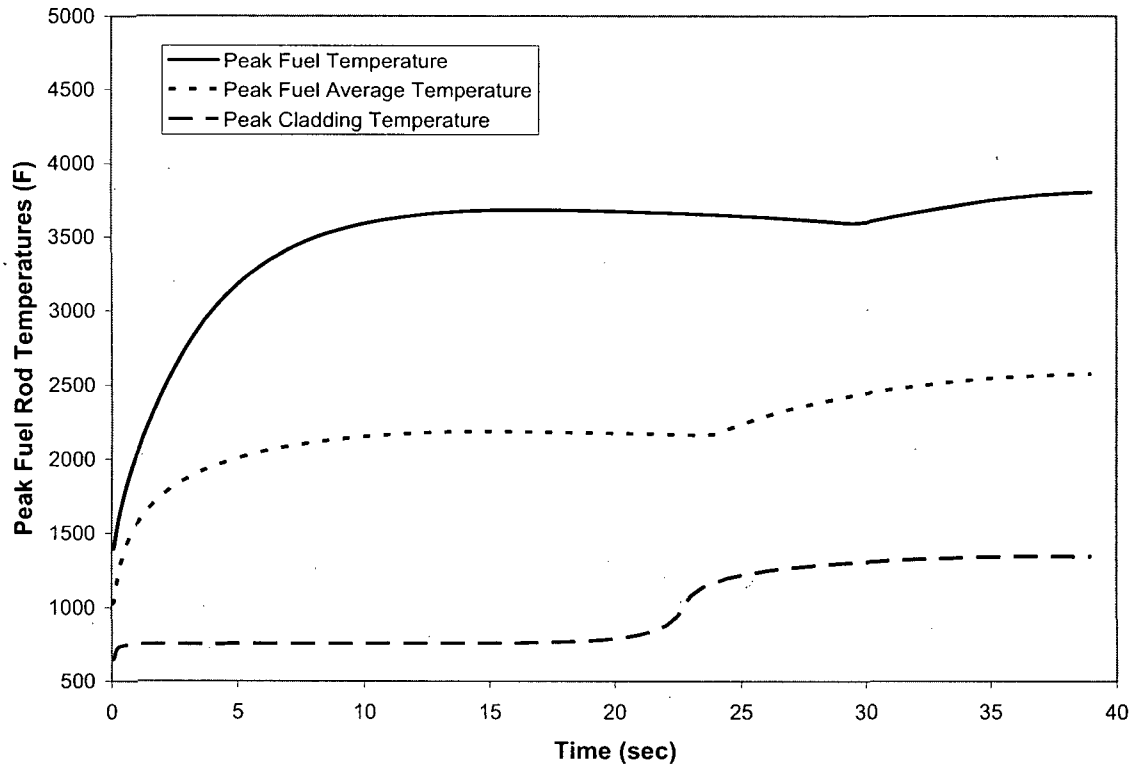

Figure 8-18 Peak Enthalpy Rise for BOC 20% Power

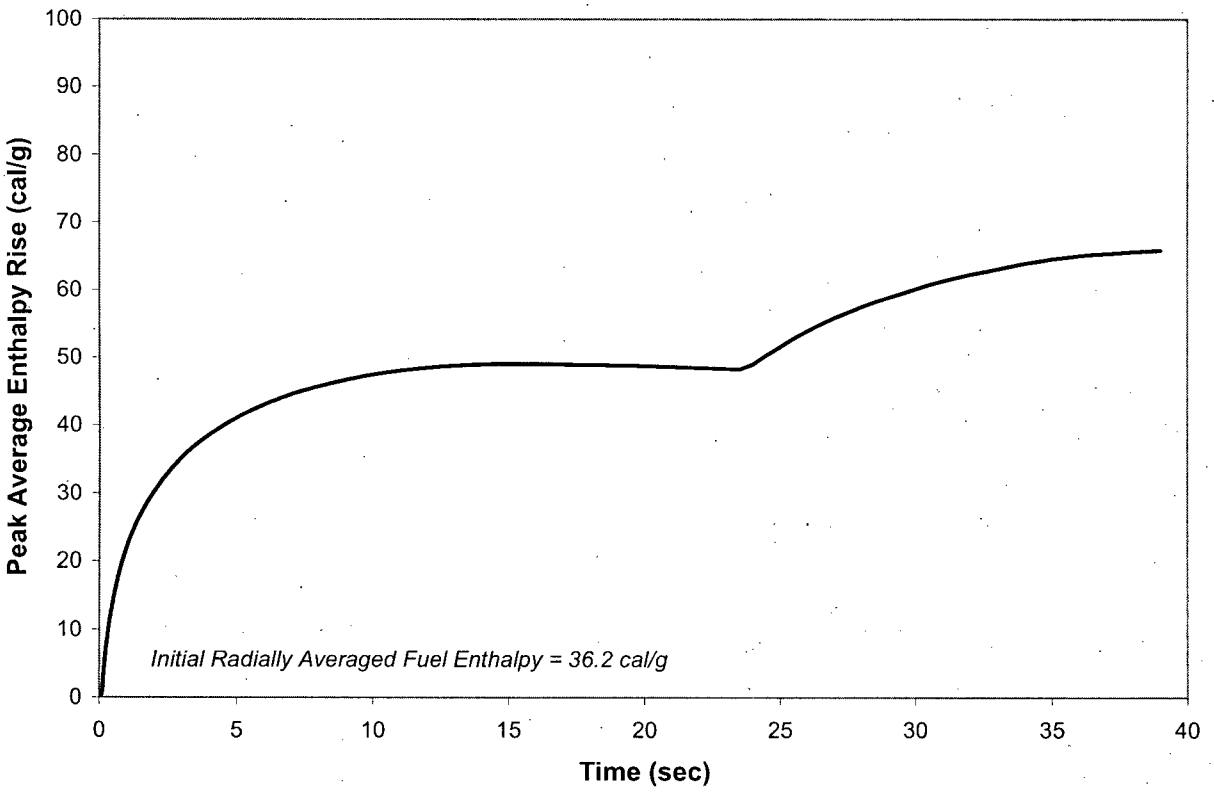

Figure 8-19 MDNBR for BOC HFP

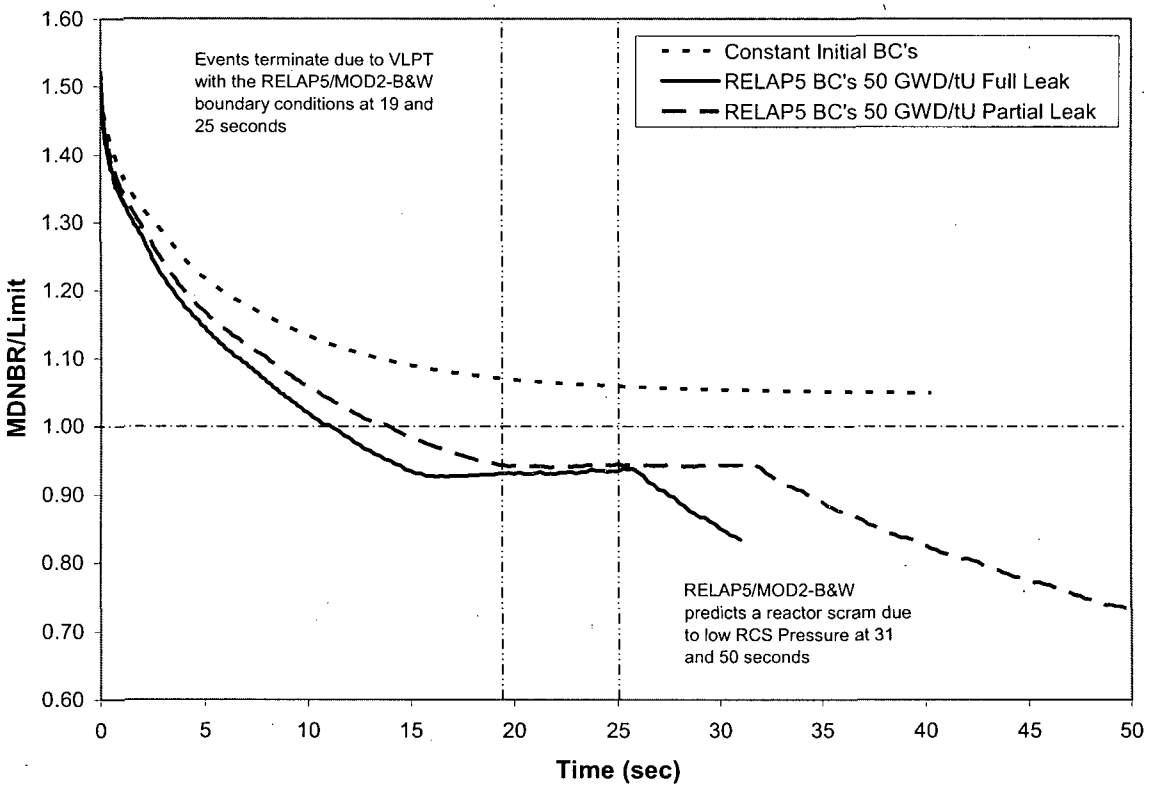

Figure 8-20 Fuel and Cladding Temperatures for BOC HFP

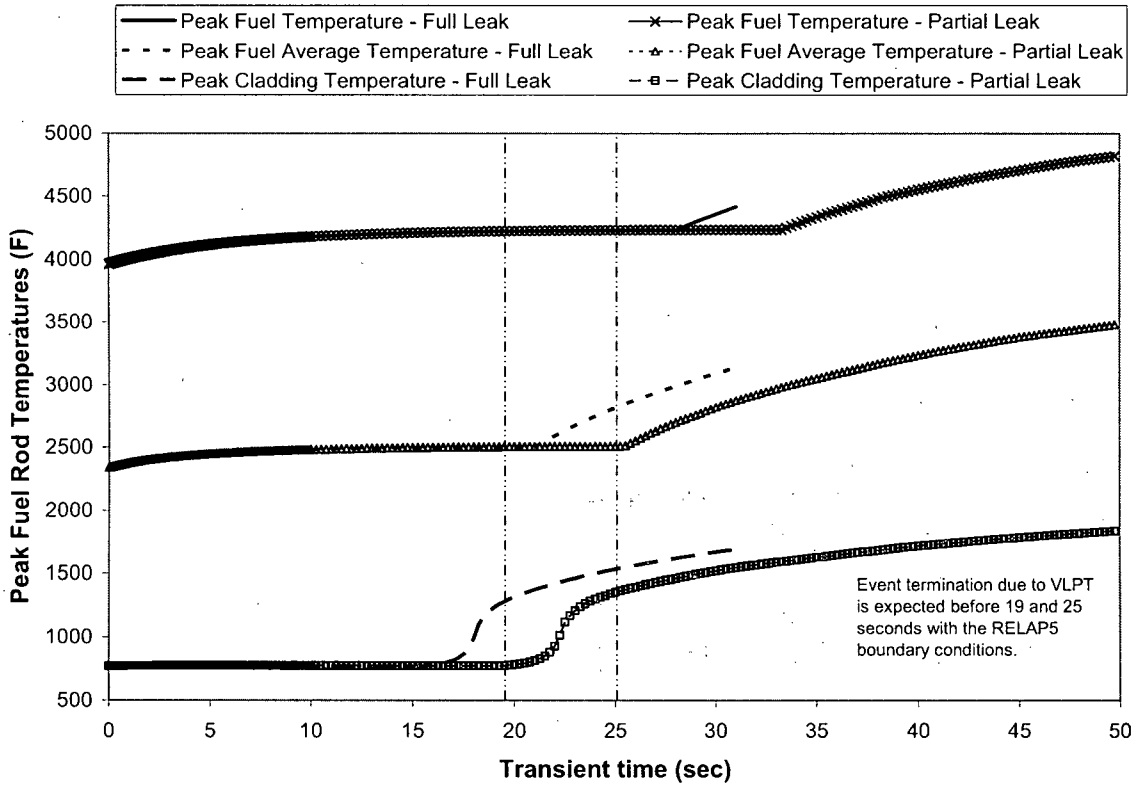

Figure 8-21 Peak Enthalpy Rise for BOC HFP

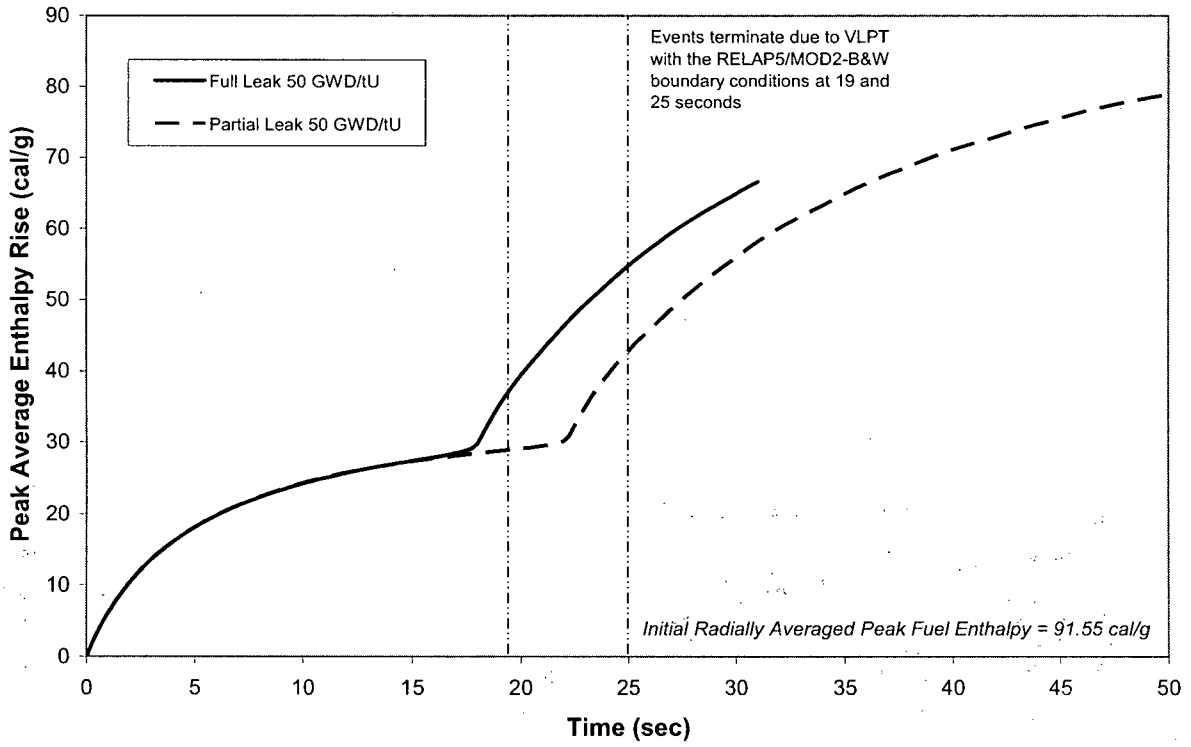

Figure 8-22 MDNBR for EOC HZP

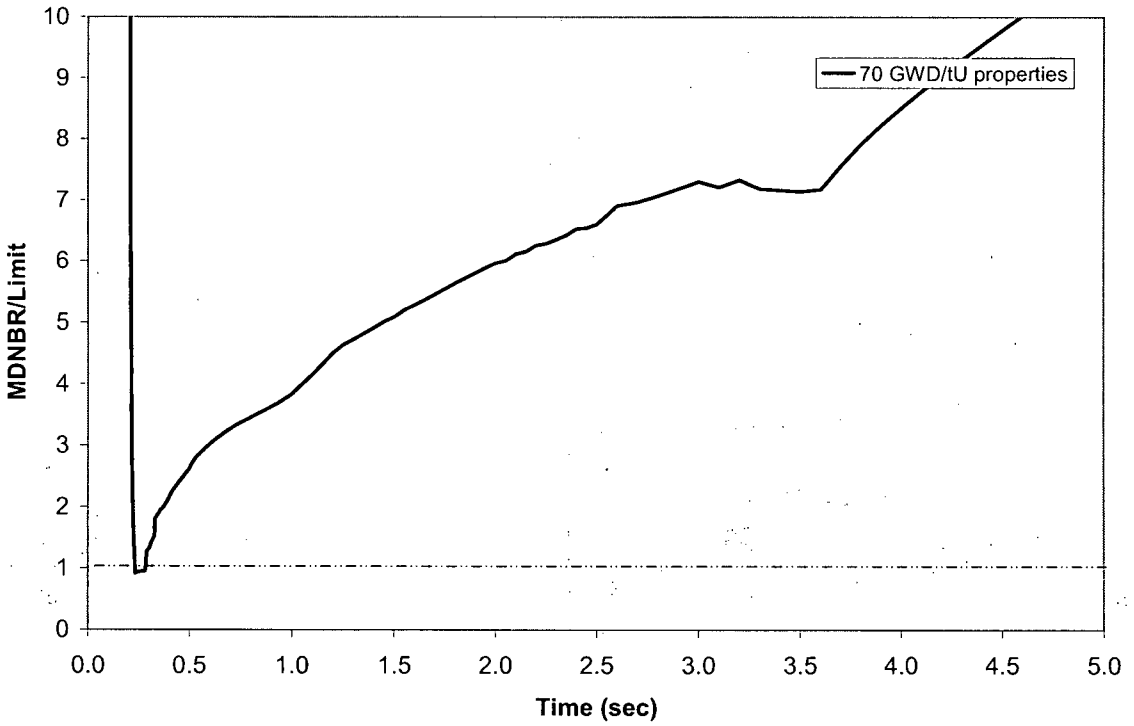

Figure 8-23 Fuel and Cladding Temperatures for EOC HZP

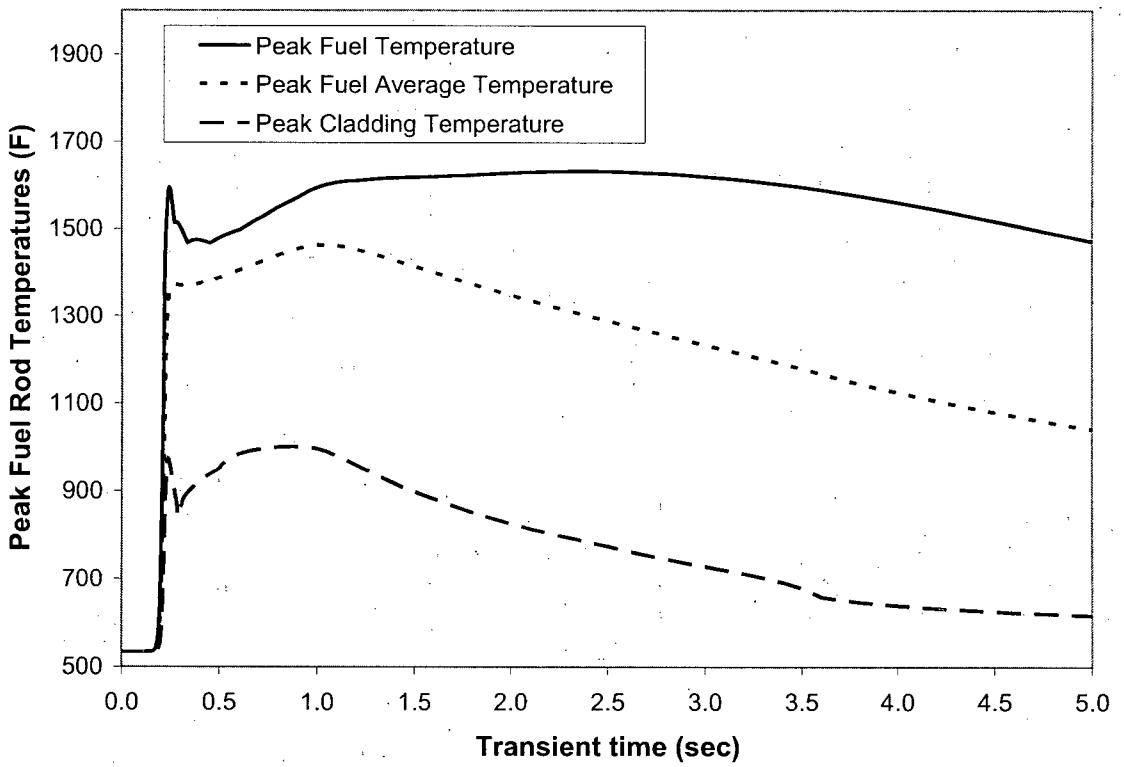

Figure 8-24 Peak Enthalpy Rise for EOC HZP

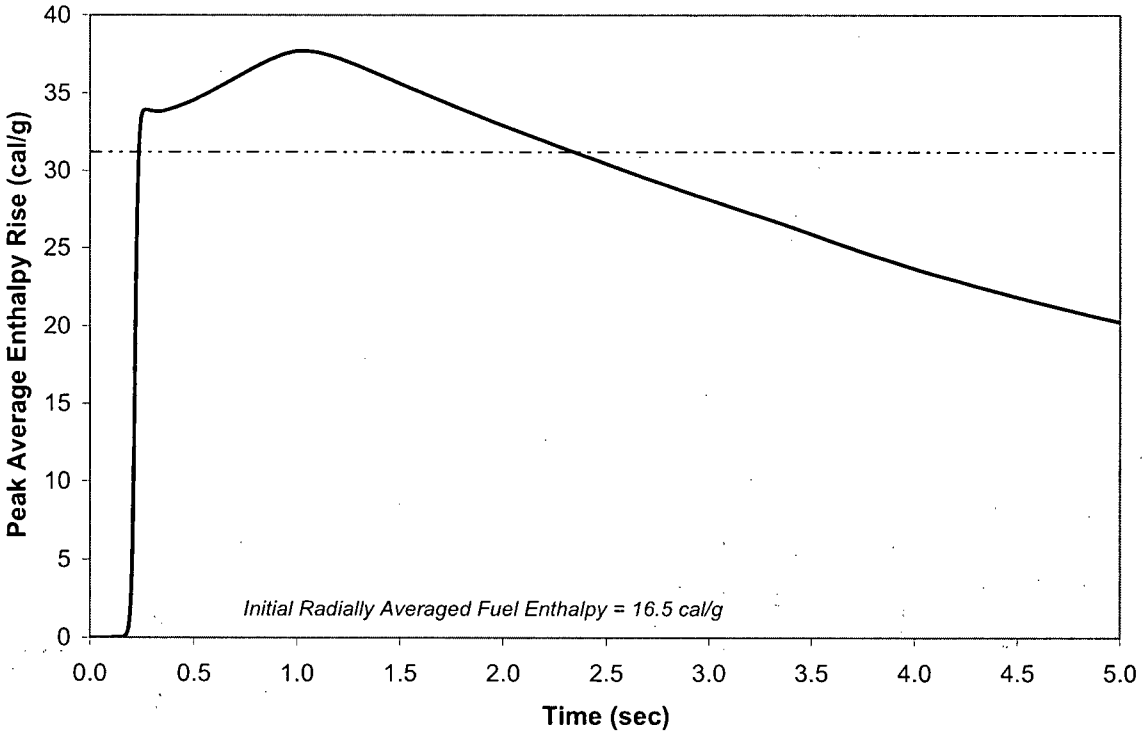

The dashed line represents the 31.2 cal/g threshold to increase fission gas release if rod fails.

Figure 8-25 MDNBR for EOC 20% Power

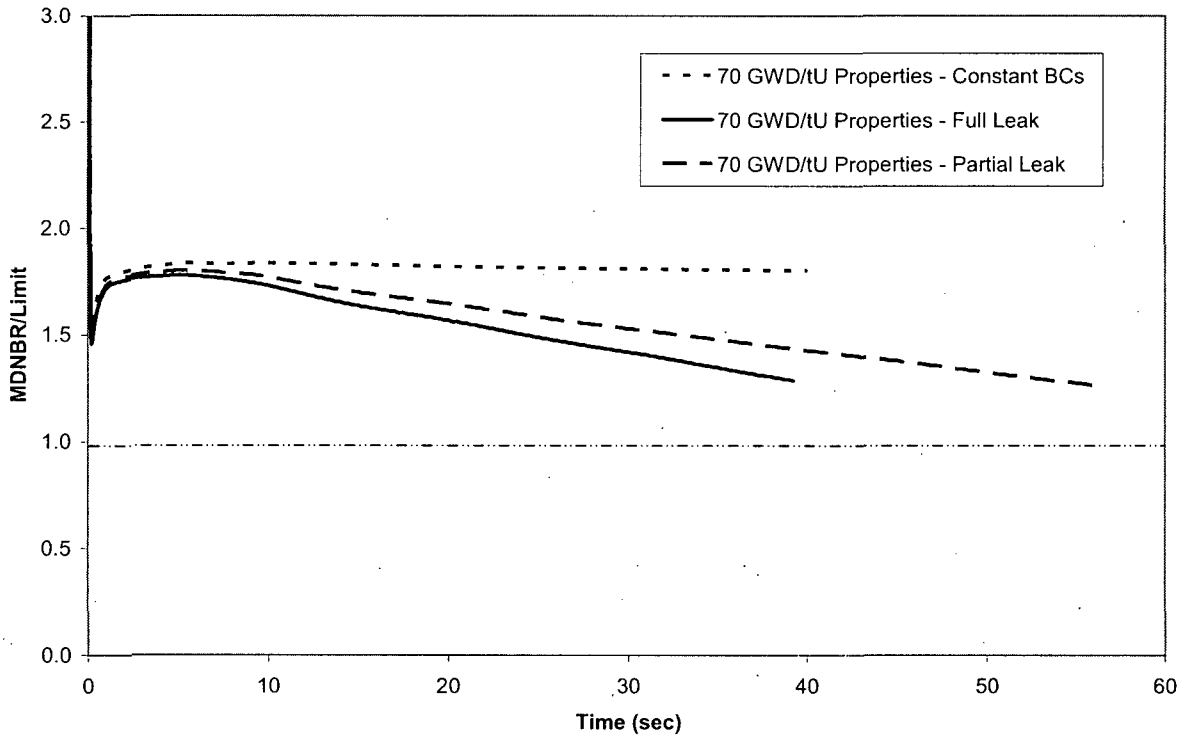

Figure 8-26 Fuel and Cladding Temperatures for EOC 20% Power

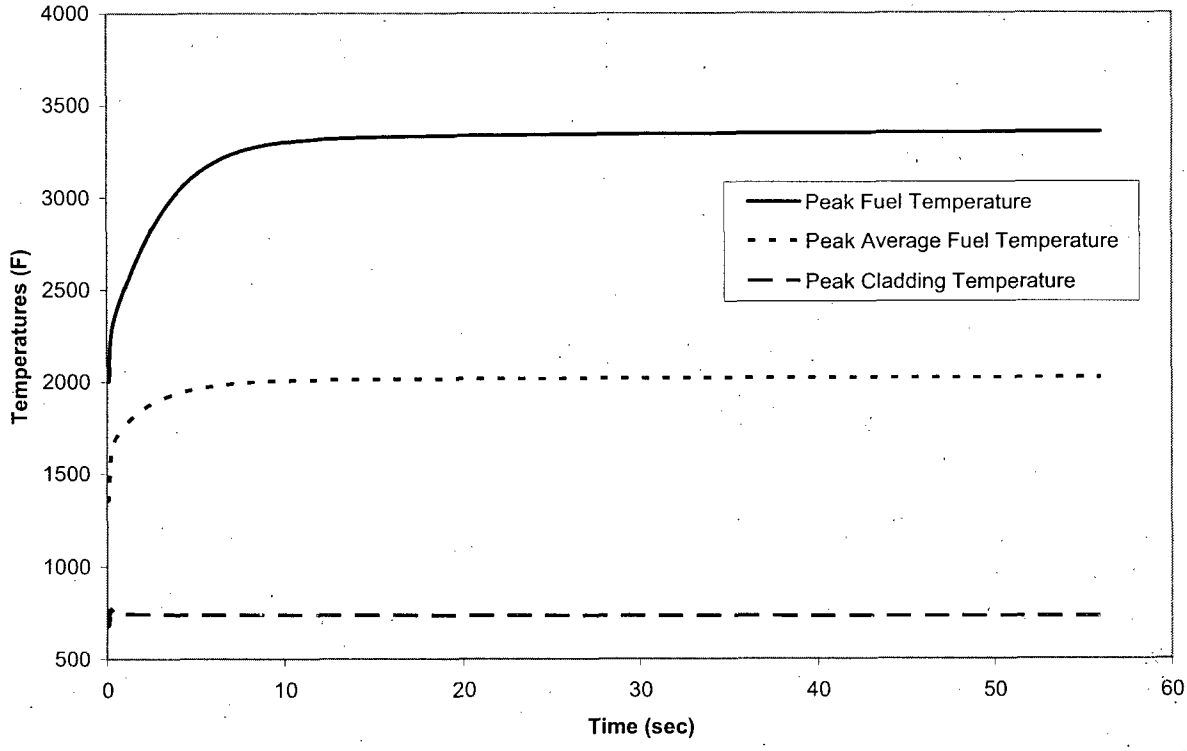

Figure 8-27 Peak Enthalpy Rise for EOC 20% Power

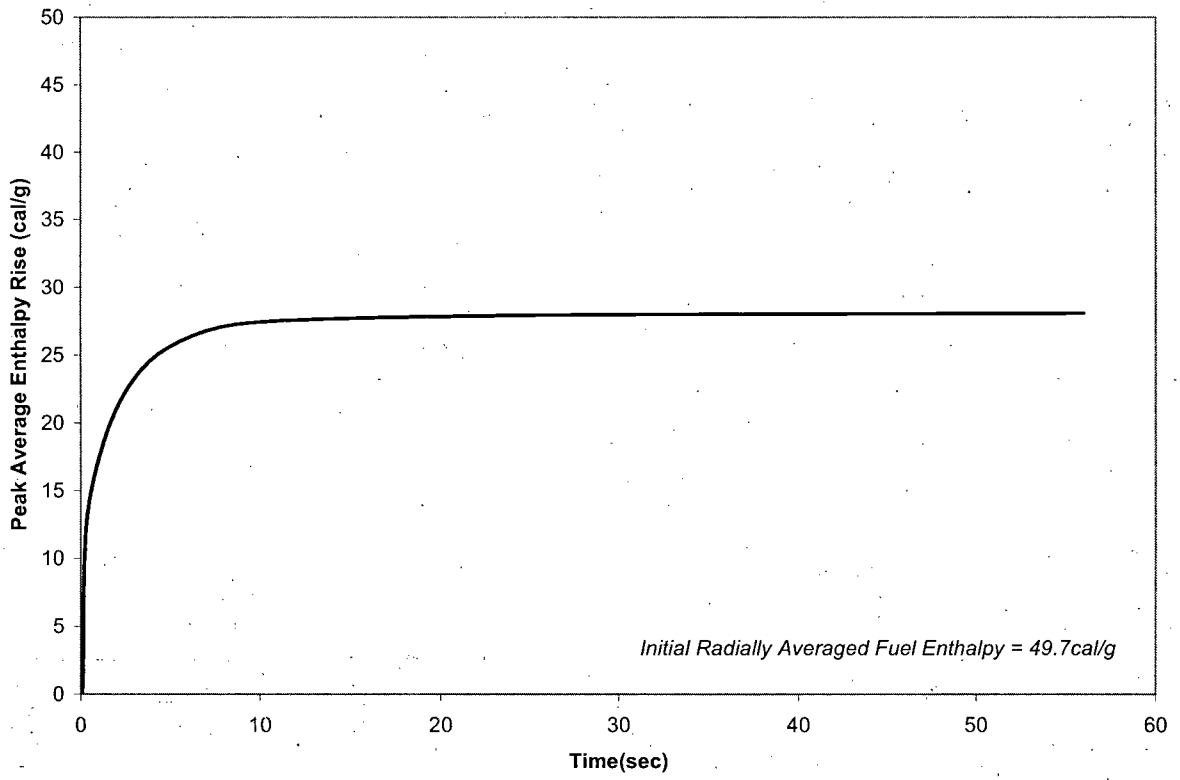

Figure 8-28 MDNBR for EOC HFP

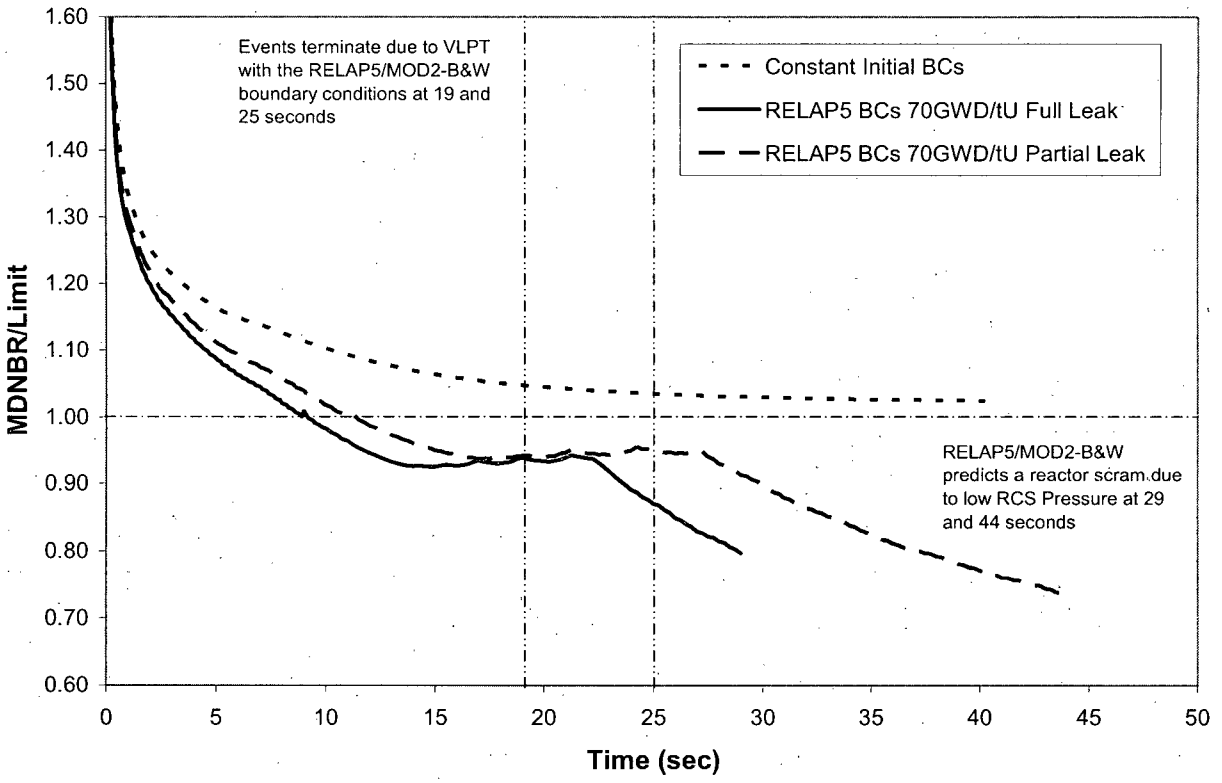

Figure 8-29 Fuel and Cladding Temperatures for EOC HFP

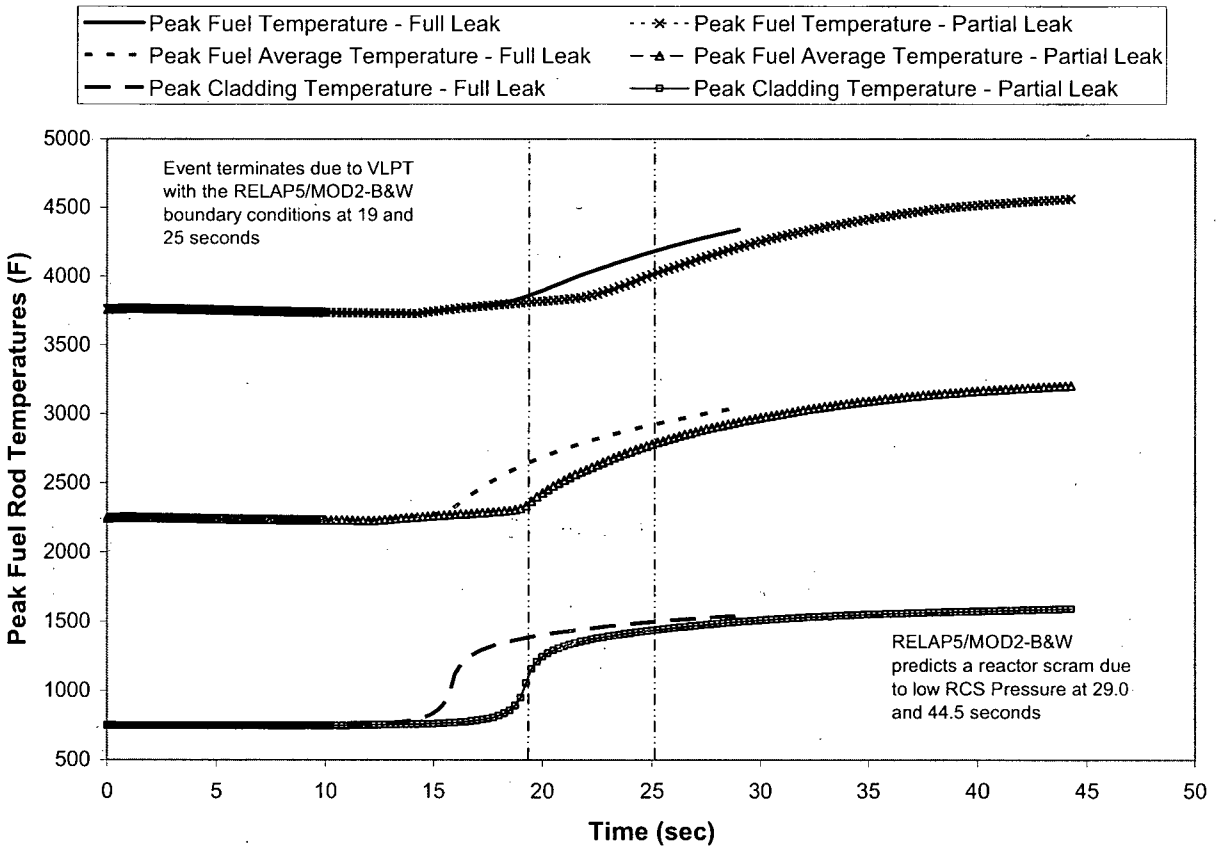

Figure 8-30 Peak Enthalpy Rise for EOC HFP

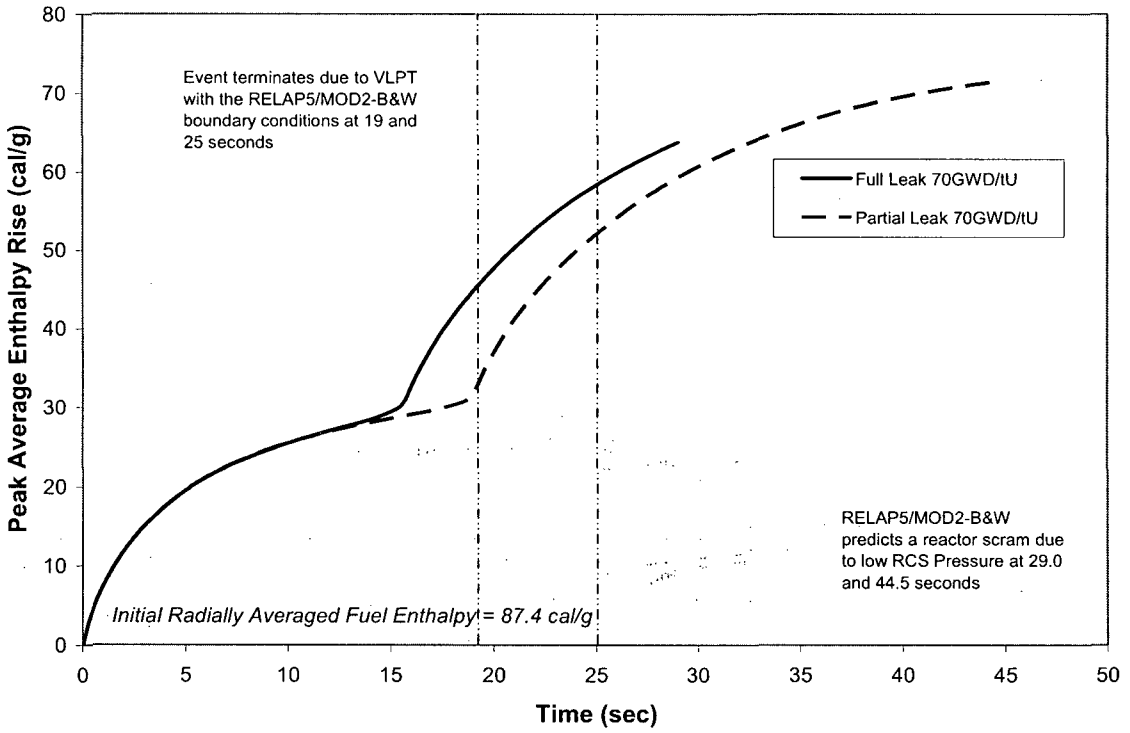

9.0 CONCLUSIONS AND CYCLE SPECIFIC CHECKS

This topical report provides a method and sample analysis to demonstrate acceptable results relative to the interim RIA criteria for Crystal River 3. One of three options can be performed in order to meet any changes in cycle design requirements:

1. Portions of the example analysis can be repeated for each cycle.
2. The current record of analysis can be shown to be applicable to another core design.
3. A complete reanalysis.

Based on the analysis results of Section 8.0, a table to check for each new fuel cycle design can be composed of the limiting values. As concluded in Section 8.0, the limiting conditions occurred at various initial power levels. Therefore, the HZP, 20 percent power, and HFP parameters need to be verified each cycle. Table 9-1 presents the checklist to validate the cycle specific verification of this sample problem. Table 9-2 presents the cycle 20 limiting values as a comparison to this sample problem. All values are found to be acceptable.

Table 9-1 Ejected Rod Analysis Checklist

Parameter	Acceptable Values	Cycle Specific Criteria					
		BOC			EOC		
		HZP	20%	HFP	HZP	20%	HFP
Maximum ejected rod worth, pcm	≤	715	556	60	741	535	73
β_{eff}	≥	0.0058	0.0058	0.0058	0.0048	0.0048	0.0048
MTC, pcm/°F	≤	2.5	0.0	-2.0	-14.5	-25.0	-26.0
DTC, pcm/°F	≤	-1.30	-1.24	-1.00	-1.40	-1.36	-1.20
Initial F_Q	≤	NA [a]	3.48	2.53	NA [a]	5.37	2.25
Static F_Q after ejection	≤	14.84	8.88	3.07	27.23	12.70	3.73
Initial $F_{\Delta H}$	≤	NA[a]	2.27	1.71	NA[a]	2.27	1.71
Static $F_{\Delta H}$ after ejection	≤	8.15	5.51	2.20	7.59	4.85	2.31
Equivalent nominal rods failed, %	≤	0	4.3[c]	4.3[c]	0	0	4.3[c]
Trip setpoints	Not Affected [b]						

Notes:
[a] Not applicable since initial stored energy above the coolant temperature is zero.
[b] Any changes to the trips listed in Table 8-1 would have to be reviewed relative to their impact on this accident analysis.
[c] As stated in Section 2.3, 4.3% failures is a conservatively low example value. The value used for Crystal River 3 will by defined by a different analysis.

Table 9-2 Cycle 20 Ejected Rod Parameters

Parameter	Acceptable Values	Cycle Specific Values					
		BOC			EOC		
		HZP	20%	HFP	HZP	20%	HFP
Maximum ejected rod worth, pcm [a]	Yes	498	339	59	362	330	69
β_{eff}	Yes	0.0063	0.0063	0.0063	0.0051	0.0051	0.0051
MTC, pcm/°F	Yes	-2.02	-4.11	-6.20	-18.83	-31.89	-32.53
DTC, pcm/°F	Yes	-1.40	-1.35	-1.13	-1.55	-1.50	-1.31
Initial F_Q [a]	Yes	NA [b]	2.97	2.18	NA [b]	4.42	1.66
Static F_Q after ejection [a]	Yes	13.61	7.17	2.82	16.66	10.30	3.02
Initial $F_{\Delta H}$ [a]	Yes	NA [b]	1.86	1.62	NA [b]	1.72	1.47
Static $F_{\Delta H}$ after ejection [a]	Yes	6.96	4.27	1.98	5.08	3.80	1.84
Equivalent nominal rods failed, %	Yes	-	0.0	0.1	-	-	0.2
Trip setpoints	Yes	-	-	-	-	-	-

Notes:

[a] Ejected rod worths and peaking are calculated with the rods inserted to the Technical Specification Limit and the highest worth/peaking from either the offset skewed to LCO limits or zero xenon for HZP.

[b] Not applicable since initial stored energy above the coolant temperature is zero.

10.0 REFERENCES

1. NUREG 800, Revision 3, "Standard Review Plan for the Review of Safety Analysis Reports for Nuclear Power Plants," March 2007, ML070740002.

2. BAW-10231PA, Revision 1, "COPERNIC Fuel Rod Design Computer Code," Framatome ANP, January 2004.

3. NUREG/CR-6742 LA-UR-99-6810, "Phenomenon Identification and Ranking Tables (PIRTs) for Rod Ejection Accidents in Pressurized Water Reactors Containing High Burnup Fuel," Los Alamos National Laboratory, September 2001.

4. NUREG/CR-0497, TREE-1280, Revision 2, D. L. Hagman, G. A. Reymann, and R.E. Mason, MATPRO Version 11 (Revision 2), "A Handbook of Material Properties for Use in the Analysis of Light Water Reactor Fuel Rod Behavior," August 1981.

5. ANP-10286P, "U.S. EPR Rod Ejection Accident Methodology Topical Report," November 2007.

6. BAW-10221PA, "NEMO-K a Kinetics Solution in NEMO," September 1998.

7. BAW-10156A, Revision 1, "LYNXT Core Transient Thermal-Hydraulic Program," B&W Fuel Company, August 1993.

8. AREVA NP Document 43-10193PA-00, RELAP5/MOD2-B&W For Safety Analysis of B&W Designed Pressurized Water Reactors.

9. AREVA NP Document 43-10164PA-06, RELAP5/MOD2-B&W An Advanced Computer Program For Light Water Reactor LOCA and Non-LOCA Transient Analysis.

10. NEACRP-L-335 (Revision 1), H. Finnemann and A. G. Galati, "NEACRP 3-D LWR Core Transient Benchmark," Final Specifications, October 1991 (January 1992).

11 BAW-10228PA, "Science," Framatome Cogema Fuels, December 2000.

12. BNWL-1962, UC-32, "COBRA-IV-I: An Interim Version of COBRA for Thermal-Hydraulic Analysis of Rod Bundle Nuclear Fuel Elements and Cores," Battelle Pacific Northwest Laboratories, March 1976.

13. BAW-10044, "TAFY – Fuel Pin Pressure and Gas Pressure Analysis," Babcock & Wilcox, April 1972.

14. BAW-10087P, "TACO – Fuel Pin Performance Analysis," Babcock & Wilcox, December 1975.

15. BAW-10141PA, "TACO2 – Fuel Pin Performance Analysis," Babcock & Wilcox, June 1983.

16. BAW-10162PA, "TACO3 – Fuel Pin thermal Analysis Computer Code," BW Fuel Company, October 1989.

17. BAW-10069A, Revision 1, "RADAR – Reactor Thermal and Hydraulic Analysis During Reactor Flow Coastdown," Babcock & Wilcox, October 1974.

18. Letter J. H. Taylor to U.S. Nuclear Regulatory Commission, "Revised Measurement Uncertainty for Control Rod Worth Calculations," JHT/96-01, January 3, 1996.

19. BAW-10180A-01, NEMO – Nodal Expansion Method Optimized, Revision 1, July 1993.

20. BAW-10120PA, "Comparison of Core Physics Calculations with Measurements," Babcock & Wilcox, July 1979.

21. BAW-10179P-A Rev. 7, "Safety Criteria and Methodology for Acceptable Cycle Reload Analyses," January 2008.